Chapter 1: Fundamental of Fluid Dynamics

Lecture 1

1.1 The Continuum Hypothesis

Fluid dynamics is a branch of ***continuum mechanics***, which studies the macroscopic mechanical behaviours of solids, liquids and gases. *Solids* tend to retain their own shapes, which deform slightly if the imposed external force is small, a property known as 'elasticity'. Because of this, in solid mechanics a linear theory has an important place. In contrast, liquids or gases, which are referred to as ***fluids***, cannot retain a definite shape, exhibiting instead 'fluidity' that large deformation occurs even under the action of weak forcing. This nature renders, as we will see, the mathematical description of fluid dynamics inherently 'nonlinear'. It should be noted that the distinction between solids and fluids is not absolute or completely exclusive; there exist many materials (e.g. jelly and polymers) which behave like something between typical solids and fluids, or switch from one to another, during the motion.

The theories of fluid dynamics and solid mechanics are both established on the foundation of continuum hypothesis, which is a mathematical abstraction of solids and fluids. In order to introduce this idea, we first look briefly at their motions from the microscopic viewpoint.

Microscopic view of fluid motion

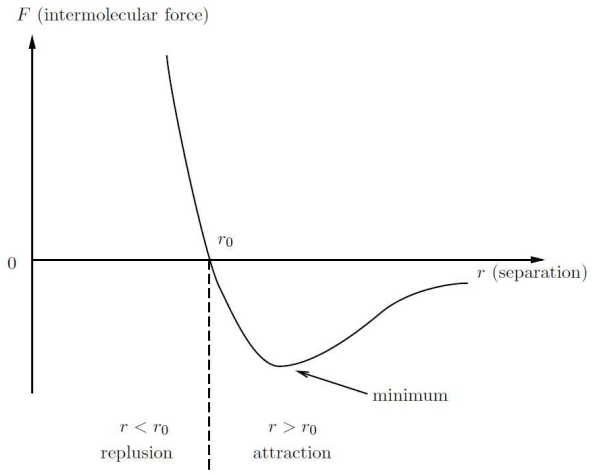

Figure 1.1: Variation of the intermolecular force with the distance r between the two molecules.

At the microscopic level, a fluid (liquid or gas) is of course composed of molecules, which move and collide under the action of the ***intermolecular force***. The nature and strength of this force between any two molecules depend on the distance between them, as is shown in figure 1.1. The force is repulsive/attractive when the distance r is less/greater than the equilibrium (critical) value r_0, which is about 3-4$\times 10^{-10}$m. Typically, for solids and liquids, the average distance between the molecules is about r_0, whereas for gases, the averaged distance is $10r_0$ or larger, implying that the force is very weak except when the

molecules are near or in collision, and the interactions are primarily through collisions. Obviously, the number of molecules is *finite* (but very large), and their spatial distribution is *discrete*.

The motion of fluid can be studied by tracing each and every molecule. This is the approach of ***Molecular Dynamics***, which includes all microscopic details. However, it is very hard to implement this approach because the number of molecules in a flow of practical application is enormous. It is also unnecessary because the flow properties that one observes and measures are the collective ones averaged over many molecules. It is usually those 'averaged', or macroscopic, properties that underpin the flow physics of scientific and engineering interest.

It is therefore desirable and possible to sacrifice the microscopic details by taking a statistical approach. This led to the ***Kinetic Theory***, in which one introduces the *probability density function* $f(t, \mathbf{r}, \mathbf{v}_m)$, which is a function of time t, the position vector $\mathbf{r}$ and the molecule velocity $\mathbf{v}_m$, such that $f\mathrm{d}\mathbf{r}\mathrm{d}\mathbf{v}_m$ represents the number of the molecules in $\mathrm{d}\mathbf{r}$ volume about $\mathbf{r}$ with velocity in a $\mathrm{d}\mathbf{v}_m$ range around $\mathbf{v}_m$. It follows that

$$\int_{-\infty}^{\infty}\int_{D} f(t, \mathbf{r}, \mathbf{v}_m)\mathbf{dr}\mathbf{dv}_m = N,$$

where N is the total number of molecules in a domain D. For gases, f satisfies the ***Boltzmann equation***[†], and the distribution of f is controlled by collisions. Fluid flows are treated as the ensemble average of the motions of molecules, which allows the macroscopic properties such as density, velocity and temperature to be calculated once f is known; f encapsulates all statistical information of the system. However, this approach is also very difficulty because f is a function of *seven* independent variables, and it is hard to characterise the collisions among the molecules in the gas as well as collision between the molecules and the boundary. It is necessary to develop a even more simplified approach, which is the *continuum approach*.

Collisions are important as they facilitate momentum and energy exchange among molecules. The mean distance that a molecule travels before colliding with another molecule is referred to as ***mean free path*** and is customarily denoted by λ. It is an important intrinsic length scale of the system.

Macroscopic view of fluid motion

A flow usually has a discernable macroscopic length L, e.g. the diameter of a sphere or the length of an aerofoil in the case of a flow past these. Typically, the mean free path λ is much smaller than L, i.e. $\lambda \ll L$. This allows a fluid to be treated as a ***continuum*** by introducing the notion of ***fluid particle***.

Definition 1.1: *A fluid particle is defined as a collection of molecules in a volume τ_D with size ℓ ($\tau_D \sim \ell^3$), which satisfies two restrictions:*

1. *ℓ is much smaller than L (i.e. $\ell \ll L$) that the volume may be treated as a geometric point;*

[†]It should be noted the Navier-Stokes equations governing fluid motions may be derived not only using the continuum mechanics approach as will be described in this course, for gases they may also be derived from the *Boltzmann equation* using the mathematical procedure called *Chapman-Enskog expansion*.

2. *ℓ is large enough that rapid random microscopic fluctuations are smoothed out when averaged over the volume and the averaged quantities become well defined, i.e. independent of the shape and size of the volume.*

For the second restriction to be met, not only the volume must contain sufficient number of molecules, there must also be sufficient momentum exchange among the molecules. This requires enough collisions to take place in the volume τ_D, which would be the case if $\ell \gg \lambda$

It follows that ℓ must be chosen such that

$$\lambda \ll \ell \ll L, \tag{1.1}$$

and the notion of fluid particle can be introduced provided that

$$\mathrm{Kn} \equiv \frac{\lambda}{L} \ll 1. \tag{1.2}$$

The ratio Kn is referred to as ***Knudsen number***. With condition (1.2), a flow field can be viewed as a *continuum* consisting of fluid particles which *distribute continuously* in space. Through this abstraction, fluid particles rather than molecules are the elementary constituents. Average quantities can be defined and attached to each moving fluid particle, or at each point. This is what the ***continuum hypothesis*** entails.

The condition (1.2), which forms the basis of continuum models, is readily satisfied in most situations, but could be violated when the gas is rarified (i.e. has extremely low density) as in high altitudes of the Earth's atmosphere, in strong shocks and in some micro-fluidic devices.

In order to elaborate the key points introduced above, let us consider a fluid flow past a rigid body, say a sphere as sketched in Figure 1.2.

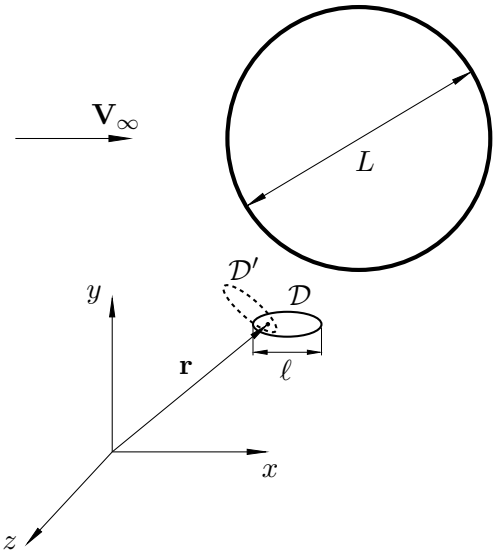

Figure 1.2: Definitions of a fluid particle and its density density $\rho(\mathbf{r}, t)$ at point $\mathbf{r}$ and time t in a fluid flow.

First, at each instant t and an arbitrary point $\mathbf{r}$, one can take a small region $\mathcal{D}$ centred at $\mathbf{r}$ with its volume be denoted by $\tau_{\mathcal{D}}$; see Figure 1.2. Let $N_{\mathcal{D}}$ and m_0 denote the number of molecules within the region $\mathcal{D}$, and the mass of an individual molecule respectively, where we assume that all the molecules in the system are identical but the ensuing arguments

can easily be extended to a mixture of different molecules. Then density $\rho(\mathbf{r}, t)$ may be defined from *microscopic point of view* as

$$\rho(\mathbf{r}, t; \mathcal{D}) = \frac{m_0 N_{\mathcal{D}}}{\tau_{\mathcal{D}}}. \tag{1.3}$$

This value would depend on the shape and size of the region (as indicated in Figure 1.3) if the region or ℓ is too small, and the variation of $m_{\mathcal{D}}/\tau_{\mathcal{D}}$ with ℓ is quite complex. However, it is known from statistical thermodynamics that the macroscopic quantities are not influenced by random fluctuations provided that the region is large enough to contain sufficiently many molecules ($N_{\mathcal{D}} \gg 1$) and sufficient collisions, i.e. $\ell \gg \lambda$. The values of ρ obtained using different regions $\mathcal{D}$ and $\mathcal{D}'$ approach the same *plateau*, independent of the shape and size of $\mathcal{D}$ as Figure 1.3 illustrates. With this condition and the consequence, formula (1.3) defines a *point-wise* quantity, which can expressed in the form of 'limit',

$$\rho(\mathbf{r}, t) = \lim_{N_{\mathcal{D}} \to \infty} \frac{m_0 N_{\mathcal{D}}}{\tau_{\mathcal{D}}} = \lim_{\ell \to \infty} \frac{m_0 N_{\mathcal{D}}}{\tau_{\mathcal{D}}}. \tag{1.4}$$

Here that the notation "$N_{\mathcal{D}} \to \infty$" does not actually imply that $N_{\mathcal{D}}$, or equivalently the region size ℓ, is indefinitely large. Rather, it means that $\ell \gg \lambda$ so that the value of ρ

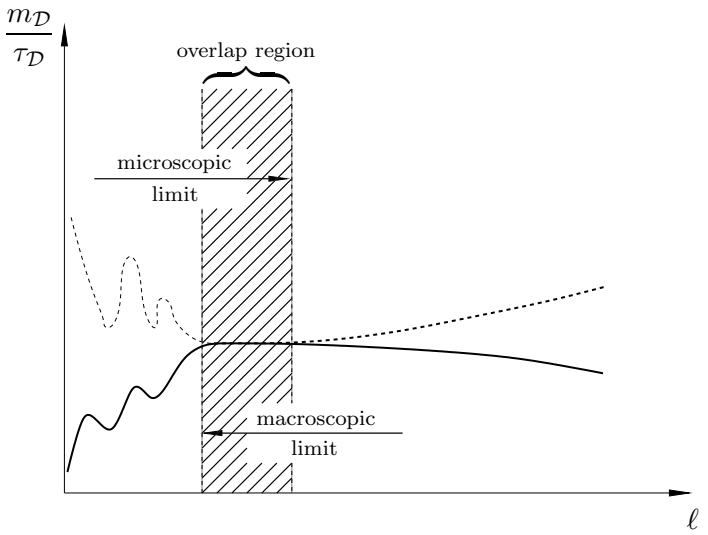

Figure 1.3: Variations of $m_{\mathcal{D}}/\tau_{\mathcal{D}}$ for different possible shapes of region $\mathcal{D}$. Here the solid and dashed lines represent the solid and dashed shapes of region $\mathcal{D}$ in Figure 1.2.

becomes independent of the size and shape of the region, and this value can be attached to a fluid particle, which occupies a geometric point when $\ell \ll L$.

Likewise, at each instant t we can define the *velocity of the fluid particle* $\mathbf{V}$ at $\mathbf{r}$ as

$$\mathbf{V}(\mathbf{r}, t) = \lim_{N_{\mathcal{D}} \to \infty} \frac{\sum m_0 \mathbf{v}_m}{m_{\mathcal{D}}} = \lim_{\ell \to \infty} \frac{\sum m_0 \mathbf{v}_m}{m_{\mathcal{D}}}, \tag{1.5}$$

where $m_{\mathcal{D}} = m_0 \tau_{\mathcal{D}}$ denotes the total mass of the molecules enclosed by $\mathcal{D}$.

The process leading to definitions (1.4) and (1.5) is called the *microscopic limit* or *coarse graining*.

Quizz: Consider a mixture consisting of s number of different molecules with masses m_1, m_2, ..., m_s. Define the density and velocity of a fluid particle.

The averaged quantities defined in terms of the microscopic ones are those measured by a macroscopic sensor that has a fine but nevertheless finite spatial resolution, because what such a sensor measures is the averaged quantities over the volume that the sensor occupies, and these quantities can be considered as being evaluated at a point as the size of volume is reduced. Let us now look at how such quantities at a point are defined in the *macroscopic limit*, taking the density for illustration purpose.

The density ρ is defined as the ratio of the mass $m_{\mathcal{D}}$ to the volume $\tau_{\mathcal{D}}$ contained in a region $\mathcal{D}$ inside the flow. If there were no variation of density throughout the flow field then the region $\mathcal{D}$ could be chosen arbitrarily. However, many fluids of practical interest are compressible and undergo density changes as they move. For example, for the situation shown in Figure 1.2, the fluid experiences deceleration near the front part of the sphere as it approaches from upstream, resulting in a process of compression. As the fluid subsequently moves around the sphere, it undergoes acceleration and a process of expansion. This is followed by a second compression occurring as the fluid decelerates near the rear portion of the sphere. The characteristic length scale associated with these variations coincides with the diameter L of the sphere.

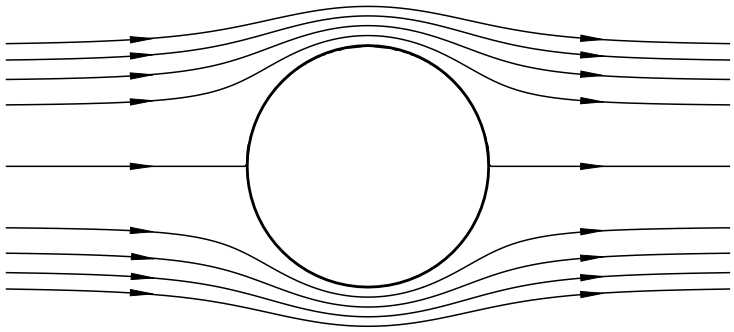

We define the density at an observation point in the flow, denoted by the vector $\mathbf{r}$ in Figure 1.2. This point is surrounded by region $\mathcal{D}$. The averaged density at time t is then evaluated as

$$\rho(\mathbf{r}, t; \mathcal{D}) = \frac{m_{\mathcal{D}}}{\tau_{\mathcal{D}}}. \tag{1.6}$$

When ℓ is comparable to the body scale L, $m_{\mathcal{D}}/\tau_{\mathcal{D}}$ would be dependent on the shape and size of region $\mathcal{D}$ due to the variation on the scale L (Figure 1.3). The dependence becomes progressively weaker as the region $\mathcal{D}$ is made smaller. One may expect that the value $\frac{m_{\mathcal{D}}}{\tau_{\mathcal{D}}}$ becomes independent of the region and a point-wise density may then be defined; this can be expressed in the form

$$\rho(\mathbf{r}, t) = \lim_{\ell \to 0} \frac{m_{\mathcal{D}}}{\tau_{\mathcal{D}}}. \tag{1.7}$$

The question of whether, or in which sense, the limit in equation (1.7) exists is crucial to the concept of a continuum. For a fluid medium which is sufficiently dense, the apparent density as measured with various shapes of region $\mathcal{D}$ approach the same plateau as $\tau_{\mathcal{D}}$ shrinks to the observation point $\mathbf{r}$, thereby indicating the existence of the limit in equation (1.7). However, this limit is only an intermediate *macroscopic limit* since further decrease in region $\mathcal{D}$ eventually reveals complex fluctuations in the apparent density which are associated with chaotic motions at the molecular level (Figure 1.3); by this stage $\tau_{\mathcal{D}}$ is so small, or ℓ is comparable with λ, that any measurement of $m_{\mathcal{D}}$ is strongly dependent on the number of molecules which happen to be in $\mathcal{D}$ at instant t.

Thus in the microscopic limit (1.4) or (1.5), the limit' $\ell \to \infty$' refers to $\ell/\lambda \to \infty$ but subject to $\ell \ll L$, while in the macroscopic (1.7), the limit '$\ell \to 0$' refers to $\ell/L \to 0$ but subject $\ell \gg \lambda$, and the two sets of limits exist only on the intermediate scale,

$$\lambda \ll \ell \ll L. \tag{1.8}$$

In this *overlapping region*, the two sets of limits, (1.4) and (1.7), give the same result (see Figure 1.3).

In summary, in the continuum mechanical description of fluid motion, the entire flow field is envisaged as being continuously filled with fluid particles; in addition all quantities describing the dynamic and thermodynamic characteristics of the fluid particles, such as the velocity vector $\mathbf{V}(\mathbf{r}, t)$, pressure $p(\mathbf{r}, t)$, density $\rho(\mathbf{r}, t)$, temperature $T(\mathbf{r}, t)$, etc., are considered to be continuous and smooth functions of the spatial coordinates $\mathbf{r} = (x, y, z)$.

2 Forces Acting on a Fluid

In order to establish the governing equations of fluid flows, it is of course necessary to consider the forces acting on a moving fluid. All possible forces may be subdivided into two classes, ***body forces*** and ***surface forces***.

A body force acts at each point in the flow field. A representative of body forces is the gravity force. Recall that any material body of mass m placed in the Earth's gravity field experiences a force

$$\mathbf{F} = m\mathbf{g},$$

where $\mathbf{g}$ is the gravity acceleration vector directed vertically downwards. Near the Earth's surface $|\mathbf{g}| = 9.8\, m/s^2$.

In fluid dynamics, one deals with a mass *continuously distributed* in space, and so it is convenient to express the body force $\mathbf{F}$ in a *local* form, and this is done through its density distribution vector $\mathbf{f}(\mathbf{r}, t)$. The latter is defined as a *body force per unit mass* and may be expressed in the form of the limit

$$\mathbf{f}(\mathbf{r}, t) = \lim_{\ell \to 0} \frac{\mathbf{F}_{\mathcal{D}}}{m_{\mathcal{D}}}, \tag{2.1}$$

where $\mathbf{F}_{\mathcal{D}}$ is the force acting on the fluid contained in a small region $\mathcal{D}$ whose characteristic length scale is denoted, as before, by ℓ, with the mass of the fluid inside $\mathcal{D}$ being $m_{\mathcal{D}}$. As $m_{\mathcal{D}} = \rho\tau_{\mathcal{D}}$, we can also write

$$\mathbf{f}(\mathbf{r}, t) = \lim_{\ell \to 0} \frac{\mathbf{F}_{\mathcal{D}}}{\rho\, \tau_{\mathcal{D}}} = \frac{1}{\rho} \lim_{\tau_{\mathcal{D}} \to 0} \frac{\mathbf{F}_{\mathcal{D}}}{\tau_{\mathcal{D}}}. \tag{2.2}$$

As the body forces act on volume elements of a fluid, they are also referred to as *volume forces*. For the gravitational force, vector $\mathbf{f}(\mathbf{r}, t)$ is simply

$$\mathbf{f}(\mathbf{r}, t) = \mathbf{g}.$$

Another common body force is the *electro-magnetic force*, which arises when an *electrically conducting fluid* is moving in a magnetic field. The branch of fluid dynamics that

studies such flows is called *magneto-hydrodynamics*. The interaction of an electric current in a fluid flow with magnetic field results in the volume force, known as the *Lorentz force*,

$$\mathbf{f} = \frac{1}{\rho}\,[\mathbf{j} \times \mathbf{B}].$$

Here vectors $\mathbf{j}$ and $\mathbf{B}$ are the electric current density and magnetic field, respectively.

In certain circumstances, the so-called *inertial forces* appear as body forces. An example of inertial force is the *Coriolis force*. This *apparent force* enters the governing equations when a fluid motion is considered in a rotating coordinate system, which is convenient, for example, when studying flows through the compressor and turbine blades inside a jet engine. For a fluid motion considered in a coordinate system $Oxyz$ which rotates with a *constant* angular velocity $\mathbf{\Omega}$ around axis OO' passing through the coordinate origin O, the inertial force is calculated as

$$\mathbf{f} = \big[(\mathbf{\Omega} \times \mathbf{r}) \times \mathbf{\Omega}\big] + 2[\mathbf{V} \times \mathbf{\Omega}],$$

where $\mathbf{r}$ and $\mathbf{V}$ denote respectively the position and velocity relative to the rotating frame. The first term on the right-hand side is referred to as *centrifugal force*, which appears even though there is no motion relative to the rotating frame, and the second term represents the *Coriolis force*, which appears only when there is a relative motion, i.e. when the velocity $\mathbf{V} \neq 0$.

The Surface Forces

In the other group are the surface forces, and they are exerted on a surface in the flow field by another part of the fluid, or by a solid surface. Surface forces exist in the form of the *pressure* and *internal viscous friction*. They play an important role in fluid flows, representing the means by which the fluid particles "communicate" with one another. The importance of the pressure forces in a moving fluid was first recognised by Euler (1757), who not only derived the differential equations for inviscid fluid motion, known as Euler equations, but also put forward a new *non-collision* concept of a flow over a rigid body. In the earlier concept, called the "Newtonian model", it was supposed that all fluid particles move towards a body along the straight trajectories and exert a force on the body by simple collision with the body surface (see Figure 2.1a). In reality the interaction of a fluid flow with a rigid body always leads to the pressure increase in front of the body, making the fluid particles to deviate from the straight-line motion and to adjust their trajectories in such a way that they smoothly flow around the body surface as is shown in Figure 2.1(b).

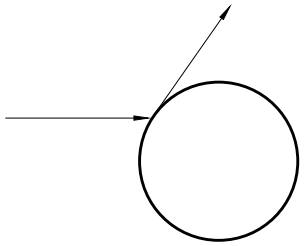

(a) Interaction of fluid particles with a rigid body surface according to the "Newtonian model".

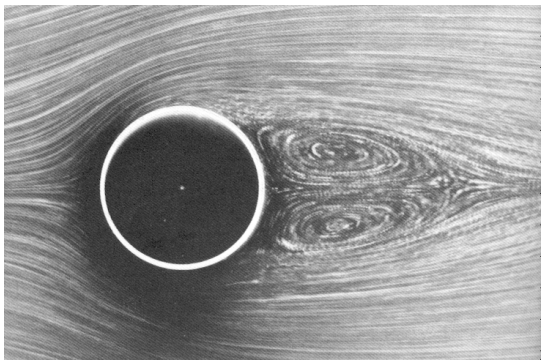

(b) Visualization of the cylinder flow by Tadeda (1956); $Re = 26$.

Figure 2.1: Comparison of the "Newtonian model" with a real flow past a circular cylinder.

Microscopic origin of surface forces

The surface forces have direct molecular origin and are produced by the interaction of molecules. The process of the interaction is better understood in gases. Gas molecules spend most of their life flying freely in space. They interact with each other primarily via collisions, in the course of which they change their velocities and directions of flight. Since the characteristic time of the collision is much smaller than the mean flight time between collisions, we do not need to describe the collision process in detail. In order to determine the surface forces in gases, it suffices to know only the result of the collisions, more exactly, the *rate of the momentum exchange among molecules* if the force on a surface in the bulk of the gas, or between gas molecules and a rigid body, is to be found.

Figure 2.2(a) illustrates what happens when molecule a crosses an imaginary surface SS' in a gas medium and after colliding with molecule b on the other side of the surface

is reflected back into the region above SS'. In this process, there is momentum change, and the rate of this change manifests as a force according to Newton's Second Law. For one collision, if the resulting change of the molecule velocity is $\Delta \mathbf{v}_m$, and the resulting force would be $m_0 \Delta \mathbf{v}_m / \Delta t$, where it may be argued that $\Delta t = O(\lambda / v_m)$ with v_m being the typical molecule velocity. The force exerted on the SS' is an integrated effect over all molecules crossing it,

$$\sum m_0 \Delta \mathbf{v}_m / \Delta t.$$

If the gas is at rest, then averaging over a large number of molecules results in the pressure force acting perpendicular to surface SS'.

If a gas is moving, then in addition to the pressure there is also a tangential force acting along SS'. It is known as the shear force and is attributed to 'internal viscosity' or 'stickiness' of the fluid. Figure 2.2(b) illustrates on the molecular scale how this force is formed. Suppose that the average velocity of molecules in region 1 above the surface SS'

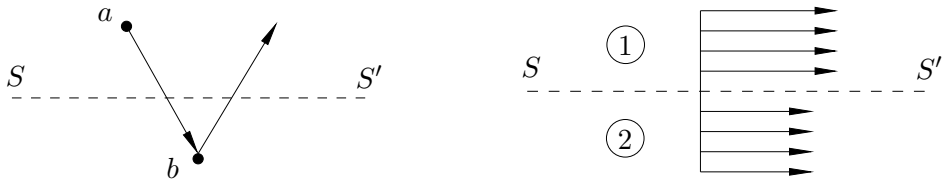

(a) Pressure production. (b) Shear stress production.

Figure 2.2: The origin of surface forces.

is larger than that in region 2 below SS', as shown by arrows in Figure 2.2(b). Suppose further that a set of molecules from region 1 migrate in their Brownian motion into the region 2. When in region 2 they have to adjust their average velocity to that of the surrounding medium, which is achieved through collisions of molecules. As a result, a certain amount of momentum is 'transmitted' to the gas in region 2. Overall such actions cause the gas in region 2 to move faster to smooth out the original velocity difference and hence are equivalent to a tangential force between regions 1 and 2. On the macroscopic scale, the force can be modelled as 'internal viscosity' of the fluid.

Molecules in liquids are "packed" much closer to each other, in fact, so close that each of them appears to be under the permanent influence of a number of surrounding molecules. Consequently, the surface forces in liquid media are dependent not only on the mean velocity of molecules in their thermal motion, but also on the manner by which they are composed in a liquid as well as on the way in which the intermolecular forces vary with the distance between molecules.

In both cases (gases or liquids), the surface forces are created by "short-range" processes taking place in a very thin layer near the surface of a body placed in a flow or an imaginary surface drawn through the bulk of the fluid. The thickness of the layer is of the order of the molecular mean free path, λ. Therefore, as $Kn = \lambda / L \to 0$ this layer appears as a surface viewed on the macroscopic scale L, and the effects of intermolecular interactions, being considered from the macroscopic point of view, turns into the true surface forces.

Stress and its representation

Again instead of a surface force, we shall be dealing with its density, referred to as the ***stress***. The formal definition of the stress applicable for any motion of a fluid may be

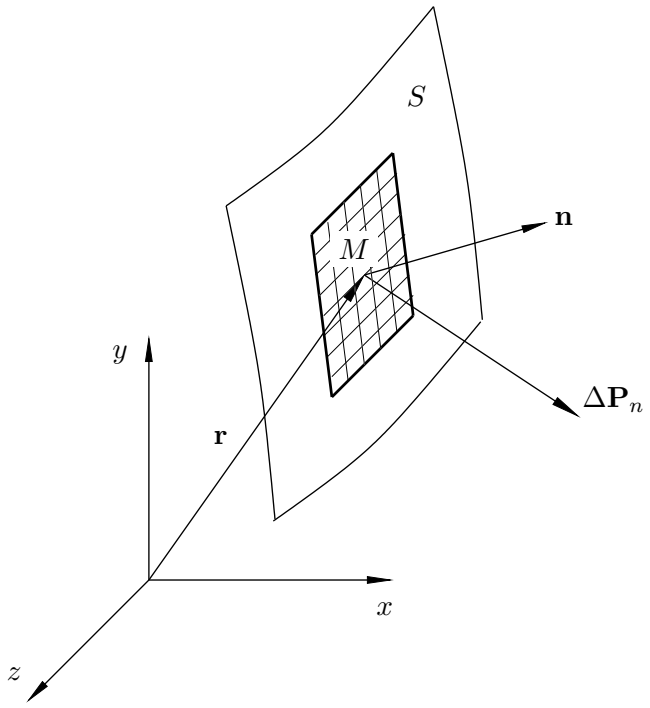

Figure 2.3: The surface element used in (2.1) to define the stress $\mathbf{p}_n$.

introduced as follows. Let M be a point where the stress is to be defined. The position of this point is defined by the position vector $\mathbf{r}$, as shown in Figure 2.3. We draw a surface S through M and choose one side of S to be its *front side*; correspondingly, the other side of S will be called its *rear* side. The unit vector $\mathbf{n}$ normal to S is introduced in such a way that it points the fluid on the *front side* of S, and serves here to define the orientation of surface S.

Let us consider a small element of surface S whose area is ΔS (it is shown in Figure 2.3 as squires ruled region), and denote by $\Delta\mathbf{P}_n$ the surface force that the fluid on the front side of S exerts through ΔS on the fluid on the rear side of S[†]. Let us further assume that the element ΔS shrinks to point M. The ***stress*** is a vector quantity defined by the limit

$$\mathbf{p}_n = \lim_{\Delta S \to 0} \frac{\Delta \mathbf{P}_n}{\Delta S}. \tag{2.1}$$

Thus simply speaking, stress is surface per unit surface area. Here the suffix n is used to indicate that the stress vector $\mathbf{p}_n$ is dependent not only on the location of the point M, but also on the orientation of the surface S drawn through M. We shall now demonstrate that the stress, $\mathbf{p}_n$, can always be expressed in terms of the nine components of the so called *stress tensor* and the unit normal direction of the surface. The stress tensor is a more fundamental quantity than the stress itself as it independent of the orientation.

To introduce the notion of the stress tensor, let us consider the special case, where a plane surface S_x is in the $x-y$ plane in a Cartesian coordinate system (x, y, z), and its normal direction is in the x-axis. We shall choose the side of S_x facing positive direction of the x-axis as its front side. The stress on S_x is denoted by $\mathbf{p}_x$ (or $\mathbf{p}_1$ in the system using numbers as subscripts for components). Like any three-dimensional vector quantity,

[†]Note that by Newton's Third Law, the force acting through ΔS on the fluid on the front side of S has the same magnitude but opposite direction, i.e. is equal to $-\Delta\mathbf{P}_n$.

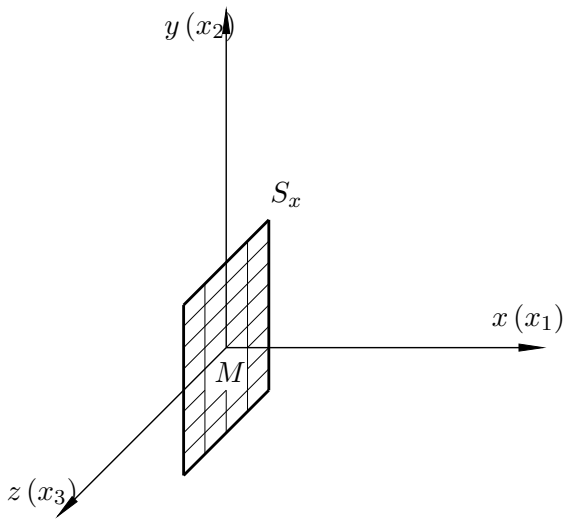

Figure 2.4: The surface element for defining $\mathbf{p}_x$ or $(\mathbf{p}_1)$.

it may be represented in the coordinate decomposition form

$$\mathbf{p}_x = p_{xx}\mathbf{i} + p_{xy}\mathbf{j} + p_{xz}\mathbf{k}, \tag{2.2}$$

or in the system using numbers as subscripts for components.

$$\mathbf{p}_1 = p_{11}\mathbf{i} + p_{12}\mathbf{j} + p_{13}\mathbf{k},$$

where $\mathbf{i}$, $\mathbf{j}$ and $\mathbf{k}$ are the unit coordinate vectors, with p_{xx}, p_{xy} and p_{xz} (or p_{11}, p_{12} and p_{13}) being the components of $\mathbf{p}_x$ $(\mathbf{p}_1)$ in these directions respectively.

Similarly, one can consider surface S_y perpendicular to the y axis and surface S_z perpendicular to the z-axis with the corresponding stresses being $\mathbf{p}_y$ and $\mathbf{p}_z$ respectively. Their coordinate decompositions are written as

$$\begin{aligned} \mathbf{p}_y &= p_{yx}\mathbf{i} + p_{yy}\mathbf{j} + p_{yz}\mathbf{k}, \\ \mathbf{p}_z &= p_{zx}\mathbf{i} + p_{zy}\mathbf{j} + p_{zz}\mathbf{k}. \end{aligned} \tag{2.3}$$

The nine components of $\mathbf{p}_x$, $\mathbf{p}_y$ and $\mathbf{p}_z$ are arrange into a 3×3 matrix

$$\mathcal{P} = \begin{pmatrix} p_{xx} & p_{xy} & p_{xz} \\ p_{yx} & p_{yy} & p_{yz} \\ p_{zx} & p_{zy} & p_{zz} \end{pmatrix} = \begin{pmatrix} p_{11} & p_{12} & p_{13} \\ p_{21} & p_{22} & p_{23} \\ p_{33} & p_{32} & p_{33} \end{pmatrix}, \tag{2.4}$$

which is called the ***stress tensor***, a central concept in continuum mechanics. Here p_{ij} stands for the j-th component of the stress $\mathbf{p}_i$ on the plane normal to $\mathbf{i}$[‡]. The diagonal components of the stress tensor are called the ***normal stresses***. For example, p_{xx} represents the x-component of the stress (2.2) acting on a surface perpendicular to the x-axis. Two other terms in (2.2) and correspondingly all the non-diagonal components of the stress tensor (2.4) are the ***tangential*** or ***shear stresses***.

We shall now deduce a formula that expresses the stress $\mathbf{p}_n$ on an arbitrarily oriented surface via the components of the stress tensor $\mathcal{P}$. For this purpose, we consider a fluid elements inside a small tetrahedron $MABC$ (see Figure 2.5). Let the area of the front face

[‡]The order of the subscripts to designate the components is the same as in the textbook of Ruban & Gajjar (2014) but differs from many other textbook. This difference disappears when $\mathcal{P}$ is shown to be symmetric.

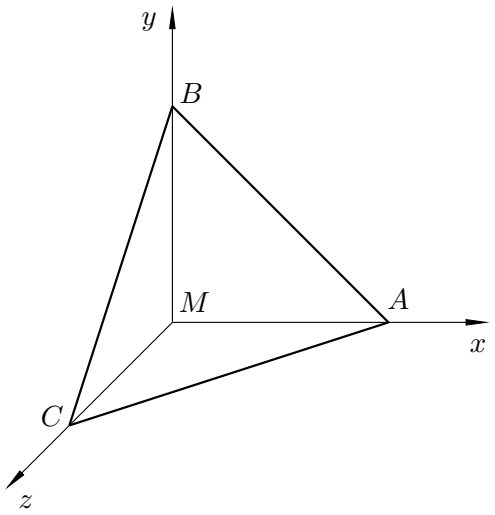

Figure 2.5: A fluid element in the shape of tetrahedron.

ABC be ΔS_n, and its outward unit normal direction is $\mathbf{n}$. The stress on this surface, $\mathbf{p}_n$, is to be expressed in terms of $\mathcal{P}$ and $\mathbf{n}$. The three other faces that are perpendicular to x-, y- and z-axes have areas ΔS_x, ΔS_y and ΔS_z respectively. These areas are the projection of S_n to the three axes, and so

$$\Delta S_x = n_x \Delta S_n, \qquad \Delta S_y = n_y \Delta S_n, \qquad \Delta S_z = n_z \Delta S_n. \tag{2.5}$$

We now apply the Newton's Second Law to the fluid element contained inside the tetrahedron $MABC$. If $\mathbf{V}$ is the velocity of the fluid element and ρ the density then

$$\rho \tau_{\mathcal{D}} \frac{d\mathbf{V}}{dt} = \rho \tau_{\mathcal{D}} \mathbf{f} + \mathbf{p}_n \Delta S_n - \mathbf{p}_x \Delta S_x - \mathbf{p}_y \Delta S_y - \mathbf{p}_z \Delta S_z. \tag{2.6}$$

Here $\tau_{\mathcal{D}}$ denotes, as before, the volume of the fluid element considered. When calculating the force acting on the fluid element through face ABM, we have been taken into account the fact that the fluid element is situated in front of ΔS_x. Meanwhile, $\mathbf{p}_x$ was introduced as the stress by the fluid on the front side of S_x (see Figure 2.4) acts upon the fluid behind S_x. Since we need to consider the surface force which acts precisely in the opposite direction, the corresponding term $\mathbf{p}_x \Delta S_x$ in (2.10) is taken with minus. The same arguments, obviously, apply to $\mathbf{p}_y \Delta S_y$ and $\mathbf{p}_z \Delta S_z$.

It is easily seen that with ℓ denoting the characteristic linear size of tetrahedron $MABC$, the left-hand side of equation (2.10) as well as the first term on the right-hand side may be estimated as $O(\ell^3)$. The rest of the terms are proportional to ℓ^2. Therefore, in the limit $\ell \to 0$, when tetrahedron $MABC$ shrinks to point M equation (2.10) reduces to a balance of the surface forces

$$\mathbf{p}_n \Delta S_n - \mathbf{p}_x \Delta S_x - \mathbf{p}_y \Delta S_y - \mathbf{p}_z \Delta S_z = 0. \tag{2.7}$$

Substitution of (2.5) into (2.7) yields

$$\mathbf{p}_n = n_x \mathbf{p}_x + n_y \mathbf{p}_y + n_z \mathbf{p}_z. \tag{2.8}$$

After using (2.2) and (2.3) in (2.8), the coordinate decomposition of the resulting equation reads

$$
\begin{aligned}
p_{nx} &= n_x p_{xx} + n_y p_{yx} + n_z p_{zx}, \\
p_{ny} &= n_x p_{xy} + n_y p_{yy} + n_z p_{zy}, \\
p_{nz} &= n_x p_{xz} + n_y p_{yz} + n_z p_{zz},
\end{aligned}
$$

or in a more compact tensor form

$$
\mathbf{p}_n = \mathcal{P}^{\mathrm{T}} \cdot \mathbf{n} \quad \text{i.e.} \quad (\mathbf{p}_n)_i = p_{ji} n_j, \tag{2.9}
$$

either of which shows that the stress on an arbitrary surface S through a point M can be expressed in terms of the normal direction of S and the *nine* components of the stress tensor $\mathcal{P}$ at point M.

Figure 2.6: Illustration of moments acting on a fluid element.

We now show that $\mathcal{P}$ is *symmetric* (i.e. $p_{ij} = p_{ji}$) by considering the conservation of angular momentum. For a fluid element in the region $\mathcal{D}$ enclosed by surface S, this can be expressed mathematically as

$$
\frac{d}{dt}\int_{\mathcal{D}} \rho\, \mathbf{r}' \times \mathbf{V} d\tau \;\; = \int_{\mathcal{D}} \rho\, \mathbf{r}' \times \mathbf{f} d\tau + \int_S \mathbf{r} \times \mathbf{p}_n ds. \tag{2.10}
$$

For a small element with dimension ℓ. The two volume integrals in (2.10) are of $O(\ell^4)$, whilst the last term, the surface integral, is $O(\ell^3)$, and so in the limit $\ell \to 0$ it must vanish,

$$
I \equiv \int_S \mathbf{r} \times \mathbf{p}_n ds = 0.
$$

The i-th component is

$$
I_i \equiv \int_S \epsilon_{ijk} x_j (\mathbf{p}_n)_k ds = \int_S \epsilon_{ijk}\, x_j\, p_{lk}\, n_l ds = 0,
$$

where use has been made of (2.9). Noting that the integrand in the last integral is the form of a scale product with $\mathbf{n}$ and a vector whose l-the component is $\epsilon_{ijk}\, x_j\, p_{lk}$, we apply the *divergence theorem* to convert it to a volume integral,

$$
I_i = \int_{\mathcal{D}} \frac{\partial \epsilon_{ijk}\, x_j\, p_{lk}}{\partial x_l} d\tau = \int_{\mathcal{D}} \epsilon_{ijk} \Big[\delta_{jl} p_{lk} + x_j \frac{\partial p_{lk}}{\partial x_l} \Big] d\tau = 0.
$$

Note the second term on the right-hand side is $O(\ell^4)$ while the first is $O(\ell^3)$, and so

$$\int_{\mathcal{D}} \epsilon_{ijk}\delta_{jl}p_{lk}d\tau = \int_{\mathcal{D}} \epsilon_{ijk}p_{jk}d\tau = 0.$$

Since the volume is arbitrary, the integrand must vanish

$$\epsilon_{ijk}p_{jk} = 0,$$

from which we can (with the detail left as an exercise) deduce that

$$p_{kj} = p_{jk}.$$

It follows that there are only *six* unknowns in $\mathcal{P}$. With symmetry of the stress tensor established, the formula (2.9) is equivalent to

$$\mathbf{p}_n = \mathcal{P}\cdot\mathbf{n} \quad \text{i.e.} \quad (\mathbf{p}_n)_i = p_{ij}\,n_j, \tag{2.11}$$

which will be the form to be used in this course. As is indicated by the second relation in (2.11), the operation $\mathcal{P}\cdot\mathbf{n}$ is the same as the multiplication of a matrix $\mathcal{P}$ with a column vector $\mathbf{n}$, or equivalently, the scalar product of each row vector in $\mathcal{P}$ with $\mathbf{n}$.

The Concept of a Fluid

The term *fluid* is generally used to describe either a liquid or a gas since they share a common feature that makes it possible to construct a unified dynamical theory, universally valid for a large range of liquids and gases. This common property is referred to as *fluidity*, which is broadly defined as a tendency of either medium to flow under action of any external force[§], no matter how small; in other words, a fluid in general moves and deforms continuously as long as an external force is applied. This behaviour may be contrasted with that of a solid, which when exposed to external forces will undergo a certain deformation, but then internal stresses will develop in the solid which will resist further deformation. As a result the solid will assume a new state as shown in Figure 2.7.

In a fluid at rest, the only surface force possible in a fluid at rest is the pressure p. It acts equally in all the directions, a result known as ***Pascal's principle***. Mathematically, this means that the stress tensor is of the simple diagonal form,

$$\mathcal{P} = \begin{pmatrix} -p & 0 & 0 \\ 0 & -p & 0 \\ 0 & 0 & -p \end{pmatrix}. \tag{2.12}$$

With (2.12) equation (2.11) reduces to

$$\mathbf{p}_n = -p\,\mathbf{n}, \tag{2.13}$$

where $p > 0$ and the negative sign reflects the fact that two portions of the fluid interact with each other through 'pushing'. Specifically, the pressure force acting upon the fluid behind the surface S_x of Figure 2.4 is perpendicular to this surface and directed opposite

[§]The only exception is the pressure; when it is distributed evenly in space it does not cause a fluid to move.

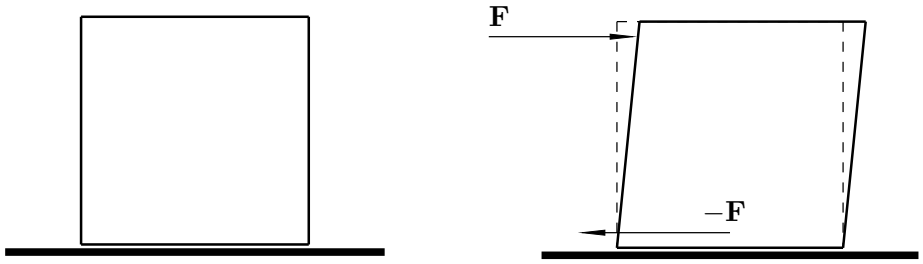

(a) Original form of a solid sample.

(b) Deformation of the sample under action of an external force **F** and reaction of the ground $-\mathbf{F}$.

Figure 2.7: Deformation of a solid body with rectangular cross-section placed on a flat ground.

to the x-axis. This suggests that the components of vector $\mathbf{p}_x$ as given by (2.2) may be written as

$$p_{xx} = -p, \qquad p_{xy} = 0, \qquad p_{xz} = 0.$$

Similarly, the components of vectors $\mathbf{p}_y$ and $\mathbf{p}_z$ may be written for a fluid at rest as

$$\begin{aligned} &p_{yx} = 0, \qquad p_{yy} = -p, \qquad p_{yz} = 0, \\ &p_{zx} = 0, \qquad p_{zy} = 0, \qquad p_{xz} = -p. \end{aligned}$$

Shear stresses would in general arise if portions of the fluid are moving relative to one another. Such stresses are associated with the internal viscosity of fluids and are called *viscous forces*. If the internal viscosity is neglected (as an approximation in the theory for the so-called 'ideal fluids'), then (2.12) and (2.13) would apply as well even when such a hypothetical fluid is moving. However, real fluids do have internal viscosity, which must be taken into accounted in order to describe their motions correctly. Characterising the shear stress in terms of the flow motion (or deformation of fluid element) is a key task in developing the mathematical theory for viscous flows. We will take on that in Lecture 6.

References

[1] Taneda, S. (1956). *J. Phys. Soc. Jpn.* **11**, 302–307.

Lecture 3

Kinematics of the Flow Field

Kinematics of the flow field is concerned with how to describe the flow motion itself, but not with the cause of the motion, which is the focus of *dynamics*, a core issue to be discussed in the coming lectures. There exist two distinct ways to describe the motion of a continuum medium in fluid dynamics, namely, ***Lagrangian*** and ***Eulerian*** descriptions.

Lagrangian approach

This approach traces each fluid particle, an idea similar to that of classical mechanics where one considers a set of material particles moving in space. In the latter problem, the number of particles is finite and so an integer number i is ascribed to each particle as its identifier, and its position with respect to a suitably chosen coordinate system (x, y, z) is given by the position vector $\mathbf{r}_i(t) = \big(x_i(t),\, y_i(t),\, z_i(t)\big)$, which is considered a function of at time t.

As in the classical mechanics, for a fluid flow the primary dependent variable is taken to be the position $\mathbf{r}(t)$. The difference and the difficult is that in a continuum model fluid particles are continuously distributed throughout the flow field, and cannot be enumerated. The immediate question is:

how can each and every fluid particle be uniquely identified, i.e. be given a unique identifier?

In the Lagrangian approach, a particle identified by its location $\mathbf{r}_0$ in the field at some initial instant $t = t_0$. This is done in the following way. Let $\mathcal{D}_0$ be a region fixed in the

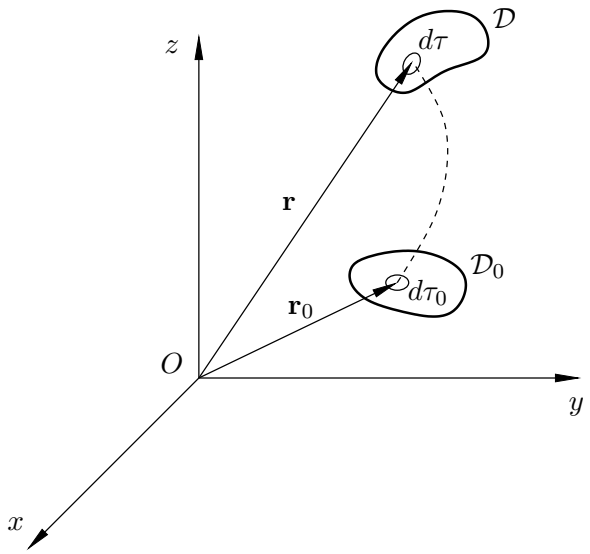

Figure 3.1: Lagrangian description of the flow field.

coordinate system (x, y, z) with fluid continually passing through it (see Figure 3.1). We shall consider a set composed of all fluid particles that happen to be inside $\mathcal{D}_0$ at an initial instant $t = t_0$. Each particle can uniquely be identified by its position $\mathbf{r}_0 \in \mathcal{D}_0$ at t_0; as far

as identifying the particle is concerned, $\mathbf{r}_0$ and t_0 act rather like the use of 'place of birth' and 'time of birth' to identify a person.

As time increases, a fluid particle moves in space and its location may be expressed in the form

$$\mathbf{r} = \mathbf{r}(t, \mathbf{r}_0; t_0) = \mathbf{r}(t, \mathbf{r}_0), \tag{3.1}$$

where in the last expression for brevity the dependence on t_0 is not explicitly expressed when no ambiguity is caused. Equation (3.1) signifies that $\mathbf{r}$ is a continuous function of two independent variables, time t and initial position vector $\mathbf{r}_0$. If the second argument $\mathbf{r}_0$ in (3.1) is fixed and time t increases, then one traces a particular particle and records its trajectory as is indicated by the dotted line in Figure 3.1. With $\mathbf{r}_0$ varying continuously in $\mathcal{D}_0$, all particles are traced.

In Lagrangian approach, in addition to the position vector (3.1) all other fluid quantities are considered as functions of t and $\mathbf{r}_0$. For example, the fluid density ρ and temperature T are written as

$$\rho = \rho(t, \mathbf{r}_0), \quad T = T(t, \mathbf{r}_0). \tag{3.2}$$

If functions $\mathbf{r}(t, \mathbf{r}_0)$, $\rho(t, \mathbf{r}_0)$ and $T(t, \mathbf{r}_0)$ were known, then all other fluid dynamic quantities could easily be obtained from well-known thermodynamic and kinematic relations. For instance, the ***velocity*** and ***acceleration*** of a fluid particle may be determined by differentiating (3.1) with respect to time, viz.

$$\mathbf{V}(t, \mathbf{r}_0) = \frac{\partial \mathbf{r}}{\partial t}\Big|_{\mathbf{r}_0}, \qquad \mathbf{a}(t, \mathbf{r}_0) = \frac{\partial^2 \mathbf{r}}{\partial t^2}\Big|_{\mathbf{r}_0} \tag{3.3}$$

with $\mathbf{r}_0$ fixed.

In order to determine functions (3.1) and (3.2), one of course has to use the conservation laws of mass, momentum and energy. Let us show here how the mass conservation law may be formulated in the Lagrangian variables. Let $\mathcal{D}$ be a region occupied at an instant $t > t_0$ by fluid particles which were in $\mathcal{D}_0$ at t_0. Consider a *small* element of volume $d\tau$ in D that originates from its counterpart $d\tau_0$ in region D_0; see Figure 3.1. Since we are dealing with the same fluid particles, the *law of conservation of mass* states

$$\rho_0 d\tau_0 = \rho d\tau. \tag{3.4}$$

Here ρ_0 and ρ denote the density of the fluid particle at times t_0 and t, respectively.

A relationship between the volumes $d\tau_0$ and $d\tau$ can be established by recalling that equation (3.1) may be interpreted as a *transformation of coordinates*, or mapping, from $\mathbf{r}_0 = (x_0, y_0, z_0)$ to $\mathbf{r} = (x, y, z)$, and vice versa[†]. For such a transformation, the volume elements are known to be related via

$$d\tau = \Big| \underbrace{\frac{\partial(x, y, z)}{\partial(x_0, y_0, z_0)}} \Big| d\tau_0, \tag{3.5}$$

Jacobian matrix of the coordinate transformation

Substitution of (3.5) into (3.4) yields

$$\left| \frac{\partial(x, y, z)}{\partial(x_0, y_0, z_0)} \right| = \frac{\rho_0}{\rho}, \tag{3.6}$$

which is the ***continuity equation*** in the Lagrangian variables.

[†]The viewpoint that Lagrangian trajectories serve as a mapping is very useful and will be employed to prove several fundamental results.

Eulerian Approach

In the *Eulerian description* of the motion, the viewpoint is entirely different. Rather than tracing individual moving fluid particles, the flow quantities are defined at each point $\mathbf{r}$ *fixed* in space, and these quantities vary in general with time t. The primary dependent variables (quantities) to be used to characterise the flow include the velocity vector, density and temperature,

$$\mathbf{V} = \mathbf{V}(t, \mathbf{r}), \quad \rho = \rho(t, \mathbf{r}), \quad T = T(t, \mathbf{r}), \tag{3.7}$$

where the position vector $\mathbf{r} = (x, y, z)$ now serves as *independent variables* as time t does, that is, $\mathbf{V}$, ρ and T are treated as *field quantities*. These quantities are defined by resorting to the corresponding ones in the Lagrangian description as follows. Let $P(t, \mathbf{r})$ represent a field quantity, which may be velocity, density or temperature. Then $P(t, \mathbf{r})$ is defined as the value of the corresponding quantity carried by the fluid particle that happens to reach $\mathbf{r}$ at time t. One may imagine that in the Eulerian description, at each point $\mathbf{r}$ sits an 'observer', who records continuously the property of the fluid particles passing through the observation $\mathbf{r}$. Mathematically, this can be expressed as

$$P(t, \mathbf{r}) = P\big[t, \mathbf{r}(t, \mathbf{r}_0)\big] = P\big[(t, x(t, \mathbf{r}_o), y(t, \mathbf{r}_0), z(t, \mathbf{r}_0)\big], \tag{3.8}$$

which links the quantities in the two frameworks. Specifically, the flow velocity $\mathbf{V}(t, \mathbf{r})$ at point $\mathbf{r}$ and time t takes the velocity of the fluid particle passing the point $\mathbf{r}$ at time t, that is,

$$\mathbf{V}(t, \mathbf{r}) = \mathbf{V}\big[t, \mathbf{r}(t, \mathbf{r}_0)\big] = \mathbf{V}\big[(t, x(t, \mathbf{r}_o), y(t, \mathbf{r}_0), z(t, \mathbf{r}_0)\big]. \tag{3.9}$$

Since a new fluid particle passes through a given point at each instant, the partial derivative of $\mathbf{V}(t, \mathbf{r})$ with respect to t for a fixed $\mathbf{r}$, $\partial \mathbf{V}(t, \mathbf{r})/\partial t$, does not represent the acceleration $\mathbf{a}$ of a fluid particle. More generally, $\partial P(t, \mathbf{r})/\partial t$ does not represent the rate of change of the property for a fixed particle, which will be referred to as *material derivative*. Yet, the latter is often needed, especially in establishing the governing equations of fluid motions since the physical laws are usually stated in terms of material derivatives. We now show how the material derivative of a property (the rate of change for a fixed fluid particle) can be expressed in the Eulerian variables.

We consider first the acceleration, or the rate of change of the velocity of a fluid particle as it passes through the field point $\mathbf{r} = (x, y, z)$. Equation (3.9) is then differentiated with respect to t for a fixed $\mathbf{r}_0$ using the chain rule,

$$\mathbf{a} = \frac{\partial \mathbf{V}}{\partial t} + \frac{\partial \mathbf{V}}{\partial x}\frac{\partial x}{\partial t}\bigg|_{\mathbf{r}_0} + \frac{\partial \mathbf{V}}{\partial y}\frac{\partial y}{\partial t}\bigg|_{\mathbf{r}_0} + \frac{\partial \mathbf{V}}{\partial z}\frac{\partial z}{\partial t}\bigg|_{\mathbf{r}_0}, \tag{3.10}$$

where suffix $\mathbf{r}_0$ indicates that the differentiation is carried out for a fixed fluid particle. Writing the first of equations (3.3) in the coordinate decomposition form we have[‡]

$$u = \frac{\partial x}{\partial t}\bigg|_{\mathbf{r}_0}, \quad v = \frac{\partial y}{\partial t}\bigg|_{\mathbf{r}_0}, \quad w = \frac{\partial z}{\partial t}\bigg|_{\mathbf{r}_0}.$$

Hence (3.10) may be written as

$$\mathbf{a} = \frac{\partial \mathbf{V}}{\partial t} + u\frac{\partial \mathbf{V}}{\partial x} + v\frac{\partial \mathbf{V}}{\partial y} + w\frac{\partial \mathbf{V}}{\partial z}$$

[‡]In fluid dynamics the components of the velocity vector $\mathbf{V}$ are usually denoted by u, v and w.

or

$$\mathbf{a} = \frac{D\mathbf{V}}{Dt} = \frac{\partial \mathbf{V}}{\partial t} + \big(\mathbf{V} \cdot \nabla\big)\mathbf{V}, \tag{3.11}$$

where the differential operator

$$\frac{D}{Dt} = \frac{\partial}{\partial t} + \big(\mathbf{V} \cdot \nabla\big)$$

is called the ***material*** or ***full derivative***. For a general property $P(t, \mathbf{r})$, we have

$$\frac{D}{Dt}P(t, \mathbf{r}) = \frac{\partial P}{\partial t} + \big(\mathbf{V} \cdot \nabla\big)P.$$

The acceleration (3.11) consists of two terms, of which the first term $\partial \mathbf{V}/\partial t$ is called the ***local derivative***. It represents an acceleration due to temporal changes in the velocity field as the fluid particle arrives at the point in question. The second term $(\mathbf{V} \cdot \nabla)\mathbf{V}$ is called the ***convective acceleration*** and is an acceleration due to the fact that the fluid particle is being convected into a point with different velocity. The convective derivative is a scalar product of the velocity vector and the gradient operator, defined by

$$\mathbf{V} = \mathbf{i}u + \mathbf{j}v + \mathbf{k}w, \qquad \nabla = \mathbf{i}\frac{\partial}{\partial x} + \mathbf{j}\frac{\partial}{\partial y} + \mathbf{k}\frac{\partial}{\partial z}$$

where $\mathbf{i}$, $\mathbf{j}$ and $\mathbf{k}$ stand for the unit vectors in the three orthogonal directions of the Cartesian coordinate system.

A flow is called a ***steady flow*** if its velocity field is independent of time, i.e.

$$\mathbf{V} = \mathbf{V}(x, y, z) \quad \text{i.e.} \quad \frac{\partial \mathbf{V}}{\partial t} = 0.$$

Steady flows play an important role in fluid dynamics. Because of the time independence, steady flows present less difficulties for theoretical and experimental investigations. They are, at the same time, of great relevance in applied engineering. Steady flows may be observed, for example, in wind tunnel experiments when in the laboratory coordinate system the velocity at each point of the flow does not change with time t. The flow over an aircraft in cruise flight is also steady for the passengers on board (but is unsteady for an observer on the earth surface).

The notion of a steady flow, obviously, makes sense only in Eulerian description. Time dependence in the Lagrangian trajectory function $\mathbf{r} = \mathbf{r}(t, \mathbf{r}_0)$ may disappear only if there is no fluid motion at all. Even in a flow which is steady from the Eulerian point of view, fluid particles experience acceleration and deceleration in the vicinity of a solid body making the analysis in Lagrangian variables as difficult as it is for non-steady flows. For that reason, Eulerian description is normally more convenient.

Streamlines, Pathlines and Streaklines

Fluid flows are usually investigated using mathematical, experimental and computational tools. In order to characterize fluid flows and also to link theoretical and experimental results, three concepts are introduced, namely, ***streamline***, ***pathline*** and ***streakline***. In particular, these concepts help make the theoretical and computational results 'visual', whereas flow visualisation is rather common technique in laboratory

In the Eulerian description, the primary dependent quantity is the velocity vector field

$$\mathbf{V} = \mathbf{V}(t, \mathbf{r}).$$

To determine the streamline pattern, one first has to choose the time of observation, t, and keeping it *fixed* make use of the following definition:

Definition 3.1: *A line $\mathcal{L}$ (see Figure 3.2) is called a* ***streamline*** *if at each point, M, on this line the velocity vector $\mathbf{V}$ is tangent to $\mathcal{L}$.*

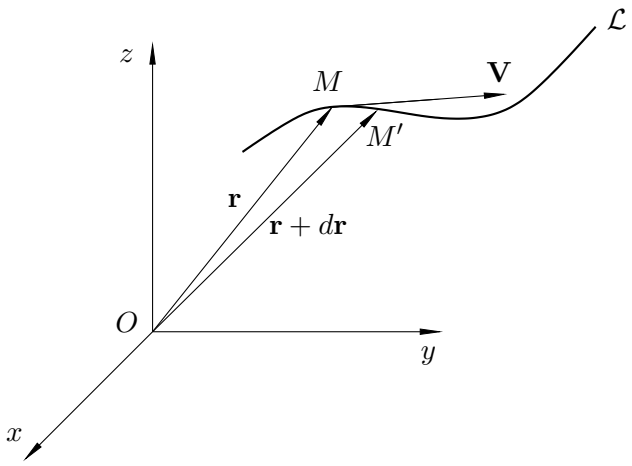

Figure 3.2: A streamline.

The above definition leads to the equations determining the streamline using the given velocity. Let $\mathbf{r}$ be the position vector of point M and $d\mathbf{r}$ be its increment along the streamline $\mathcal{L}$ connecting point M with a neighbouring point M'. Then $d\mathbf{r}$ should be parallel to $\mathbf{V}$ for small enough $|d\mathbf{r}|$. Therefore, the vector product of $d\mathbf{r}$ and $\mathbf{V}$ should be zero,

$$d\mathbf{r} \times \mathbf{V} = 0. \tag{3.12}$$

More explicitly equation (3.12) may be written as

$$d\mathbf{r} \times \mathbf{V} = \begin{vmatrix} \mathbf{i} & \mathbf{j} & \mathbf{k} \\ dx & dy & dz \\ u & v & w \end{vmatrix} =$$

$$= \mathbf{i}(wdy - vdz) + \mathbf{j}(udz - wdx) + \mathbf{k}(vdx - udy) = 0. \tag{3.13}$$

Since each component in (3.13) must be zero, the differentials dx, dy and dz are related to each other by the equations

$$\frac{dx}{u(t,x,y,z)} = \frac{dy}{v(t,x,y,z)} = \frac{dz}{w(t,x,u,z)}, \tag{3.14}$$

where the coordinate arguments x, y, z of the velocity components u, v, w are varying along the streamline considered. Equations (3.14) are integrated for fixed t, implying that a streamline is a *snap shot*. When the flow is unsteady, i.e. $\partial \mathbf{V}/\partial t \neq 0$, streamlines at different instants are different in general. At each instant, there is a streamline passing each point, and flow particles move along the streamlines. This gives an instantaneous picture of the flow field.

Figure 3.3: Illustration of streamline and a streamline tube.

The role of streamlines in characterizing the flow can be appreciated by considering *streamline tube*. Let C be a closed curve in the flow field. Then from each point on C emanates a streamline. Streamlines emanating from all the points on C form a ***streamline tube***. Let σ and σ' be two cross sections of the tube, which enclose, with the tube surface Σ, a closed region $\mathcal{D}$. Let the unit normal vectors of σ and σ' be denoted by $\mathbf{n}$ (pointing out of the region D) and $\mathbf{n}'$ (point into the region D), respectively. Then based on the law of mass conservation, we have

$$\iint_{\sigma} \rho\big(\mathbf{V}\cdot\mathbf{n}\big)\,ds = \iint_{\sigma'} \rho'\big(\mathbf{V}\cdot\mathbf{n}'\big)\,ds,$$

since the left-hand and right-hand sides represent the mass leaving/entering the region D per unit time, while no fluid particles cross the tube surface. Thus a streamline tube acts like a physical tube at each instant. However, the former does change its shape for any unsteady flow.

When the density remains constant, then we have

$$\iint_{\sigma} \big(\mathbf{V}\cdot\mathbf{n}\big)\,ds = \iint_{\sigma'} \big(\mathbf{V}\cdot\mathbf{n}'\big)\,ds.$$

Definition 3.2: *A **pathline** represents the trajectory of a fluid particle.*

With a known velocity field $\mathbf{V}(t,\mathbf{r})$, the equation for a pathline of a particle that is at $\mathbf{r}_0$ when $t = t_0$ is

$$\frac{d\mathbf{r}}{dt} = \mathbf{V}(t,\mathbf{r}) \quad \text{with the initial condition} \quad \mathbf{r}(t_0) = \mathbf{r}_0. \tag{3.15}$$

The ordinary differential equation (3.15) consists of three components

$$\frac{dx}{dt} = u(t,x,y,z), \quad \frac{dy}{dt} = v(t,x,y,z), \quad \frac{dz}{dt} = w(t,x,y,z). \tag{3.16}$$

The solution to the initial-value problem can be written as

$$\mathbf{r}(t) = \mathbf{r}(t, \mathbf{r}_0; t_0) \quad \text{or} \quad \big(x(t), y(t), z(t)\big) = \big(x(t, \mathbf{r}_0; t_0), y(t, \mathbf{r}_0; t_0), z(t, \mathbf{r}_0; t_0)\big). \tag{3.17}$$

The pathline of a fluid particle is given by $\mathbf{r}$ as a function of t. As $\mathbf{r}_0$ is varied continuously, we have a family of pathlines.

Definition 3.3: *A* ***streakline*** *at a* fixed *instant t is a line which consists of all particles passing from the same point at earlier times.*

Mathematically, a streakline passing $\mathbf{r}_0$ is given by $\mathbf{r} = \mathbf{r}(t, \mathbf{r}_0; t_0)$ as *a function of t_0 with $\mathbf{r}_0$ and t fixed*. Clearly, a streakline is snap shot picture.

Figure 3.4: Illustration of a streakline.

Streamlines, pathlines and streaklines are all different concepts for a general unsteady flow. They are related to different means of visualising the flow. When a tiny drop of dye is introduced at a point $\mathbf{r}_0$ instantaneously at t_0, it marks the particle that happens to pass through this point, and the the subsequent positions of this marked particle for $t > t_0$ trace out a pathline. In contrast, if dye starts to be discharge at a point $\mathbf{r}_0$ *continuously* from time t_0, all fluid particles passing through this discharge site will be marked and form a line. A snap-shot photo of the marked particles at any later time $t > t_0$, would give a streakline, which can be described by

$$\mathbf{r} = \mathbf{r}(t, \mathbf{r}_0; \tau) \quad \text{with} \quad t_0 \le \tau \le t$$

as a *function of τ with both t and $\mathbf{r}_0$ fixed* (Figure 3.4). In fluid dynamics, it is more useful to figure out streamlines of the flow, but unfortunately it is harder to visualise them directly in unsteady flows. As a matter of fact, streaklines are sometimes mistaken for streamlines.

The difference between a streamline and pathline is rather obvious by their definitions as the latter involves history of the motion while the former does not. However, since both lines have the feature of being tangent to the local velocity, it is necessary to demonstrate the difference more closely. Let us choose a point in the flow field (in Figure 3.5 it is shown as point M) and draw the streamline and pathline originating from M.

In accordance with their definitions, both the streamline and pathline must follow the direction of the velocity vector. Streamline is a snap shot, and so we take $t = \tau$, the velocity $\mathbf{V}$ at point M and place point M_1 small distance from M in the direction of $\mathbf{V}$. It will be a common point for both the streamline and pathline. Now, if the streamline is to be plotted, the velocity vector $\mathbf{V}_1$ at point M_1 must be taken at the same time $t = \tau$ as at

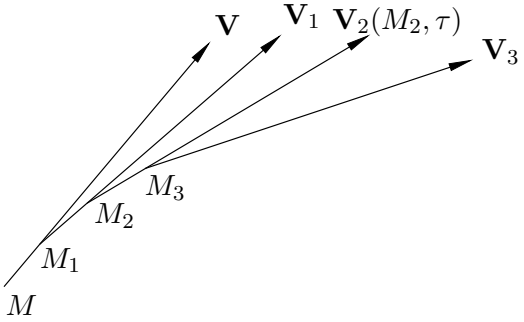

(a) Construction of a streamline (snap shot) at $t = \tau$.

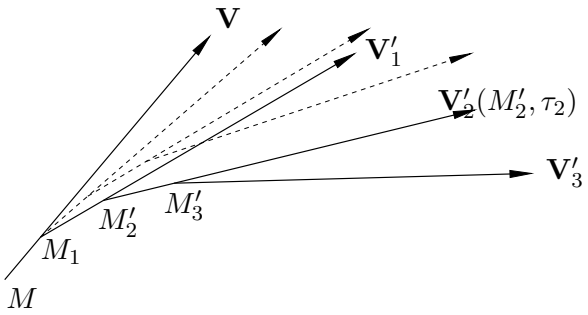

(b) Pathline traced in time $t \geq \tau$; the 'dashed' vectors reproduce vectors $\mathbf{V}_1$, $\mathbf{V}_2$, etc. from panel (a).

Figure 3.5: Comparison of a streamline with the corresponding pathline.

point M. The next point on the streamline will be M_2, see Figure 3.5(a). This procedure being repeated many times results in a broken line $MM_1M_2\ldots$ which tends to the actual streamline as the distances between points M, M_1, M_2, etc. tend to zero.

If the pathline is to be constructed, one has to take into account the fact that while the fluid particle travels from M to M_1, its velocity vector, being dependent on time, changes to $\mathbf{V}'_1(\tau_1)$ $(\tau_1 > \tau)$, see Figure 3.5(b). So the next point on the pathline will be M'_2, not M_2. The more steps are made along the pathline, its deviation from the streamline become more significant. For a steady flow, since its velocity field is independent of time

$$\mathbf{V} = \mathbf{V}(x, y, z) \quad \text{i.e.} \quad \frac{\partial \mathbf{V}}{\partial t} = 0,$$

then the streamline and the pathline obviously coincide with each other. It can be shown that streamlines, pathlines and streaklines are same for *steady flows.*

Quiz: Show that for a steady flow each streakline corresponds to a pathline and vice versa.

Lecture 4

Vorticity

In addition to velocity, ***vorticity*** is also an important, sometimes better, quantity to characterise the fluid motion. In terms of the velocity $\mathbf{V} = \mathbf{V}(t, \mathbf{r})$, the vorticity field $\boldsymbol{\omega}$, is defined as

$$\boldsymbol{\omega} = \operatorname{curl} \mathbf{V}.$$

Here "curl" is a differential operator defined as the vector product of the gradient operator

$$\nabla = \mathbf{i}\frac{\partial}{\partial x} + \mathbf{j}\frac{\partial}{\partial y} + \mathbf{k}\frac{\partial}{\partial z}$$

and the velocity vector

$$\mathbf{V} = \mathbf{i}u + \mathbf{j}v + \mathbf{k}w.$$

In the coordinate decomposition form it may be written as

$$\boldsymbol{\omega} = \operatorname{curl} \mathbf{V} = \big[\nabla \times \mathbf{V}\big] = \begin{vmatrix} \mathbf{i} & \mathbf{j} & \mathbf{k} \\ \frac{\partial}{\partial x} & \frac{\partial}{\partial y} & \frac{\partial}{\partial z} \\ u & v & w \end{vmatrix} =$$

$$= \mathbf{i}\left(\frac{\partial w}{\partial y} - \frac{\partial v}{\partial z}\right) + \mathbf{j}\left(\frac{\partial u}{\partial z} - \frac{\partial w}{\partial x}\right) + \mathbf{k}\left(\frac{\partial v}{\partial x} - \frac{\partial u}{\partial y}\right). \tag{4.1}$$

The vorticity $\boldsymbol{\omega}$ serves to describe local rotation of fluid particles about their "centres". In order to see this interpretation, let us consider a special form of fluid flow, namely, the fluid moves as if it was a rigid body[†]. It is known from classical mechanics that any rigid body motion may be represented as a *superposition of (i) translational motion of arbitrary chosen "centre" O inside the body* (see Figure 4.1) *and (ii) rotation around the axis OO' which is drawn through the centre O parallel to the angular velocity vector* $\boldsymbol{\Omega} = (\Omega_x, \Omega_y, \Omega_z)$, where Ω_x, Ω_y and Ω_z are the projections of the angular velocity vector, $\boldsymbol{\Omega}$, on the x-, y- and z-axes, respectively. It follows that the velocity field can be written as

$$\mathbf{V} = \mathbf{V}_0 + \big[\boldsymbol{\Omega} \times (\mathbf{r} - \mathbf{r}_0)\big]. \tag{4.2}$$

The meaning of different terms in formula (4.2) is demonstrated by Figure 4.1. Vector $\mathbf{V}$ on the left hand side of (4.2) is the velocity of an arbitrary chosen point A whose position vector is $\mathbf{r}$. The first term on the right hand side is translational velocity, $\mathbf{V}_0$, of the centre O and the second term, $\big[\boldsymbol{\Omega} \times (\mathbf{r} - \mathbf{r}_0)\big]$, is circumferential velocity of the body rotation around the axis OO'; the latter is drawn through centre O in the direction of the angular velocity vector $\boldsymbol{\Omega}$. Notice that in a rigid body motion $\boldsymbol{\Omega}$ is independent of a choice of the centre O and remains the same for any A inside the body (see Figure 4.1).

Coordinate decomposition of equation (4.2) is written as

$$\begin{aligned} u &= u_0 + \Omega_y(z - z_0) - \Omega_z(y - y_0), \\ v &= v_0 + \Omega_z(x - x_0) - \Omega_x(z - z_0), \\ w &= w_0 + \Omega_x(y - y_0) - \Omega_y(x - x_0). \end{aligned} \tag{4.3}$$

[†]The term "rigid body" is used in situations when a solid body may be treated as undeformable.

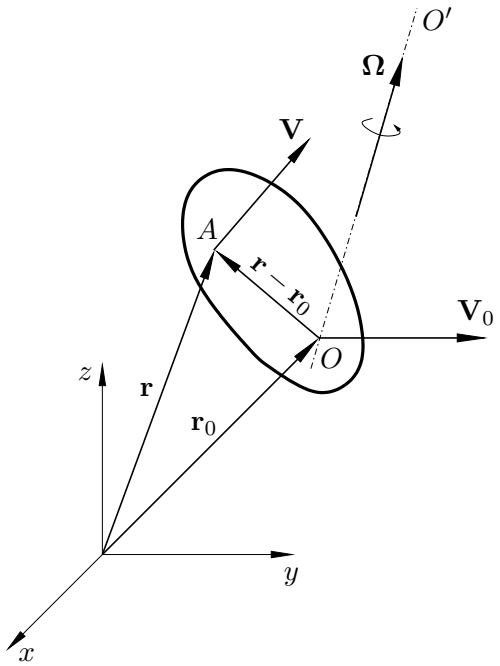

Figure 4.1: Graphical illustration of formula (4.2).

Substitution of (4.3) into (4.1) yields

$$\boldsymbol{\omega} = \mathbf{i}\, 2\Omega_x + \mathbf{j}\, 2\Omega_y + \mathbf{k}\, 2\Omega_z = 2\boldsymbol{\Omega}$$

which implies that the vorticity $\boldsymbol{\omega}$ is simply twice the angular velocity $\boldsymbol{\Omega}$.

In the general case, the vorticity $\boldsymbol{\omega}$ varies with position rather than being a constant. Nevertheless, the above interpretation remains valid in the local sense with small $|\mathbf{r} - \mathbf{r}_0|$, and $\boldsymbol{\omega}/2$ represents the *local* angular velocity of fluid particles, as will be in the next Lecture.

If $\boldsymbol{\omega} = 0$ almost everywhere (i.e. except at a finite, or infinite but countable, number of points) in the flow field, then the flow is referred to as ***irrotational flow*** or ***potential flow***.

Circulation

Another important quantity to describe the flow motion is *circulation*. Let C be a closed contour inside a moving fluid. The ***circulation*** Γ of the velocity vector $\mathbf{V}$ along C is defined as a line (contour) integral along C,

$$\Gamma = \oint_C \big(\mathbf{V} \cdot d\mathbf{r}\big). \tag{4.4}$$

As it stands, Γ depends on both the velocity and the contour chosen. However, there are important flows which are, to a good degree of approximation, irrotational and two-dimensional, and then Γ is independent of C as long as the latter does not cross any of those exceptional points. An example is the flow around a two-dimensional aerofoil, and as we will see, its lift is intrinsically linked to the circulation.

Vortex Tube and Circulation

There exists a more general result about the role of C and the connection between the circulation Γ and vorticity. To derive this result, we introduce the concepts of a *vortex line* and *vortex tube*.

Definition 4.1: *Line $\mathcal{L}$ is call a **vortex-line** if at each point M on $\mathcal{L}$ the vorticity vector $\boldsymbol{\omega}$ is tangent to $\mathcal{L}$.*

Let us consider a closed contour C. Through each point on C, a vortex line can be drawn. The vortex lines emanating from all the points on C then forms a ***vortex tube***. In Figure 4.2 the vortex tube is shown as surface Σ. Let us now draw another contour C' on Σ and "close" the tube from both sides using surface σ which rests on C and surface σ' which rests on C'. We shall call the region bounded by Σ, σ and σ' as region $\mathcal{D}$. Using Gauss' divergence theorem, we can write

$$\iint_S \left(\boldsymbol{\omega}\cdot\mathbf{n}\right) ds = \iiint_{\mathcal{D}} \operatorname{div}\boldsymbol{\omega}\, d\tau, \tag{4.5}$$

where S is the surface surrounding $\mathcal{D}$ and $\mathbf{n}$ is the unit vector outward normal to S. Equation (4.5) is valid for *any* arbitrary vector $\boldsymbol{\omega}$, but here $\boldsymbol{\omega}$ stands for the vorticity.

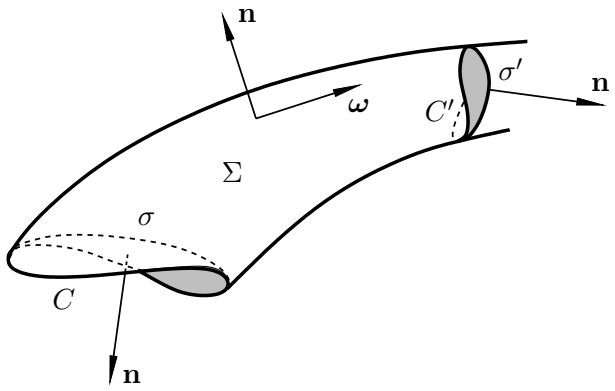

Figure 4.2: Vortex tube.

The divergence of $\boldsymbol{\omega}$ is given by the formula

$$\operatorname{div}\boldsymbol{\omega} = \frac{\partial\omega_x}{\partial x} + \frac{\partial\omega_y}{\partial y} + \frac{\partial\omega_z}{\partial z}. \tag{4.6}$$

Using (4.1) in (4.6) it is easy to find that for any velocity field

$$\operatorname{div}\boldsymbol{\omega} = 0,$$

which is just a mathematical identity:

$$\operatorname{div}(\operatorname{curl}\mathbf{V}) = \nabla\cdot(\nabla\times\mathbf{V}) = 0,$$

valid for any vector $\mathbf{V}$.

On the vortex tube surface Σ, the vorticity vector $\boldsymbol{\omega}$ is perpendicular to $\mathbf{n}$, that is, $\boldsymbol{\omega} \cdot \mathbf{n} = 0$, and it follows that (4.5) reduces to

$$\iint\limits_{\sigma} \big(\boldsymbol{\omega} \cdot \mathbf{n}\big)\, ds + \iint\limits_{\sigma'} \big(\boldsymbol{\omega} \cdot \mathbf{n}\big)\, ds = 0.$$

If we change the direction of the normal vector $\mathbf{n}$ on σ' onto the opposite one making it the same as on σ, then we will have

$$\iint\limits_{\sigma} \big(\boldsymbol{\omega} \cdot \mathbf{n}\big)\, ds = \iint\limits_{\sigma'} \big(\boldsymbol{\omega} \cdot \mathbf{n}'\big)\, ds \quad (\mathbf{n}' = -\mathbf{n}). \tag{4.7}$$

We have proven that the flux of the vorticity through a cross-section of a vortex tube does not depend either on the form of the cross-section or on its position along the tube. Both sides of (4.7) represent the *vorticity flux* through the vortex tube, and this flux is constant along the tube.

On the other hand, using the Stokes theorem, we have

$$\iint\limits_{\sigma} \big(\boldsymbol{\omega} \cdot \mathbf{n}\big)\, ds = \oint\limits_{C} (\mathbf{V} \cdot d\mathbf{r}) = \Gamma.$$

The above result is stated as the ***Helmholtz's First Theorem***.

Theorem 1 *The circulation of the velocity vector along a closed contour C embracing a vortex tube is an invariant quantity. It is called the* ***intensity*** *of the vortex tube.*

The conservation of the circulation explains, for example, the existence of a strong vortex originating from the tip of a finite aspect ratio wing; see Figure 4.3.

Figure 4.3: Trailing vortices.

Rate-of-Strain Tensor

We have seen earlier (in Lecture 4) a special form of fluid motion which behaves like that of a rigid body, and thus can be decomposed into translation and rotation of fluid particles. However, in general fluid elements also undergo deformation, which is a crucial difference between a continuum and a rigid body. We now examine the general character of the *local relative motion* of fluid particles as this information is required to establish the relation between the deformation and the force acting on them (see Lecture 2).

Let us consider a small fluid element (see Figure 5.1) in the flow with the velocity $\mathbf{V} = \mathbf{V}(t, \mathbf{r})$ defined in the Euler variables. We choose a point M inside the element as its "centre". The position of this point at instance t is defined by the position vector $\mathbf{r}_0$. We then consider (at the same instant) a neighbouring point M' whose position vector is $\mathbf{r} = \mathbf{r}_0 + \delta\mathbf{r}$. Here the symbol δ is used to signify that the variation of coordinates is taken at the same instance, t.

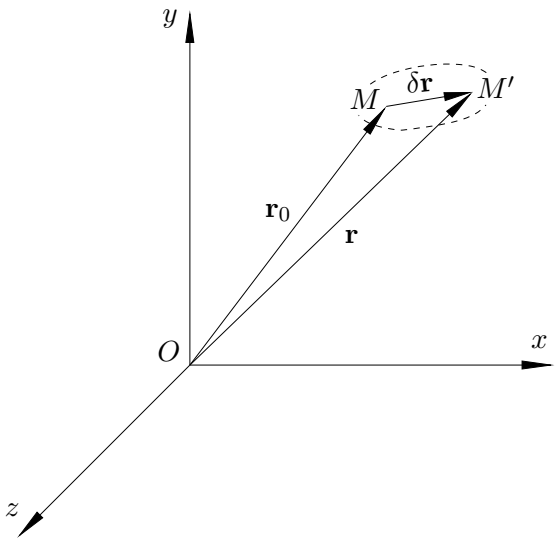

Figure 5.1: Deformation of a fluid element.

Taking into account that the viscous forces would usually act to smooth out possible discontinuities in flow functions, we suppose that the velocity components are differentiable, and therefore we shall represent the velocity at $\mathbf{r}_0 + \delta\mathbf{r}$ by the Taylor expansions about $\mathbf{r}_0$. We shall perform the expansions in a compact manner using simple vector/tensor notations and algebra. (The much longer analysis using the components of the velocity and coordinates will be given later.)

First we introduce the necessary notations and conventions[†].

$$\mathbf{r} = (x_1, x_2, x_3) = (x, y, z), \quad \mathbf{V} = (u_1, u_2, u_3) = (u, v, w);$$

$$\delta\mathbf{r} = (\delta x_1, \delta x_2, \delta x_3) = (\delta x, \delta y, \delta z); \quad \delta\mathbf{V} = (\delta u_1, \delta u_2, \delta u_3) = (\delta u, \delta v, \delta w),$$

where the correspondences between the two sets of notations are indicated.

[†]To be consistent with notations used earlier, u_1, u_2 and u_3 should be identified with v_1, v_2 and v_3, respectively.

Now the Taylor expansion of $u_i(t, x_1, x_2, x_3)$ $(i = 1, 2, 3)$ can be expressed as

$$u_i(t, \mathbf{r}) = u_i(t, \mathbf{r}_0) + \frac{\partial u_i}{\partial x_j}\delta x_j. \tag{5.1}$$

where use has been made of Einstein's convention: a repeated index indicates summation. Equation (5.1) can be rewritten as

$$u_i(t, \mathbf{r}) - u_i(t, \mathbf{r}_0) = \frac{1}{2}\Big(\frac{\partial u_i}{\partial x_j} - \frac{\partial u_j}{\partial x_i}\Big)\delta x_j + \frac{1}{2}\Big(\frac{\partial u_i}{\partial x_j} + \frac{\partial u_j}{\partial x_i}\Big)\delta x_j. \tag{5.2}$$

Note that the three non-zero $\left(\frac{\partial u_i}{\partial x_j} - \frac{\partial u_j}{\partial x_i}\right)$ are the components of $\boldsymbol{\omega}$, and the first term on the high-hand side of (5.2) is the $i-$th component of $\frac{1}{2}\boldsymbol{\omega} \times \delta\mathbf{r}$. With the second term in (5.2), we introduce notation

$$\varepsilon_{ij} = \frac{1}{2}\Big(\frac{\partial u_i}{\partial x_j} + \frac{\partial u_j}{\partial x_i}\Big),$$

and then the 3×3 matrix

$$\mathcal{E} = \big(\varepsilon_{ij}\big)_{3\times 3} = \begin{pmatrix} \varepsilon_{11} & \varepsilon_{12} & \varepsilon_{13} \\ \varepsilon_{21} & \varepsilon_{22} & \varepsilon_{23} \\ \varepsilon_{31} & \varepsilon_{32} & \varepsilon_{33} \end{pmatrix} = \begin{pmatrix} \varepsilon_{xx} & \varepsilon_{xy} & \varepsilon_{xz} \\ \varepsilon_{yx} & \varepsilon_{yy} & \varepsilon_{yz} \\ \varepsilon_{zx} & \varepsilon_{zy} & \varepsilon_{zz} \end{pmatrix}, \tag{5.3}$$

which is called the ***rate-of-strain tensor***, a crucial concept in continuum mechanics; it has the symmetric property: $\varepsilon_{ij} = \varepsilon_{ji}$, and has 6 (instead of 9) elements. The second term in (5.2) represents the $i-$th component of the vector $\mathcal{E} \cdot \delta\mathbf{r}$ (which can be understood as the product of the 3×3 matrix with the vector $\delta\mathbf{r}$).

Using this tensor and $\boldsymbol{\omega}$, the relation (5.2) can now be written as

$$\delta\mathbf{V} \equiv \mathbf{V}(t, \mathbf{r}) - \mathbf{V}(t, \mathbf{r}_0) = \big[\frac{1}{2}\boldsymbol{\omega} \times \delta\mathbf{r}\big] + \mathcal{E} \cdot \delta\mathbf{r}. \tag{5.4}$$

The first term on the right-hand side describe the "locally rigid" motion of the fluid element, which would be its only motion if the fluid element suddenly solidifies. Consequently, the second term on the right-hand side of (5.4),

$$\mathbf{V}_{\text{def}} = \mathcal{E} \cdot \delta\mathbf{r},$$

should be attributed to the *deformational motion* of the fluid, which proves the ***Helmholtz's Second Theorem***.

Theorem 1 *The local relative motion of a small fluid element is a superposition of (i) locally-rigid motion represented by the first of the two terms in* (5.4)*, and (ii) deformational motion with the velocity* $\mathbf{V}_{\text{def}} = \mathcal{E} \cdot \delta\mathbf{r}$.

In terms of individual components, (5.1) reads

$$\begin{aligned}
u(t,\mathbf{r}) = u(t,\mathbf{r}_0+\delta\mathbf{r}) &= u(t,x_0+\delta x, y_0+\delta y, z_0+\delta z) = \\
&= u(t,\mathbf{r}_0) + \frac{\partial u}{\partial x}\delta x + \frac{\partial u}{\partial y}\delta y + \frac{\partial u}{\partial z}\delta z, \\
v(t,\mathbf{r}) = v(t,\mathbf{r}_0+\delta\mathbf{r}) &= v(t,x_0+\delta x, y_0+\delta y, z_0+\delta z) = \\
&= v(t,\mathbf{r}_0) + \frac{\partial v}{\partial x}\delta x + \frac{\partial v}{\partial y}\delta y + \frac{\partial v}{\partial z}\delta z, \\
w(t,\mathbf{r}) = w(t,\mathbf{r}_0+\delta\mathbf{r}) &= w(t,x_0+\delta x, y_0+\delta y, z_0+\delta z) = \\
&= w(t,\mathbf{r}_0) + \frac{\partial w}{\partial x}\delta x + \frac{\partial w}{\partial y}\delta y + \frac{\partial w}{\partial z}\delta z,
\end{aligned}$$

which can, after regrouping, be rewritten as

$$\left.\begin{aligned}
u(t,\mathbf{r}) - u(t,\mathbf{r}_0) =& \frac{1}{2}\left(\frac{\partial u}{\partial z} - \frac{\partial w}{\partial x}\right)\delta z - \frac{1}{2}\left(\frac{\partial v}{\partial x} - \frac{\partial u}{\partial y}\right)\delta y + \\
&+ \frac{\partial u}{\partial x}\delta x + \frac{1}{2}\left(\frac{\partial u}{\partial y} + \frac{\partial v}{\partial x}\right)\delta y + \frac{1}{2}\left(\frac{\partial u}{\partial z} + \frac{\partial w}{\partial x}\right)\delta z, \\
v(t,\mathbf{r}) - v(t,r_0) =& \frac{1}{2}\left(\frac{\partial v}{\partial x} - \frac{\partial u}{\partial y}\right)\delta x - \frac{1}{2}\left(\frac{\partial w}{\partial y} - \frac{\partial v}{\partial z}\right)\delta z + \\
&+ \frac{1}{2}\left(\frac{\partial v}{\partial x} + \frac{\partial u}{\partial y}\right)\delta x + \frac{\partial v}{\partial y}\delta y + \frac{1}{2}\left(\frac{\partial v}{\partial z} + \frac{\partial w}{\partial y}\right)\delta z, \\
w(t,\mathbf{r}) - w(t,\mathbf{r}_0) =& \frac{1}{2}\left(\frac{\partial w}{\partial y} - \frac{\partial v}{\partial z}\right)\delta y - \frac{1}{2}\left(\frac{\partial u}{\partial z} - \frac{\partial w}{\partial x}\right)\delta x + \\
&+ \frac{1}{2}\left(\frac{\partial w}{\partial x} + \frac{\partial u}{\partial z}\right)\delta x + \frac{1}{2}\left(\frac{\partial w}{\partial y} + \frac{\partial v}{\partial z}\right)\delta y + \frac{\partial w}{\partial z}\delta z.
\end{aligned}\right\} \tag{5.5}$$

These are equivalent to (5.2). The first lines in the expressions (5.5) for u, v and w represent the "locally rigid" motion of the fluid element, while the second lines in (5.5) are associated with the *deformational motion* of the fluid,

$$\left.\begin{aligned}
u_{\rm def} &= \frac{\partial u}{\partial x}\delta x + \frac{1}{2}\left(\frac{\partial u}{\partial y} + \frac{\partial v}{\partial x}\right)\delta y + \frac{1}{2}\left(\frac{\partial u}{\partial z} + \frac{\partial w}{\partial x}\right)\delta z, \\
v_{\rm def} &= \frac{1}{2}\left(\frac{\partial v}{\partial x} + \frac{\partial u}{\partial y}\right)\delta x + \frac{\partial v}{\partial y}\delta y + \frac{1}{2}\left(\frac{\partial v}{\partial z} + \frac{\partial w}{\partial y}\right)\delta z, \\
w_{\rm def} &= \frac{1}{2}\left(\frac{\partial w}{\partial x} + \frac{\partial u}{\partial z}\right)\delta x + \frac{1}{2}\left(\frac{\partial w}{\partial y} + \frac{\partial v}{\partial z}\right)\delta y + \frac{\partial w}{\partial z}\delta z.
\end{aligned}\right\} \tag{5.6}$$

The tensor composed of the coefficients of δx, δy and δz in (5.6) is

$$\mathcal{E} = \begin{pmatrix} \varepsilon_{xx} & \varepsilon_{xy} & \varepsilon_{xz} \\ \varepsilon_{yx} & \varepsilon_{yy} & \varepsilon_{yz} \\ \varepsilon_{zx} & \varepsilon_{zy} & \varepsilon_{zz} \end{pmatrix} = \begin{pmatrix} \frac{\partial u}{\partial x} & \frac{1}{2}\left(\frac{\partial u}{\partial y} + \frac{\partial v}{\partial x}\right) & \frac{1}{2}\left(\frac{\partial u}{\partial z} + \frac{\partial w}{\partial x}\right) \\ \frac{1}{2}\left(\frac{\partial v}{\partial x} + \frac{\partial u}{\partial y}\right) & \frac{\partial v}{\partial y} & \frac{1}{2}\left(\frac{\partial v}{\partial z} + \frac{\partial w}{\partial y}\right) \\ \frac{1}{2}\left(\frac{\partial w}{\partial x} + \frac{\partial u}{\partial z}\right) & \frac{1}{2}\left(\frac{\partial w}{\partial y} + \frac{\partial v}{\partial z}\right) & \frac{\partial w}{\partial z} \end{pmatrix}, \tag{5.7}$$

which is (5.3). The symmetry is reflected by the fact that

$$\varepsilon_{yx} = \varepsilon_{xy}, \quad \varepsilon_{zx} = \varepsilon_{xz}, \quad \varepsilon_{zy} = \varepsilon_{yz}.$$

Equations (5.5) may be expressed in the vector form (5.4) as expected.

The six elements of the tensor (5.3) or (5.7) represent possible elementary 'modes' of the deformation of a fluid particle. To reveal their physical content, it is convenient to use a Cartesian coordinate system $Oxyz$ with the origin, O, being at the fluid element "centre" at all times, and the coordinate moves with the velocity at O and its axes x, y, z rotate together with the angular velocity $\mathbf{\Omega} = \frac{1}{2}\mathrm{curl}\mathbf{V}$. The only fluid motion that may be observed in this coordinate system is the deformation of the fluid element with respect to the centre. At any point inside the fluid particle the deformation velocity is calculated as

$$\mathbf{V} = \mathcal{E} \cdot \delta\mathbf{r},$$

where $\delta\mathbf{r}$ is the position vector of the point of interest.

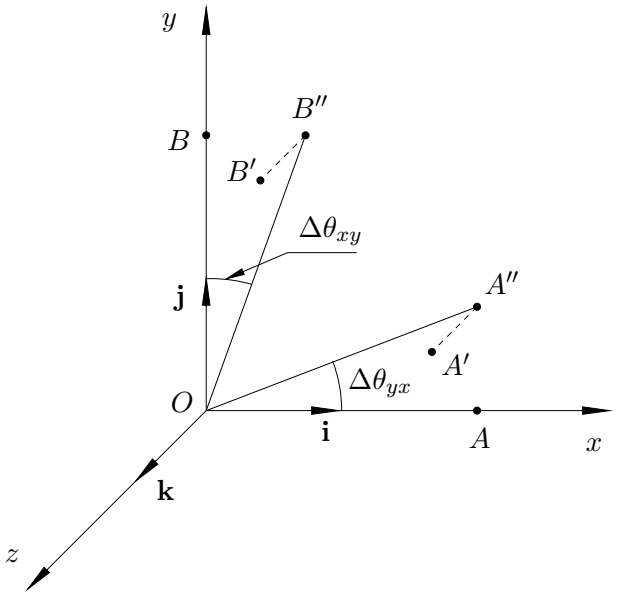

Figure 5.2: Deformation of a fluid element.

In order to see the meaning of the components in the rate-of-strain tensor, let us consider point A situated on the x-axis as shown in Figure 5.2. The position vector for this point may be written as $\delta\mathbf{r} = \mathbf{i}\delta x$, where $\mathbf{i}$ is the unit vector along the x-axis. The fluid velocity at point A is

$$\mathbf{V} = \mathcal{E} \cdot \delta\mathbf{r} = \begin{pmatrix} \varepsilon_{xx} & \varepsilon_{xy} & \varepsilon_{xz} \\ \varepsilon_{yx} & \varepsilon_{yy} & \varepsilon_{yz} \\ \varepsilon_{zx} & \varepsilon_{zy} & \varepsilon_{zz} \end{pmatrix} \begin{pmatrix} \delta x \\ 0 \\ 0 \end{pmatrix} = \begin{pmatrix} \varepsilon_{xx}\delta x \\ \varepsilon_{yx}\delta x \\ \varepsilon_{zx}\delta x \end{pmatrix},$$

which is written, in terms of components, as

$$u = \varepsilon_{xx}\delta x, \quad v = \varepsilon_{yx}\delta x, \quad w = \varepsilon_{zx}\delta x.$$

Consequently, the fluid particle that was at point A at an initial instance, t, translates shortly afterwards to a new position A' (see Figure 5.2) with the coordinates

$$x = \delta x + \varepsilon_{xx}\delta x\Delta t, \quad y = \varepsilon_{yx}\delta x\Delta t, \quad z = \varepsilon_{zx}\delta x\Delta t. \tag{5.8}$$

Here Δt denotes the time spent by the fluid particle when travelling between points A and A'.

The distance between the new location A' of the fluid particle and the coordinate origin O is

$$l_{OA'} = \delta x\sqrt{(1+\varepsilon_{xx}\Delta t)^2 + (\varepsilon_{yx}\Delta t)^2 + (\varepsilon_{yz}\Delta t)^2} =$$
$$= \delta x\sqrt{1 + 2\varepsilon_{xx}\Delta t + O\big[(\Delta t)^2\big]} = \delta x(1+\varepsilon_{xx}\Delta t) + O\big[\delta x(\Delta t)^2\big].$$

It differs from the distance, $l_{OA} = \delta x$, between the original location A and the coordinate origin O by the value

$$\Delta l = l_{OA'} - l_{OA} = \varepsilon_{xx}\delta x\Delta t. \tag{5.9}$$

Formula (5.9), obviously, holds for any fluid particle situated on the x-axis in a vicinity of centre O. Therefore, if we consider a *material line* composed of the fluid particles occupying the interval (O, A) on the x-axis then we can see that the material line experiences uniform *extension* at a relative rate

$$\frac{1}{\delta x}\lim_{\Delta t\to 0}\frac{\Delta l}{\Delta t} = \varepsilon_{xx}$$

In addition to the extension, the material line deviates from the x-axis. According to (5.8), its projection (O, A'') upon the (x, y)-plane (see Figure 5.2) makes an angle

$$\Delta\theta_{yx} = \arctan\frac{y}{x} \tag{5.10}$$

with the x-axis. Substituting (5.8) into (5.10), we have

$$\Delta\theta_{yx} = \arctan\frac{\varepsilon_{yx}\Delta t}{1+\varepsilon_{xx}\Delta t},$$

which for small Δt reduces to

$$\Delta\theta_{yx} = \arctan\big(\varepsilon_{yx}\Delta t\big) = \varepsilon_{yx}\Delta t.$$

In the same way, it may be shown that the material line composed of the fluid particles in the interval (O, B) on the y-axis experiences extension with the rate ε_{yy} and deviates from the y-axis such that its projection (O, B'') upon the (x, y)-plane makes an angle

$$\Delta\theta_{xy} = \varepsilon_{xy}\Delta t$$

with the y-axis (see Figure 5.2). Consequently, the original right angle between the material lines (O, A) and (O, B) decreases by the value

$$\Delta\theta_{yx} + \Delta\theta_{xy} = (\varepsilon_{yx} + \varepsilon_{xy})\Delta t.$$

We can conclude that the angle between the x- and y-axes changes with the rate

$$\lim_{\Delta t\to 0}\frac{\Delta\theta_{yx} + \Delta\theta_{xy}}{\Delta t} = \varepsilon_{yx} + \varepsilon_{xy} = 2\varepsilon_{xy},$$

where use is made of the symmetry $\varepsilon_{yx} = \varepsilon_{xy}$.

The same arguments may, of course, be applied to a material line on the z-axis. Taking the results together, we have shown that

- the three diagonal elements ε_{xx}, ε_{yy}, ε_{zz} of the rate-of-strain tensor (5.7) describe linear expansion of a small fluid element in the x-, y- and z-directions, respectively;

- the non-diagonal elements ε_{xy}, ε_{xz}, ε_{yz} and their symmetric counterparts ε_{yx}, ε_{zx}, ε_{zy} characterise angular compression of the fluid element in the (x, y)-, (x, z)- and (y, z)-planes, which leads to deformation of the shape.

Constitutive Equation

We have discussed earlier (see Lecture 2) the origin of the surface forces acting in fluids, and we recall that these are the short-range forces produced by the interaction of molecules, which move under the mutual forces of attraction and repulsion. In particular, in gasses the dominant mechanism is a transport of momentum from one fluid layer to another due to collisions of molecules taking place in the neighbourhood of the surface, within distances of a few mean free paths.

We have also shown that the stress acting on surface can be expressed in terms of the unit normal vector of the surface and the stress tensor $\mathcal{P}$. In a *fluid at rest*, the only surface force possible is the pressure p acting equally in all the directions, with the stress tensor assuming the form of equation (2.12),

$$\mathcal{P} = \begin{pmatrix} -p & 0 & 0 \\ 0 & -p & 0 \\ 0 & 0 & -p \end{pmatrix} = -pI, \tag{6.1}$$

where

$$I = \begin{pmatrix} 1 & 0 & 0 \\ 0 & 1 & 0 \\ 0 & 0 & 1 \end{pmatrix}$$

is the unit tensor.

In the special case of a fluid moving like a *rigid body* (translation and rotation), the interaction between the molecules will remain the same as it would be in this fluid at rest. The stress tensor will therefore remain unchanged, i.e. could be represented by (6.1). Keeping this in mind, we write the stress tensor (2.4) for an arbitrarily moving fluid as

$$\mathcal{P} = -pI + \mathcal{T}, \tag{6.2}$$

where the tensor

$$\mathcal{T} = \begin{pmatrix} \tau_{xx} & \tau_{xy} & \tau_{xz} \\ \tau_{yx} & \tau_{yy} & \tau_{yz} \\ \tau_{zx} & \tau_{zy} & \tau_{zz} \end{pmatrix}$$

is called the ***deviatoric stress tensor***. Its existence is entirely attributable to the deformational motion of a fluid, which is fully characterised by the rate-of-strain tensor $\mathcal{E}$.

The purpose of the following analysis is to establish an explicit form of the relationship between the ***deviatoric stress tensor*** $\mathcal{T}$ and the rate-of-strain tensor $\mathcal{E}$. Such a relationship is termed the ***constitutive equation***, which describes the physical property of the medium, the fluid in the case of fluid dynamics.

Since the rate-of-strain tensor (5.6) is symmetric, there exists a privileged Cartesian coordinate system $(\hat{x}, \hat{y}, \hat{z})$ where $\mathcal{E}$ assumes a diagonal form

$$\begin{pmatrix} \varepsilon_{\hat{x}\hat{x}} & 0 & 0 \\ 0 & \varepsilon_{\hat{y}\hat{y}} & 0 \\ 0 & 0 & \varepsilon_{\hat{z}\hat{z}} \end{pmatrix}. \tag{6.3}$$

These coordinates are called the *principal axes* of the rate-of-strain tensor.

Our strategy will be to deduce the constitutive equation in the principal axes $(\hat{x}, \hat{y}, \hat{z})$ and then we will return to the original Cartesian coordinates (x, y, z). If we write the deviatoric stress tensor in the $(\hat{x}, \hat{y}, \hat{z})$-axes

$$\mathcal{T} = \begin{pmatrix} \tau_{\hat{x}\hat{x}} & \tau_{\hat{x}\hat{y}} & \tau_{\hat{x}\hat{z}} \\ \tau_{\hat{y}\hat{x}} & \tau_{\hat{y}\hat{y}} & \tau_{\hat{y}\hat{z}} \\ \tau_{\hat{z}\hat{x}} & \tau_{\hat{z}\hat{y}} & \tau_{\hat{z}\hat{z}} \end{pmatrix}, \tag{6.4}$$

then each element in (6.4) has to be a function of the three elements of the tensor (6.3).

In order to establish the constitutive relation, it is necessary to make assumptions about the *physical property*, the so-called *rheology*, of the fluids. Fluids which are common and have received most attention are the so-called ***Newtonian fluids***, which satisfy the following two postulates.

1. ***Linearity postulate***. *All the elements of the deviatoric stress tensor* (6.4) *are linear functions of the three elements of the rate-of-strain tensor* (6.3). For example, the first diagonal element may be written as

$$\tau_{\hat{x}\hat{x}} = a_1 \varepsilon_{\hat{x}\hat{x}} + a_2 \varepsilon_{\hat{y}\hat{y}} + a_3 \varepsilon_{\hat{z}\hat{z}} \,. \tag{6.5}$$

   Here the coefficients a_1, a_2 and a_3 are assumed to be independent of the velocity field but might depend on the local thermodynamic state of the fluid.

2. ***Isotropy postulate***. *The form of the equations, like* (6.5)*, relating the elements of the deviatoric stress tensor* (6.4) *to the elements of the rate-of-strain tensor* (6.3) *should be independent on the choice of Cartesian coordinates aligned with the principal axes.*

The assumed properties are underlined by the physics at the molecule level, and indeed for gases they could be deduced from the kinetic gas theory. The two assumptions made are however of *phenomenological* nature. Fortunately, they turn to be valid for all gases and most common liquids, allowing motions of fluids and gases to be treated in a unified framework. Fluid-like materials which do not satisfy either of the assumptions are referred to as ***Non-Newtonian*** fluids, of which there are quite many. The study of those fluids forms the subject of *Non-Newtonian Fluid Dynamics*.

Applying the first postulate to the second diagonal element of tensor (6.4), we can write

$$\tau_{\hat{y}\hat{y}} = b_1 \varepsilon_{\hat{x}\hat{x}} + b_2 \varepsilon_{\hat{y}\hat{y}} + b_3 \varepsilon_{\hat{z}\hat{z}} \,, \tag{6.6}$$

and a similar linear relation holds for $\tau_{\hat{z}\hat{z}}$. We shall prove next that the coefficients b_1, b_2, b_3 in (6.6) are not independent of the coefficients a_1, a_2, a_3 in (6.5), by rotating the coordinate system and making use the second postulate.

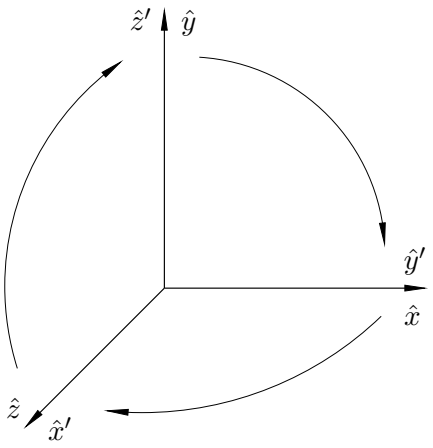

Figure 6.1: Rotation of the principal axes: rotate first about the y-axis by the angle of $\pi/2$, followed by the rotation about the z-axis by $\pi/2$ angle.

First, we rotate the coordinate system as is shown in Figure (6.1). According to the second postulate, the equation (6.6) is invariant with respect to the rotation, and in the "new coordinates", $(\hat{x}', \hat{y}', \hat{z}')$, it should remain of the same as (6.6) and be written as

$$\tau_{\hat{y}'\hat{y}'} = b_1 \varepsilon_{\hat{x}'\hat{x}'} + b_2 \varepsilon_{\hat{y}'\hat{y}'} + b_3 \varepsilon_{\hat{z}'\hat{z}'} \,,$$

It is obvious that $\tau_{\hat{y}'\hat{y}'}$ and $\tau_{\hat{x}\hat{x}}$ represent the same physical quantity, the projection on the $\hat{x}$-axis of the stress acting on a surface element drawn perpendicular to the $\hat{x}$-axis (with the pressure subtracted). Hence, we can write

$$\tau_{\hat{x}\hat{x}} = \tau_{\hat{y}'\hat{y}'} = b_1 \varepsilon_{\hat{x}'\hat{x}'} + b_2 \varepsilon_{\hat{y}'\hat{y}'} + b_3 \varepsilon_{\hat{z}'\hat{z}'} \,. \tag{6.7}$$

It easily seen further from Figure 6.1 that

$$\begin{aligned} &\hat{x}' = \hat{z}, \qquad \hat{y}' = \hat{x}, \qquad \hat{z}' = \hat{y}, \\ &\hat{u}' = \hat{w}, \qquad \hat{v}' = \hat{u}, \qquad \hat{w}' = \hat{v}. \end{aligned}$$

Consequently, using the formula for the first diagonal element of $\mathcal{E}$ in (5.6), we find

$$\varepsilon_{\hat{x}'\hat{x}'} = \frac{\partial \hat{u}'}{\partial \hat{x}'} = \frac{\partial \hat{w}}{\partial \hat{z}} = \varepsilon_{\hat{z}\hat{z}}. \tag{6.8}$$

Similarly, it can be deduced that

$$\varepsilon_{\hat{y}'\hat{y}'} = \varepsilon_{\hat{x}\hat{x}}, \qquad \varepsilon_{\hat{z}'\hat{z}'} = \varepsilon_{\hat{y}\hat{y}}. \tag{6.9}$$

Substitution of (6.8) and (6.9) into equation (6.7) turns it into

$$\tau_{\hat{x}\hat{x}} = b_1 \varepsilon_{\hat{z}\hat{z}} + b_2 \varepsilon_{\hat{x}\hat{x}} + b_3 \varepsilon_{\hat{y}\hat{y}}. \tag{6.10}$$

Comparing (6.10) with (6.5), and we can conclude that $b_1 = a_3$, $b_2 = a_1$ and $b_3 = a_2$, which allows us to write (6.6) as

$$\tau_{\hat{y}\hat{y}} = a_1 \varepsilon_{\hat{y}\hat{y}} + a_2 \varepsilon_{\hat{z}\hat{z}} + a_3 \varepsilon_{\hat{x}\hat{x}} \,. \tag{6.11}$$

Similarly, it may be shown that

$$\tau_{\hat{z}\hat{z}} = a_1 \varepsilon_{\hat{z}\hat{z}} + a_2 \varepsilon_{\hat{x}\hat{x}} + a_3 \varepsilon_{\hat{y}\hat{y}} \,. \tag{6.12}$$

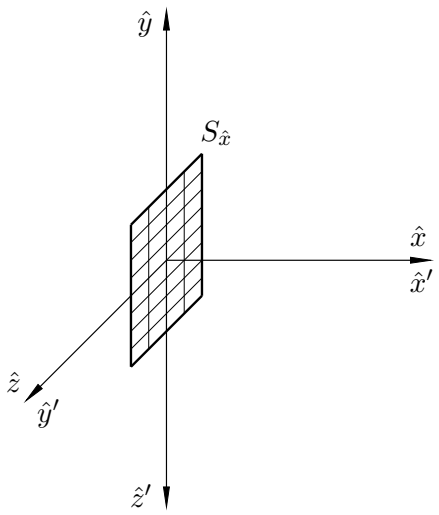

Figure 6.2: Rotation of the principle axes about the $\hat{x}$-axis by the angle $\pi/2$.

Let us now show that $a_2 = a_3$. For this purpose, we rotate the coordinate system about the $\hat{x}$-axis by the right angle as is shown in Figure 6.2. The new axes $\hat{x}'$, $\hat{y}'$ and $\hat{z}'$ lie along the principal axes of the rate-of-strain tensor $\mathcal{E}$, and therefore, according to the second postulate, we can still use equation (6.5). In the new coordinates, it is written as

$$\tau_{\hat{x}'\hat{x}'} = a_1\varepsilon_{\hat{x}'\hat{x}'} + a_2\varepsilon_{\hat{y}'\hat{y}'} + a_3\varepsilon_{\hat{z}'\hat{z}'}\,. \tag{6.13}$$

The new and old coordinates and the components of the velocity vector are related to one another as

$$\begin{aligned} &\hat{x}' = \hat{x}, \qquad \hat{y}' = \hat{z}, \qquad \hat{z}' = -\hat{y},\\ &\hat{u}' = \hat{u}, \qquad \hat{v}' = \hat{w}, \qquad \hat{w}' = -\hat{v}. \end{aligned}$$

Consequently,

$$\varepsilon_{\hat{x}'\hat{x}'} = \frac{\partial\hat{u}'}{\partial\hat{x}'} = \frac{\partial\hat{u}}{\partial\hat{x}} = \varepsilon_{\hat{x}\hat{x}}\,, \qquad \varepsilon_{\hat{y}'\hat{y}'} = \frac{\partial\hat{v}'}{\partial\hat{y}'} = \frac{\partial\hat{w}}{\partial\hat{z}} = \varepsilon_{\hat{z}\hat{z}}\,,$$
$$\varepsilon_{\hat{z}'\hat{z}'} = \frac{\partial\hat{w}'}{\partial\hat{z}'} = \frac{\partial\hat{v}}{\partial\hat{y}} = \varepsilon_{\hat{y}\hat{y}}\,.$$

Using these in (6.13), we find

$$\tau_{\hat{x}'\hat{x}'} = a_1\varepsilon_{\hat{x}\hat{x}} + a_3\varepsilon_{\hat{y}\hat{y}} + a_2\varepsilon_{\hat{z}\hat{z}}\,. \tag{6.14}$$

Now (6.14) can be compared with (6.5) since $\tau_{\hat{x}'\hat{x}'}$ and $\tau_{\hat{x}\hat{x}}$ represent the same physical quantity, namely, the normal component of the stress acting upon surface $S_{\hat{x}}$ drawn perpendicular the $\hat{x}$-axis, with the pressure subtracted. We see that a_2 and a_3 are really equal to one another.

Two factors a_1, a_2 in (6.5), (6.11), (6.12) still remain independent of one another. If instead of them we introduce parameters λ and μ such that

$$a_1 = \lambda + 2\mu, \qquad a_2 = a_3 = \lambda,$$

then the equations (6.5), (6.11), (6.12) assume the form

$$\left.\begin{aligned}\tau_{\hat{x}\hat{x}} &= \lambda(\varepsilon_{\hat{x}\hat{x}} + \varepsilon_{\hat{y}\hat{y}} + \varepsilon_{\hat{z}\hat{z}}) + 2\mu\varepsilon_{\hat{x}\hat{x}}\,,\\ \tau_{\hat{y}\hat{y}} &= \lambda(\varepsilon_{\hat{x}\hat{x}} + \varepsilon_{\hat{y}\hat{y}} + \varepsilon_{\hat{z}\hat{z}}) + 2\mu\varepsilon_{\hat{y}\hat{y}}\,,\\ \tau_{\hat{z}\hat{z}} &= \lambda(\varepsilon_{\hat{x}\hat{x}} + \varepsilon_{\hat{y}\hat{y}} + \varepsilon_{\hat{z}\hat{z}}) + 2\mu\varepsilon_{\hat{z}\hat{z}}\,.\end{aligned}\right\} \tag{6.15}$$

Since

$$\varepsilon_{\hat{x}\hat{x}} + \varepsilon_{\hat{y}\hat{y}} + \varepsilon_{\hat{z}\hat{z}} = \frac{\partial\hat{u}}{\partial\hat{x}} + \frac{\partial\hat{v}}{\partial\hat{y}} + \frac{\partial\hat{w}}{\partial\hat{z}} = \mathrm{div}\mathbf{V},$$

equations (6.15) may be written as

$$\left.\begin{aligned}\tau_{\hat{x}\hat{x}} &= \lambda\,\mathrm{div}\mathbf{V} + 2\mu\varepsilon_{\hat{x}\hat{x}}\,,\\ \tau_{\hat{y}\hat{y}} &= \lambda\,\mathrm{div}\mathbf{V} + 2\mu\varepsilon_{\hat{y}\hat{y}}\,,\\ \tau_{\hat{z}\hat{z}} &= \lambda\,\mathrm{div}\mathbf{V} + 2\mu\varepsilon_{\hat{z}\hat{z}}\,.\end{aligned}\right\} \tag{6.16}$$

We shall now show that all the non-diagonal elements of the deviatoric stress tensor (6.4) vanish when $\mathcal{T}$ is written in the principal axes $\hat{x}$, $\hat{y}$, $\hat{z}$ of the rate-of-strain tensor $\mathcal{E}$. It is suffices to prove that $\tau_{\hat{x}\hat{y}} = 0$. According to the first postulate, we can write

$$\tau_{\hat{x}\hat{y}} = c_1\varepsilon_{\hat{x}\hat{x}} + c_2\varepsilon_{\hat{y}\hat{y}} + c_3\varepsilon_{\hat{z}\hat{z}}\,. \tag{6.17}$$

If we rotate the coordinate system about the $\hat{x}$-axis by the angle π, as is shown in Figure 6.3, then, using postulate 2, we can also write

$$\tau_{\hat{x}'\hat{y}'} = c_1\varepsilon_{\hat{x}'\hat{x}'} + c_2\varepsilon_{\hat{y}'\hat{y}'} + c_3\varepsilon_{\hat{z}'\hat{z}'}. \tag{6.18}$$

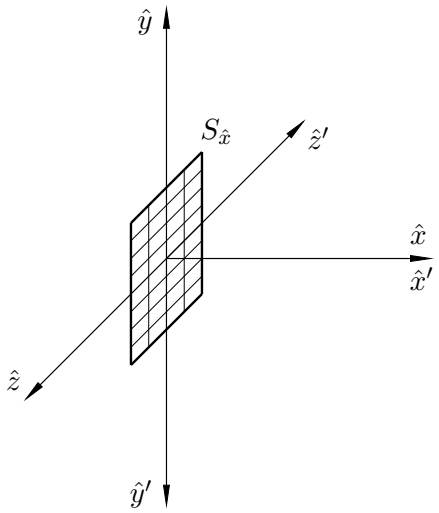

Figure 6.3: Rotation the coordinate system about the $\hat{x}$-axis by the angle π.

The new and old coordinates, and the corresponding velocity components are related as

$$\hat{x}' = \hat{x}, \quad \hat{y}' = -\hat{y}, \quad \hat{z}' = -\hat{z},$$
$$\hat{u}' = \hat{u}, \quad \hat{v}' = -\hat{v}, \quad \hat{w}' = -\hat{w}.$$

Consequently,

$$\varepsilon_{\hat{x}'\hat{x}'} = \frac{\partial \hat{u}'}{\partial \hat{x}'} = \frac{\partial \hat{u}}{\partial \hat{x}} = \varepsilon_{\hat{x}\hat{x}}\,, \qquad \varepsilon_{\hat{y}'\hat{y}'} = \frac{\partial \hat{v}'}{\partial \hat{y}'} = \frac{\partial \hat{v}}{\partial \hat{y}} = \varepsilon_{\hat{y}\hat{y}}\,,$$
$$\varepsilon_{\hat{z}'\hat{z}'} = \frac{\partial \hat{w}'}{\partial \hat{z}'} = \frac{\partial \hat{w}}{\partial \hat{z}} = \varepsilon_{\hat{z}\hat{z}}\,,$$

which, being substituted into to the equation (6.18) renders it in the form

$$\tau_{\hat{x}'\hat{y}'} = c_1\varepsilon_{\hat{x}\hat{x}} + c_2\varepsilon_{\hat{y}\hat{y}} + c_3\varepsilon_{\hat{z}\hat{z}}. \tag{6.19}$$

Since the right hand sides in (6.19) and (6.17) are identical, we can conclude that

$$\tau_{\hat{x}'\hat{y}'} = \tau_{\hat{x}\hat{y}}. \tag{6.20}$$

The second relation between these quantities may be deduced by simply recalling the physical meaning of $\tau_{\hat{x}\hat{y}}$ and $\tau_{\hat{x}'\hat{y}'}$; the former is the $\hat{y}$-projection of the stress acting upon the surface $S_{\hat{x}}$ drawn perpendicular to the $\hat{x}$-axis (see Figure 6.3), while the latter is the projection of the same stress on the $\hat{y}'$-axis. Since the $\hat{y}$- and $\hat{y}'$-axes are directed opposite to one another,

$$\tau_{\hat{x}'\hat{y}'} = -\tau_{\hat{x}\hat{y}}. \tag{6.21}$$

It follows from (6.20) and (6.21) that $\tau_{\hat{x}\hat{y}} = 0$.

By a similar procedure, we can shown that $\tau_{xz} = \tau_{yz} = 0$, and thus we can conclude that the deviatoric stress tensor (6.4) assumes a diagonal form

$$\mathcal{T} = \begin{pmatrix} \tau_{\hat{x}\hat{x}} & 0 & 0 \\ 0 & \tau_{\hat{y}\hat{y}} & 0 \\ 0 & 0 & \tau_{\hat{z}\hat{z}} \end{pmatrix}. \tag{6.22}$$

Using (6.16) on the right hand side of (6.4), we find that the sought constitutive equation has the form

$$\mathcal{T} = \lambda\,\mathrm{div}\mathbf{V} \begin{pmatrix} 1 & 0 & 0 \\ 0 & 1 & 0 \\ 0 & 0 & 1 \end{pmatrix} + 2\mu \begin{pmatrix} \varepsilon_{\hat{x}\hat{x}} & 0 & 0 \\ 0 & \varepsilon_{\hat{y}\hat{y}} & 0 \\ 0 & 0 & \varepsilon_{\hat{z}\hat{z}} \end{pmatrix}$$

or, equivalently,

$$\mathcal{T} = \lambda\,\mathrm{div}\mathbf{V}\, I + 2\mu\,\mathcal{E}. \tag{6.23}$$

Tensor (or vector) equations, like (6.23), do not depend on the choice of the coordinate system, i.e. the forms of the equations remain (but the tensors and vectors of course would have the specific representations pertaining to the coordinate system). Therefore, we can now simply go from the principal axes $(\hat{x}, \hat{y}, \hat{z})$ to arbitrarily oriented Cartesian coordinates, (x, y, z) with equation (6.23) remaining valid. Substituting (6.23) into (6.2), we will find that the stress tensor

$$\mathcal{P} = (-p + \lambda\,\mathrm{div}\mathbf{V})\, I + 2\mu\,\mathcal{E}, \tag{6.24}$$

or in the coordinate decomposition form

$$\begin{pmatrix} p_{xx} & p_{xy} & p_{xz} \\ p_{yx} & p_{yy} & p_{yz} \\ p_{zx} & p_{zy} & p_{zz} \end{pmatrix} = \big(-p + \lambda\,\mathrm{div}\mathbf{V}\big) \begin{pmatrix} 1 & 0 & 0 \\ 0 & 1 & 0 \\ 0 & 0 & 1 \end{pmatrix} + 2\mu \begin{pmatrix} \varepsilon_{xx} & \varepsilon_{xy} & \varepsilon_{xz} \\ \varepsilon_{yx} & \varepsilon_{yy} & \varepsilon_{yz} \\ \varepsilon_{zx} & \varepsilon_{zy} & \varepsilon_{zz} \end{pmatrix}.$$

Expressing the elements of the rate-of-strain tensor through the velocity components as in equation (5.3) (or equivalent (5.7)), we have that

$$p_{ij} = \big(-p + \lambda \, \mathrm{div}\mathbf{V} \big) \, \delta_{ij} + \mu \bigg(\frac{\partial V_i}{\partial x_j} + \frac{\partial V_j}{\partial x_i} \bigg), \qquad i, j = 1,\, 2,\, 3. \tag{6.25}$$

Here we use the index notations, with coordinates (x, y, z) denoted as (x_1, x_2, x_3) and the velocity components (u, v, w) as (V_1, V_2, V_3), respectively; δ_{ij} is the Kronecker delta,

$$\delta_{ij} = \begin{cases} 1 & \text{if} \quad i = j \\ 0 & \text{if} \quad i \neq j \end{cases}$$

Fluids satisfying equation (6.25) are called ***Newtonian fluids***; the parameter μ is called the ***first viscosity coefficient***, and parameter λ the ***second viscosity coefficient***. They reflect the physical properties and are thus independent of the flow motion (directly), although they may depend on the thermodynamic state of the fluid, e.g. the temperature; the mathematical relations expressing the dependence of the (first) viscosity coefficient is referred to as *viscosity laws*.

Experiments show that all the gasses and the majority of common liquids, like water, belong to are extremely well described by the constitutive relation for Newtonian fluids. However, for some liquids, like paint or blood, the constitutive equations can be more complicated. These fluids are called *non-Newtonian*, and the forms an important research area but will not be studied in this course.

Continuity Equation in Eulerian Variables.

The first of the fundamental physical laws to be employed to derive the governing equations of fluid flows is that of the mass conservation. To express this for a continuum in the Eulerian variables, we consider an arbitrary region $\mathcal{D}$ *fixed* in space (see Figure 7.1a) with fluid passing through $\mathcal{D}$ as time t increases; this region $\mathcal{D}$ is called a *control volume*. We denote the surface surrounding region $\mathcal{D}$ by S, and the *outward* unit vector normal to S by $\mathbf{n}$. The fluid mass contained in $\mathcal{D}$ at instant t may be expressed by the integral

$$m(t) = \iiint_{\mathcal{D}} \rho(t, \mathbf{r})\, d\tau, \tag{7.1}$$

where $d\tau$ is a volume element in $\mathcal{D}$.

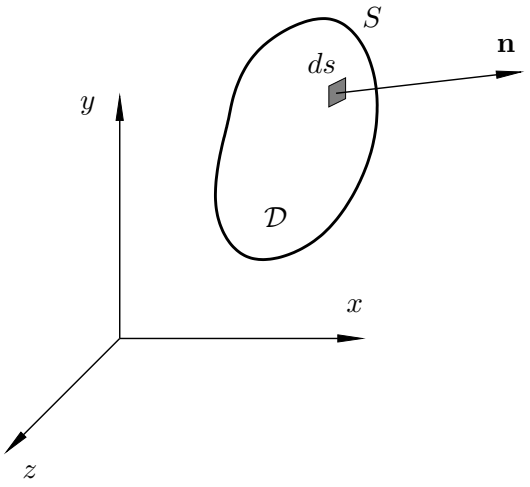

(a) Region $\mathcal{D}$ used in derivation of the mass concervation law.

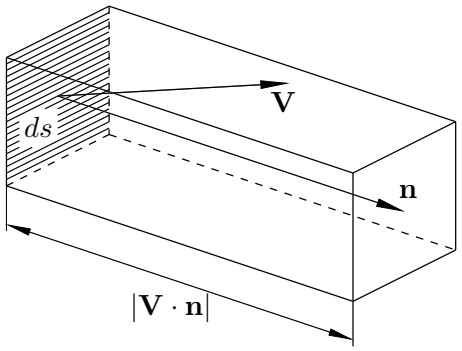

(b) Zoomed surface element ds and cylindrical region filled by the fluid passing through ds per unit time.

Figure 7.1: Schematic of the derivation of the mass conservation law.

Since region $\mathcal{D}$ does not change with time, the differentiation of (7.1) involves variation of the integrand only. We have

$$\frac{dm}{dt} = \iiint_{\mathcal{D}} \frac{\partial \rho}{\partial t}\, d\tau, \tag{7.2}$$

which represents the rate of change of mass inside $\mathcal{D}$. Provided that there are no sources or sinks of fluid inside $\mathcal{D}$, this mass variation must be only due to feeding of fluid through the surface S. The mass flux through a small element ds of the surface S is given by

$$\rho\big(\mathbf{V}\cdot\mathbf{n}\big)ds.$$

It equals to the local density ρ multiplied by volume of the parallelepiped (see Figure 7.1b) swept by the fluid passing through ds per unit time. The area of the base of the parallelepiped is ds and its ribs are $|\mathbf{V}\cdot\mathbf{n}|$ long.

The total mass flux (i.e. the mass per unit time) *out of* $\mathcal{D}$ through the entire surface S obviously is

$$\iint\limits_S \left(\rho \mathbf{V} \cdot \mathbf{n}\right) ds. \tag{7.3}$$

The mass conservation law, applied to $\mathcal{D}$, should be written as

$$\iint\limits_S \left(\rho \mathbf{V} \cdot \mathbf{n}\right) ds = -\frac{dm}{dt}.$$

Applying the Gauss's *divergence theorem* to the left hand side of this equation we have

$$\iiint\limits_{\mathcal{D}} \operatorname{div}(\rho \mathbf{V})\, d\tau = -\frac{dm}{dt}. \tag{7.4}$$

Combining (7.2) with (7.4) results in

$$\iiint\limits_{\mathcal{D}} \left[\frac{\partial \rho}{\partial t} + \operatorname{div}(\rho \mathbf{V})\right] d\tau = 0. \tag{7.5}$$

Suppose that both ρ and $\mathbf{V}$ have continuous derivatives. Then the region $\mathcal{D}$ is arbitrary, the integrand in (7.5) should be zero everywhere in the flow field,

$$\frac{\partial \rho}{\partial t} + \operatorname{div}(\rho \mathbf{V}) = 0. \tag{7.6}$$

Equation (7.6) is called the ***continuity equation***. Now it is expressed in the Eulerian variables. In this course our main focus will be on the so called ***incompressible flows***, which refer to the flows where the fluid density ρ remains constant, i.e. $\frac{d\rho}{dt} \equiv 0$, and so the continuity equation (7.6) reduces to

$$\operatorname{div}(\mathbf{V}) = 0. \tag{7.7}$$

Momentum Equation

The second fundamental physical law to be employed is that of conservation of momentum, or *Newton's Second Law*. It will be applied to a continuum of a fluid, which is a rather substantial step.

Recall first that when applied to a solid body, Newton's Second Law is written as

$$m\mathbf{a} = \mathbf{F} \qquad \text{or} \qquad m\frac{d\mathbf{V}}{dt} = \mathbf{F}. \tag{7.8}$$

Here m is the mass of the body, $\mathbf{a}$ acceleration and $\mathbf{F}$ the force applied to the body.

A few remarks should be made concerning equation (7.8). First, this equation is valid if a body motion is analyzed in the framework of an *inertial* coordinate system. Second, when more than one force is applied to the body then vector $\mathbf{F}$ in (7.8) must be interpreted as the vector sum of all forces acting on the body. Third, if the body is not "small" and its different parts experience different acceleration, then equation (7.8) serves to determine the acceleration $\mathbf{a}$ of the *mass center*. A convenient idealization, made when the body size is much smaller the characteristic path traced by the body during the time of observation,

is that the body is thought as a *material point*. In fluid dynamics the role of material points is played by the fluid particles.

Let us consider an ensemble of N material points. Each particle obeys the Newton's Second Law, that is,

$$m_i \frac{d\mathbf{V}_i}{dt} = \mathbf{F}_i. \tag{7.9}$$

Here suffix i is used to enumerate the particles in the assemble, and the acceleration $\mathbf{a}_i$ of the i-th particle is written via the velocity derivative $d\mathbf{V}_i/dt$. Since the mass m_i does not vary with time, equation (7.9) may be also written as

$$\frac{d\mathbf{K}_i}{dt} = \mathbf{F}_i \tag{7.10}$$

with $\mathbf{K}_i = m_i\mathbf{V}_i$ being the momentum of i-th material point. The force $\mathbf{F}_i$ is a superposition of external and internal forces

$$\mathbf{F}_i = \mathbf{F}_{ie} + \sum_{j=1,\, j\neq i}^{N} \mathbf{F}_{ij}, \tag{7.11}$$

where $\mathbf{F}_{ie}$ is the external force produced by any physical agents outside the system under consideration, while $\mathbf{F}_{ij}$ is the force exerted by the particle with number j upon the particle with number i. Due to *Newton's Third Law*, which states that an action and its reaction are equal in magnitude and opposite in direction, we have

$$\mathbf{F}_{ij} = -\mathbf{F}_{ji}.$$

Substitution of (7.11) into (7.10) and summation over all the particle in the system yields the momentum equation

$$\frac{d\mathbf{K}}{dt} = \sum_{i=1}^{N} \mathbf{F}_{ie}, \tag{7.12}$$

where $\mathbf{K}$ is the momentum of the entire material system

$$\mathbf{K} = \sum_{i=1}^{N} m_i\mathbf{V}_i; \tag{7.13}$$

internal forces obviously cancel in the course of summation due to the fact that $\mathbf{F}_{ij} = -\mathbf{F}_{ji}$.

Now we shall apply equation (7.12) to a continuum, a moving fluid. When expressing the derivative $d\mathbf{K}/dt$ on the left hand side of (7.12) in terms of the fluid dynamic variables, it is important to keep in mind that the momentum equation (7.12) is valid for a *material system consisting of the same elements*; no exchange of matter between the system under consideration and surrounding medium is allowed.

As opposed to a control volume fixed in space, we now consider an arbitrary region $\mathcal{D}$ containing the same fluid particles all the time. Such a region $\mathcal{D}$ is called *material volume*, and moves with the fluid particles, changing its shape and size with time, a fact that we indicate by writing $\mathcal{D}(t)$. At each instant t, the surface surrounding $\mathcal{D}(t)$ is denoted by S and its outward unit vector normal to S by $\mathbf{n}$ (see Figure 7.2). We then follow this volume of fluid particles as time increases, which may be considered as forming a *fluid body*, and

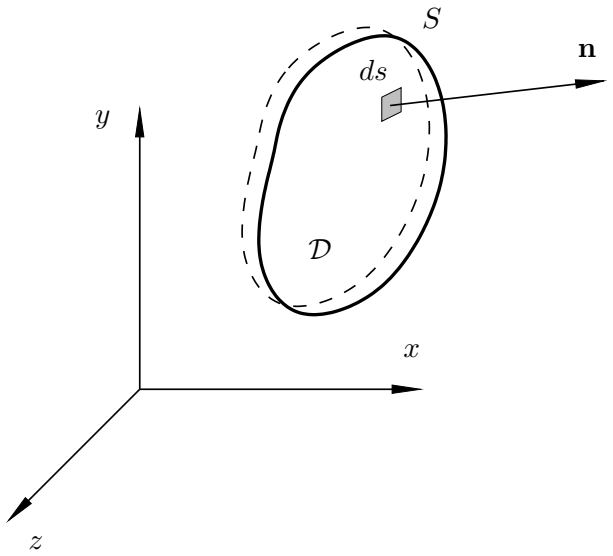

Figure 7.2: Motion of a volume of fluid particles. The dashed line stands for the deformed volume at time $t + \delta t$.

apply the momentum equation (7.12) to it. The momentum (7.13) of this 'fluid body' is expressed by the integral

$$\mathbf{K}(t) = \iiint\limits_{\mathcal{D}(t)} \rho(t, \mathbf{r})\mathbf{V}(t, \mathbf{r})\, d\tau. \tag{7.14}$$

Direct differentiation of (7.14) with respect to t involves differentiation of the integrand $\rho\mathbf{V}$ as well as an analysis of the fluid body deformation, which is significantly more intricate. This may be avoided if prior to differentiating $\mathbf{K}(t)$ a transformation of integration variables is performed in (7.14) with new integration variables chosen in such a way that the region is mapped into one that is fixed in space. A natural choice for the latter is the region occupied by the same particles at $t = t_0$, which we denote as $\mathcal{D}_0$. This mapping can be accomplished by the Lagrangian trajectories of the particles in $\mathcal{D}_0$:

$$\mathbf{r} = \mathbf{r}(t, \mathbf{r}_0), \tag{7.15}$$

which relates the "initial location" $\mathbf{r}_0$ of a fluid particle in $\mathcal{D}_0$ at time t_0 to its current location $\mathbf{r}$ in $\mathcal{D}(t)$ at time t. Formula (7.15) serves as a transformation of variables from (x, y, z) to (x_0, y_0, z_0) and vice versa. Using (7.15) in (7.14) results in

$$\mathbf{K}(t) = \iiint\limits_{\mathcal{D}_0} \rho\big[t, \mathbf{r}(t, \mathbf{r}_0)\big]\, \mathbf{V}\big[t, \mathbf{r}(t, \mathbf{r}_0)\big] \left|\frac{\partial(x, y, z)}{\partial(x_0, y_0, z_0)}\right| d\tau_0\,. \tag{7.16}$$

It follows from the continuity equation in Lagrangian variables (3.6) that

$$\left|\frac{\partial(x, y, z)}{\partial(x_0, y_0, z_0)}\right| = \frac{\rho_0}{\rho}.$$

Hence, (7.16) may be rewritten as

$$\mathbf{K}(t) = \iiint\limits_{\mathcal{D}_0} \rho_0 \mathbf{V}\big[t, \mathbf{r}(t, \mathbf{r}_0)\big]\, d\tau_0\,. \tag{7.17}$$

Here both the initial density ρ_0 and initial region $\mathcal{D}_0$ are independent on t. Therefore differentiation of (7.17) yields

$$\frac{d\mathbf{K}}{dt} = \iiint_{\mathcal{D}_0} \rho_0 \left[\frac{\partial \mathbf{V}}{\partial t} + \frac{\partial \mathbf{V}}{\partial x}\frac{\partial x(t,\mathbf{r}_0)}{\partial t} + \frac{\partial \mathbf{V}}{\partial y}\frac{\partial y(t,\mathbf{r}_0)}{\partial t} + \frac{\partial \mathbf{V}}{\partial z}\frac{\partial z(t,\mathbf{r}_0)}{\partial t} \right] d\tau_0 \,.$$

Noting that the expression in the square brackets is the acceleration of a fluid particle (3.10) we can further write

$$\frac{d\mathbf{K}}{dt} = \iiint_{\mathcal{D}_0} \rho_0 \frac{D\mathbf{V}}{Dt}\, d\tau_0.$$

Now using (7.15) to transform the integration over $\mathcal{D}_0$ back to that over $\mathcal{D}(t)$, we have

$$\frac{d\mathbf{K}}{dt} = \iiint_{\mathcal{D}} \rho \frac{D\mathbf{V}}{Dt} d\tau. \tag{7.18}$$

We have now managed to express the rate of change of the momentum in terms of the velocity field, which is an important step in deriving the moment equations.

The result (7.18) may be obtained directly, albeit perhaps less rigorously than the procedure above, from (7.14) by noting that $\rho d\tau$ stands for the mass contained in the infinitesimal volume $d\tau$ and remains constant by the law of mass conversation.

Quiz: Can you show the following? For ***any*** *physical quality G, a vector or a scalar,*

$$\frac{d}{dt}\iiint_{\mathcal{D}} \rho\, G\, d\tau = \iiint_{\mathcal{D}} \rho \frac{DG}{Dt}\, d\tau,$$

and

$$\frac{d}{dt}\iiint_{\mathcal{D}} G\, d\tau = \iiint_{\mathcal{D}} \Big[\frac{DG}{Dt} + G\mathrm{div}\mathbf{V} \Big]\, d\tau;$$

the second is referred to as ***Reynolds transport theorem****.*

Having considered the rate of the change of the momentum in this 'fluid body', we will exam the other side of the coin (Newton's Second Law), the forces (especially surface force) acting on the 'fluid body'.

Momentum Equations (continued)

We now consider the forces acting on the fluid element inside region $\mathcal{D}$ (see Figure 8.1). As we know, all the forces acting on a moving fluid fall into two classes, body forces and

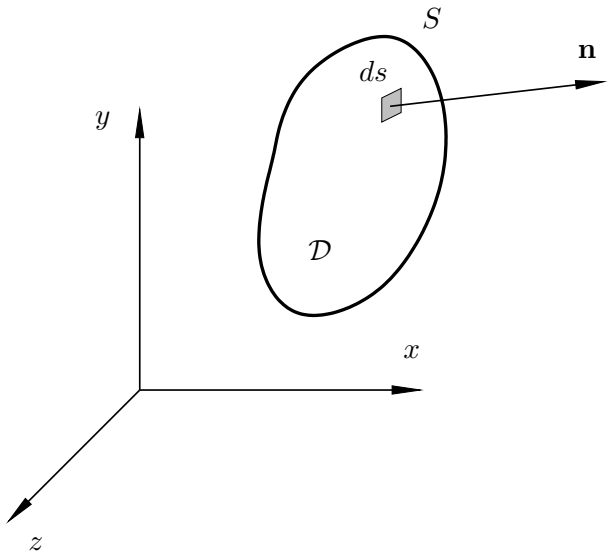

Figure 8.1: Forces acting on a fluid element occupying region $\mathcal{D}$.

surface forces. With $\mathbf{f}(\mathbf{r}, t)$ denoting the *body force* upon a unit mass, the force acting on a volume element $d\tau$ inside $\mathcal{D}$ is expressed as

$$\rho(\mathbf{r}, t)\mathbf{f}(\mathbf{r}, t)d\tau,$$

and the entire body force acting upon the fluid contained in region $\mathcal{D}$ is given by

$$\iiint\limits_{\mathcal{D}} \rho(\mathbf{r}, t)\mathbf{f}(\mathbf{r}, t)d\tau. \tag{8.1}$$

Let us now turn to the *surface forces*. According to its definition (2.1), a small element ds of the surface S surrounding region $\mathcal{D}$ experiences the force (see Figure 2.2)

$$d\mathbf{P}_n = \mathbf{p}_n ds = \mathcal{P} \cdot \mathbf{n}\, ds, \tag{8.2}$$

where we have used the stress representation formula (2.11). The total force acting on the fluid in $\mathcal{D}$ through S is expressed as a surface integral

$$\iint\limits_{S} \mathcal{P} \cdot \mathbf{n}\, ds. \tag{8.3}$$

The sum of (8.3) and (8.1) amounts to the total force acting on the fluid element, and should be used on the right-hand side of equation (7.12). Using for the left-hand side formula (7.18), we arrive at the ***integral form of the momentum equation***

$$\iiint\limits_{\mathcal{D}} \rho \frac{D\mathbf{V}}{Dt} d\tau = \iiint\limits_{\mathcal{D}} \rho\, \mathbf{f}\, d\tau + \iint\limits_{S} \mathcal{P} \cdot \mathbf{n}\, ds. \tag{8.4}$$

To express this equation in a differential form, we need to convert the integral for the surface force

$$\mathbf{P} \equiv \iint_S \mathcal{P} \cdot \mathbf{n}\, ds \tag{8.5}$$

into a volume integral, which would involve again use of the *Divergence Theorem*. To this end, we recall that $\mathcal{P} \cdot \mathbf{n}$ simply represents a vector resulting from the scalar product of each row vector of $\mathcal{P}$ with $\mathbf{n}$.

Thus, use of the Divergence Theorem to each row gives a volume integral

$$\mathbf{P} = \iiint_{\mathcal{D}} \mathrm{div}\mathcal{P}\, d\tau = \iiint_{\mathcal{D}} \nabla \cdot \mathcal{P}\, d\tau, \tag{8.6}$$

where the divergence is taken of, or equivalently the operator ∇ acts on, each row vector of $\mathcal{P}$. Using this volume integral for the surface force in (8.4), and noting that $\mathcal{D}$ is arbitrary, we conclude that

$$\rho \frac{D\mathbf{V}}{Dt} = \rho\, \mathbf{f} + \nabla \cdot \mathcal{P}. \tag{8.7}$$

This is the ***differential form of the momentum equation***, established first by Cauchy (1827). In terms of the components, it can be written as[†]

$$\rho\Big[\frac{\partial V_i}{\partial t} + V_j \frac{\partial V_i}{\partial x_j}\Big] = \rho f_i + \frac{\partial p_{ij}}{\partial x_j}.$$

It is worth noting that (8.7) has been derived for a rather general continuum, and hence is valid for both fluids and solids, the different physical properties of which are characterized by their respective constitutive relations.

The detail leading to (8.6) is given as follow, where use is made of the index notations with (x, y, z) denoting (x_1, x_2, x_3). According to (2.13), the projection of the vector equation (8.5) onto the x_i-axis may be written as

$$P_i = \iint_S n_j p_{ij}\, ds \qquad (i = 1,\ 2,\ 3). \tag{8.8}$$

Let the i-the row of $\mathcal{P}$ be denoted by the vector $\mathbf{A} = (A_1, A_2, A_3) = (p_{i1}, p_{i2}, p_{i3})$. The integrand on right-hand side of (8.8) is the scalar product of $\mathbf{A}$ and the unit normal vector $\mathbf{n}$, and so we have

$$P_i = \iint_S \big(\mathbf{A} \cdot \mathbf{n}\big) ds.$$

[†]Here and in what follows we use the Einstein's summation convention: terms containing a repeated suffix are to be regarded as summed over all three possible values of the suffix.

Using Gauss's divergence theorem, we can further write

$$P_i = \iiint_{\mathcal{D}} \mathrm{div}\mathbf{A}\, d\tau = \iiint_{\mathcal{D}} \frac{\partial p_{ij}}{\partial x_j}\, d\tau, \tag{8.9}$$

where use has been made of

$$\mathrm{div}\mathbf{A} = \frac{\partial A_j}{\partial x_j} = \frac{\partial p_{ij}}{\partial x_j}.$$

The relation (8.9) is nothing other than the i-th component of the vector equation (8.6).

The final jigsaw to be fitted into the equation is the constitutive equation (6.25) for Newtonian fluids, which states that

$$p_{ij} = (-p + \lambda\, \mathrm{div}\mathbf{V})\delta_{ij} + \mu\left(\frac{\partial V_i}{\partial x_j} + \frac{\partial V_j}{\partial x_i}\right).$$

In this lecture course, we restrict our attention to incompressible flows, for which the continuity equation (7.6) reduces to

$$\mathrm{div}\mathbf{V} = 0,$$

and the constitutive equation simplifies to

$$p_{ij} = -p\delta_{ij} + \mu\left(\frac{\partial V_i}{\partial x_j} + \frac{\partial V_j}{\partial x_i}\right). \tag{8.10}$$

The factor μ is known as ***dynamic viscosity coeffecient***. Its value for a fluid is normally found through experimental measurements. It depends on the temperature of the fluid, but varies insignificantly in a range close to the room temperature. However, the dependence must be accounted for if the temperature varies appreciably in the flow field. The mathematical relation describing the change of μ with the temperature is referred to as *viscosity law*.

With a *constant* μ, we differentiate (8.10) with respect to x_j to obtain

$$\frac{\partial p_{ij}}{\partial x_j} = -\frac{\partial p}{\partial x_i} + \mu\frac{\partial}{\partial x_j}\left(\frac{\partial V_i}{\partial x_j}\right) + \mu\frac{\partial}{\partial x_j}\left(\frac{\partial V_j}{\partial x_i}\right). \tag{8.11}$$

Note that repeating indices imply the summation, namely,

$$\frac{\partial V_j}{\partial x_j} = \mathrm{div}\mathbf{V} = 0, \quad \frac{\partial}{\partial x_j}\left(\frac{\partial V_i}{\partial x_j}\right) = \nabla^2 V_i,$$

where $\nabla^2 = \frac{\partial^2}{\partial x^2} + \frac{\partial^2}{\partial y^2} + \frac{\partial^2}{\partial z^2}$ denotes the Laplace operator. Use of the above relations in (8.11) gives

$$(\nabla \cdot \mathcal{P})_i = \frac{\partial p_{ij}}{\partial x_j} = -\frac{\partial p}{\partial x_i} + \mu\nabla^2 V_i,$$

or in the vector form,

$$\nabla \cdot \mathcal{P} = -\nabla p + \mu\nabla^2\mathbf{V}. \tag{8.12}$$

Here ∇p stands for the gradient of the pressure p, and $\nabla^2\mathbf{V}$ denotes a vector whose components are $(\nabla^2 u, \nabla^2 v, \nabla^2 w)$.

Substitution of (8.12) into (8.7)), we finally obtain the momentum equation[‡]

$$\frac{\partial \mathbf{V}}{\partial t} + (\mathbf{V}\cdot\nabla)\mathbf{V} = \mathbf{f} - \frac{1}{\rho}\nabla p + \nu\nabla^2\mathbf{V}. \tag{8.13a}$$

Here $\nu = \mu/\rho$ is called the ***kinematic viscosity***. The momentum equation (8.13a) and the continuity equation

$$\mathrm{div}\mathbf{V} = 0 \tag{8.13b}$$

form a closed set of the ***Navier-Stokes equations***, which are the fundamental equations governing incompressible flows.

For compressible flows, the density and hence the temperature are two more dependent variables to be found along with the velocity and the pressure. Therefore, two more equations are needed. One of the additional equation is that governing the energy and can be derived by applying the law of energy conservation, while the other is the so-called state equation. In this course, we focus on incompressible flows.

In the vector form, equations (8.13a) and (8.13b) are valid in any coordinate system. When a specific coordinate system is adopted (for the convenience of investigating particular problems), all that is required is that the differential operators in the equations assume the appropriate forms as defined in vector calculus. In the Cartesian coordinate decomposition form, the Navier-Stokes equations (8.13a) and (8.13b) are written as

$$\Big[\frac{\partial}{\partial t} + u\frac{\partial}{\partial x} + v\frac{\partial}{\partial y} + w\frac{\partial}{\partial z}\Big]u = f_x - \frac{1}{\rho}\frac{\partial p}{\partial x} + \nu\left(\frac{\partial^2}{\partial x^2} + \frac{\partial^2}{\partial y^2} + \frac{\partial^2}{\partial z^2}\right)u, \tag{8.14a}$$

$$\Big[\frac{\partial}{\partial t} + u\frac{\partial}{\partial x} + v\frac{\partial v}{\partial y} + w\frac{\partial}{\partial z}\Big]v = f_y - \frac{1}{\rho}\frac{\partial p}{\partial y} + \nu\left(\frac{\partial^2}{\partial x^2} + \frac{\partial^2}{\partial y^2} + \frac{\partial^2}{\partial z^2}\right)v, \tag{8.14b}$$

$$\Big[\frac{\partial}{\partial t} + u\frac{\partial}{\partial x} + v\frac{\partial}{\partial y} + w\frac{\partial}{\partial z}\Big]w = f_z - \frac{1}{\rho}\frac{\partial p}{\partial z} + \nu\left(\frac{\partial^2}{\partial x^2} + \frac{\partial^2}{\partial y^2} + \frac{\partial^2}{\partial z^2}\right)w, \tag{8.14c}$$

$$\frac{\partial u}{\partial x} + \frac{\partial v}{\partial y} + \frac{\partial w}{\partial z} = 0. \tag{8.14d}$$

These four equations involve four unknown functions, the velocity components u, v, w and pressure p.

In the momentum equation (8.13a), the nonlinear term $(\mathbf{V}\cdot\nabla)\mathbf{V}$ is referred to as ***inertial term***, while $\nu\nabla^2\mathbf{V}$ is referred to as ***viscous diffusion***. With the latter being present, the equation is second order in space, but if this term is neglected as is done in the so-called inviscid approximation, the equation reduces to the ***Euler equations***, which are of first order. This has a serious implication on how the boundary conditions should be imposed.

The nonlinear term $(\mathbf{V}\cdot\nabla)\mathbf{V}$ underpins the exceedingly rich and complex behaviours of fluid flows, and is the primary cause of difficulty for the investigation of the Navier-Stokes equations. The reason is that this nonlinear term generates motions on increasingly small scales, exhibited as rapidly variation in time and space, until a cut-off is provided by the viscous dissipation. At the same time, it is also through this nonlinear term that small-scale motions could also transfer part of their energy to large-scale motions.

[‡] *Quiz: In certain flows, the coefficient may not be constant due to its dependence on temperature. What is the form of the momentum equation in this case?*

By taking the curl of the momentum equation (8.13a) and making use of the continuity equation, one may derive the equation for the vorticity $\boldsymbol{\omega}$,

$$\frac{\partial \boldsymbol{\omega}}{\partial t} + (\mathbf{V} \cdot \nabla)\boldsymbol{\omega} = (\boldsymbol{\omega} \cdot \nabla)\mathbf{V} + \nu \nabla^2 \boldsymbol{\omega}, \tag{8.15}$$

the derivation of which is left as an exercise. The first term on the right-hand side of(8.15) represents the *'stretching'* and *'tilting'* of the vortex line by the strain rate of the flow as is illustrated in Figure 8.2. The former tends to intensify the vorticity.

Figure 8.2: Illustration of 'stretching' and 'tilting' of a vortex line.

For two-dimensional flows, the vorticity is perpendicular to the flow velocity, and the vortex stretching and tilting are absent. This represents a fundamental difference between two- and three-dimensional flows.

Non-dimensionalisation of the Navier-Stokes Equations

As is common in physical sciences, when studying fluid motions it is informative to introduce non-dimensional independent and dependent variables by using the representative time T_{ref}, length L_{ref}, velocity V_{ref}, etc., as references, and rewrite the Navier-Stokes equations in a dimensionless form. The dimensionless coordinate, time and velocity are

$$\bar{\mathbf{r}} = \mathbf{r}/L_{\text{ref}} = (x, y, z)/L_{\text{ref}}, \quad \bar{t} = t/T_{\text{ref}}, \quad \bar{\mathbf{V}} = \mathbf{V}/V_{\text{ref}} = (u, v, w)/V_{\text{ref}}, \tag{8.16}$$

while the pressure $\bar{p}$ is introduced by writing

$$p = p_0 + \rho V_{\text{ref}}^2 \bar{p},$$

where p_0 is a constant, taken to be the pressure at a reference point; the choice of p_0 does not affect the equations since the pressure appears in the gradient operator (and furthermore does not affect the solution if no interface surface is involved in the flow). In terms of the non-dimensional variables, the Navier-Stokes equations become

$$\text{St}\frac{\partial \bar{\mathbf{V}}}{\partial \bar{t}} + (\bar{\mathbf{V}} \cdot \nabla)\bar{\mathbf{V}} = -\nabla \bar{p} + \frac{1}{\text{Re}}\nabla^2 \bar{\mathbf{V}},$$

where the differential operators are now defined with respect to $\bar{t}$ and $\bar{\mathbf{r}}$, and the body force is neglected. In the equations, St and Re are two non-dimensional parameters, defined as

$$\text{St} = \frac{L_{\text{ref}}}{V_{\text{ref}} T_{\text{ref}}}, \quad \text{Re} = \frac{V_{\text{ref}} L_{\text{ref}}}{\nu};$$

they are called ***Strouhal number*** and ***Reynolds number***, respectively. The Strouhal number measures the unsteadiness of the flow. Note if there is no externally imposed time scale, then the natural time scale is $T_{\text{ref}} = L_{\text{ref}}/V_{\text{ref}}$, for which $\text{St} = 1$. The Reynolds number measures the size of the inertial $(\mathbf{V} \cdot \nabla)\mathbf{V}$ relative to that of the viscous diffusion $\nu\nabla^2\mathbf{V}$.

The choice of the reference quantities depends on the problem under consideration. A representative example is the air flow around an aerofoil that may be undergoing pitching movement with a frequency ω. Suppose that the length of the aerofoil is L and the velocity

Figure 8.3: Sketch of a flow around a pitching aerofoil.

of the uniform flow approaching the aerofoil is V_∞. The obvious choice is

$$L_{\text{ref}} = L, \qquad T_{\text{ref}} = \omega^{-1}, \qquad V_{\text{ref}} = V_\infty.$$

The non-dimensionalisation brings about a few benefits. First, the number of parameters is reduced. For the aerofoil under consideration, there are 5 dimensional parameters: ρ and μ in the momentum equation plus L, ω and V_∞ specifying the flow, but only two dimensionless parameters, St and Re, appear after non-dimensionalisation. Second, after non-dimensionalisation, it transpires that what control the flow are the resultant dimensionless parameters, and that the dimensional ones do not play an independent role. This implies that if two flows are *geometrically similar* and have the same non-dimensional parameters, they would be identical in the non-dimensional variables, regardless the differences in the values of the dimensional parameters. This property is referred to as ***dynamic similarity***, and forms the basis for laboratory experiments using rescaled models, e.g. wind tunnel tests of scaled-down wing models. Third, the non-dimensionalised form of the equations shows the relative importance of different terms according to the sizes of the dimensionless parameters. In particular, when Re is very small ($\mathrm{Re} \ll 1$), the inertial and unsteady terms may be neglected as a first approximation, with the Navier-Stokes equations being reduced to linear equations, known as *Stokes equations*. This type of flows is referred to as ***Stokes flows***. In the opposite limit of Re being very large ($\mathrm{Re} \gg 1$), the viscous terms can be neglected and the flow may be treated as being inviscid as a first approximation. This approximation works well for the majority of the flow field.

It should be pointed out that non-dimensionalisation is not merely a simple formality, and it requires a careful judgment of how 'big' and how fast of the phenomenon under investigation. The choice of references quantities may not at all be as obvious as it looks in the above problem, especially when more than one length, time and velocity scales are present. Furthermore, the non-dimensionalization can be rather intricate when one probes into the details of the flow. For example, the three coordinates may not always be scaled by the same reference length, and accordingly the velocity components not by the same reference velocity. For the flow past an aerofoil, in a thin layer adjacent to the aerofoil surface, which is known as *boundary layer*, the coordinate and velocity in the wall-normal direction should be scaled by $\mathrm{Re}^{-1/2}L$ and $\mathrm{Re}^{-1/2}V_\infty$, rendering the viscous diffusion to balance the inertia.

The discussions indicates that the question of whether viscosity is important or not is not merely determined by the physical property μ or ν of the fluid. Rather it depends on Re, which characterizes the *flow* rather than just the *fluid* itself, as well as on which part or aspect of the flow is considered. For a flow of the same viscous fluid, air past an aerofoil say, the *flow* away from the surface may be inviscid if the Reynolds number Re is large, but the flow near the surface is viscous. If the Reynolds number is moderate, then the majority flow field is viscous. From this standpoint, the term *inviscid fluids* that is widely used is inappropriate. There is no such a thing as an 'inviscid fluid' (except the so-called super-fluids such as liquid helium-3 and 4 at extremely low temperatures). We will therefore refrain from using this term as much as possible, and will use instead *inviscid flows*.

Boundary Conditions

In order to determine the flow motions, appropriate boundary conditions must be imposed. Two broad types of boundaries may arise.

Boundary on a solid surface

The solid surface may be at rest or in motion with a velocity $\mathbf{V}_s$ say.

Figure 8.4: Sketch of different types of boundaries.

For *viscous flows*, the velocity of the fluid is required to be the same as $\mathbf{V}_s$, i.e.

$$\mathbf{V} = \mathbf{V}_s, \tag{8.17}$$

on the surface. The velocity can be decomposed into a component perpendicular to the surface, and a component in the tangent plane. Both components of the fluid are required to be the same as the counterparts of the solid surface. The condition on the normal component can be expressed as

$$\mathbf{V} \cdot \mathbf{n} = \mathbf{V}_s \cdot \mathbf{n}, \tag{8.18}$$

which $\mathbf{n}$ denotes the unit normal of the surface. This is referred to as ***no-penetration*** or ***impermeability condition***. The condition on the tangent component is called the***no-slip condition***. The no-penetration is rather obvious, but the reason for the no-slip condition is not. This condition is attributed to the nature to molecular interaction between the fluid and the solid, however a complete theoretical justification is yet to be developed for a general fluid flow[§], and therefore its correctness relied upon the available experimental evidence. Indeed, all experiments on flows on the macroscopic scale support the view that the no-slip condition is a universal law of fluid dynamics.

For flows bounded by solid surfaces, no condition is required on the stress at the surface. Instead the surface stress can be calculated once the velocity is known, and indeed the prediction of the surface stress and hence the drag is one of the primary reasons for studying the flow.

[§]For a perfect gas the *kinetic gas theory* may be used for this purpose. In order to deduce the boundary condition for the Navier-Stokes equations on a rigid body surface, one needs to solve the Boltzmann equation in the so-called Knudsen layer which occupies a small vicinity of the surface with the characteristic thickness being comparable with the molecular mean free path. If this approach is applied, for example, to the flow near a stationary solid surface, then it may be shown that the tangential velocity does not really vanish on the wall. Instead, it is proportional to its gradient in the wall-normal direction,

$$u = \alpha \frac{\partial u}{\partial n}.$$

However, the factor α is small in the sense that $\alpha \to 0$ as $Kn \to 0$, such that taking the macroscopic limit reduces the above result to the no-slip condition.

However, if the flow is considered (approximated) as being *inviscid*, the no-slip condition, i.e. continuity of the tangent velocity, must be abandoned, and only the velocity normal to the surface is required to be equal to that of the solid surface, that is, only the impermeability condition (8.18) can be imposed.

There also exist so-called *perforated porous surfaces*, through which a fluid may be injected or sucked out for flow control purpose. In such a situation, (8.18) and (8.17) remain valid provided that $\mathbf{V}_s$ is taken to be the injection or suction velocity.

Fluid/fluid interface

Between two fluids of different physical properties (e.g. density or viscosity), an interface forms between them. The interface may conveniently be described by a contour of a

Figure 8.5: Interface between two fluids.

function $F(t, \mathbf{r})$,

$$F(t, \mathbf{r}) = 0,$$

where the function F is part of the solution to be determined along with the flow field. The unit normal at an arbitrary point on the interface is given by

$$\mathbf{n} = \frac{\nabla F}{|\nabla F|}.$$

The two fluid fields interact through the boundary conditions.

If both flows are treated as being viscous, the velocities of the two fluids, which we distinguish by superscripts 1 and 2, are required to be equal at the interface, i.e.

$$\mathbf{V}^{(1)} = \mathbf{V}^{(2)}.$$

As the interface is part of the solution to be determined, we need also to impose the condition on the stress. The latter is required to be continuous across the interface, that is,

$$\mathcal{P}^{(1)} \cdot \mathbf{n} = \mathcal{P}^{(2)} \cdot \mathbf{n}.$$

Note that each side is a vector representing the surface stress, and so the above relation implies continuity of both the stress components normal and tangent to the surface.

For inviscid flows on both sides, the continuity of the velocity is imposed on its component normal to the interface,

$$\mathbf{V}^{(1)} \cdot \mathbf{n} = \mathbf{V}^{(2)} \cdot \mathbf{n}.$$

The stress then degenerates to the pressure, which is required to be continuous at the interface, and so

$$p^{(1)} = p^{(2)}.$$

In particular, if one of the fluid fields, fluid 2 say, is deemed to be dynamically insignificant, then the pressure $p^{(2)}$ is a constant. This is the so-called ***free surface (boundary)***.

In order to fix the flow fields and the interface, a so-called ***kinematic condition*** has to be imposed, which asserts that any fluid particle that is initially on the interface remains on the surface. Mathematically, this requirement can be expressed as

$$\frac{\partial F}{\partial t} + (\mathbf{V} \cdot \nabla) F = 0, \tag{8.19}$$

the proof of which is left as an exercise. It should be noted that fluid particles do not necessarily 'stick' to the interface, and may actually 'slide' along it.

Exact Solutions of the Navier-Stokes Equations.

The term *exact solution* refers to situations where the governing fluid dynamics equations may be solved in an analytical form (in terms of elementary functions), or where they may be reduced to ordinary differential equations.

As the Navier-Stokes equations are nonlinear, exact solutions are possible only in a small number of simple configurations, where the nonlinear terms often vanish identically, and/or a similarity reduction is possible. It should also be noted that solutions to the Navier-Stokes equations are not unique even for the same configuration (i.e. boundary conditions). Very often, an exact solution represents a simple form, which may be unstable and hence not always observable in reality, and what is observed instead are more complex states. Nevertheless, it is important to seek typical exact solutions in order to illustrate fundamental flow physics. Furthermore, those exact solutions provide a starting point for the investigation of *instability* that leads to more complex states of the flow.

For the most common body force, the gravity force, a potential U can be found such that $\mathbf{f} = -\nabla U$. The body force can be absorbed into the refined pressure $p + U/\rho$, which means that gravity plays no role if the flow involves no interface or free surface. We shall assume that no other body force is present.

Unidirectional Flows

A class of flows which admit exact solution is the so-called *unidirectional flows*, where the fluid moves only in one direction. The context of these flows is provided by the flow through a *straight pipe of an arbitrary cross section.*

Figure 9.1: Configuration of unidirectional flows

We now describe this class of flows in the Cartesian coordinates (x, y, z) with the x-axis aligned with the flow direction, and $y-$ and $z-$axes are on the cross section plane. The velocity is then expressed as

$$\mathbf{V} = \big(u(t, x, y, z), 0, 0\big).$$

The governing equation for u can be deduced as follows.

Since $v = w = 0$, the continuity equation (8.14d) reduces to

$$\frac{\partial u}{\partial x} = 0,$$

which indicates that u is independent of x, and so

$$u = u(t, y, z).$$

The y and z-momentum equations (8.14b,c) reduce to

$$\frac{\partial p}{\partial y} = 0, \quad \frac{\partial p}{\partial z} = 0,$$

implying that p is a function of x and t only,

$$p = p(t, x).$$

The x-momentum equation (8.14a) becomes

$$\frac{\partial u}{\partial t} = -\frac{1}{\rho}\frac{\partial p}{\partial x} + \nu\big(\frac{\partial^2}{\partial y^2} + \frac{\partial^2}{\partial z^2}\big)u,$$

which is linear. Rearranging, we have

$$\frac{\partial u}{\partial t} - \nu\big(\frac{\partial^2}{\partial y^2} + \frac{\partial^2}{\partial z^2}\big)u = -\frac{1}{\rho}\frac{\partial p}{\partial x}. \tag{9.1}$$

Note that the left-hand side is a function of y, z and t only, whereas the right-hand side depends only on x and t. It follows that the pressure gradient must a function of t only.

Equation (9.1) covers several flows that are unidirectional including the plane Couette flow, plane Poiseuille flow, Hagen-Poiseuille flow (flow through a circular pipe), in the unsteady case the Rayleigh layer and the Stokes layer.

Couette Flow

This is the incompressible flow between two parallel flat plates, which are infinitely large and separated by a distance h as shown in Figure 9.2; the lower plate is kept stationary in the laboratory frame, while the upper moves parallel itself with *constant* velocity U. The flow is brought into motion purely by the moving plate through the viscous shear stress. We use Cartesian coordinates with the x-axis drawn along the surface of the lower plate in the direction of the upper plate motion, y-axis perpendicular to the plates, and z-axis perpendicular to the sketch plane in Figure 9.2.

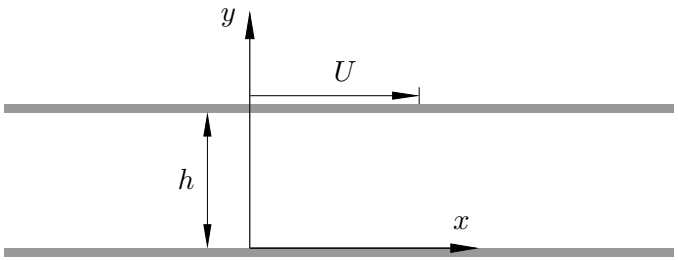

Figure 9.2: The problem layout.

The presumed unidirectional flow is certainly consistent with the boundary conditions that $v = w = 0$ at both plates. Since the plates are infinitely large (or in practice treated

as such when their size is much greater than h), the flow may be invariant in z-direction, i.e.

$$\frac{\partial u}{\partial z} = 0.$$

Also, no pressure gradient is imposed to push the fluid through, and so

$$\frac{\partial p}{\partial x} = 0. \tag{9.2}$$

The flow is also steady and so

$$\frac{\partial u}{\partial t} = 0.$$

Therefore for the Couette flow, (9.1) simplifies further to

$$\frac{\partial^2 u}{\partial y^2} = 0. \tag{9.3}$$

Alternatively, the admissible form of the solution and equation (9.3) can be deduced from the Navier-Stokes equations (8.14) based on the following simplifications:

1. The velocity of the upper plate has been kept constant for long enough for the flow to become steady, i.e.
$$\frac{\partial u}{\partial t} = \frac{\partial v}{\partial t} = \frac{\partial w}{\partial t} = 0. \tag{9.4}$$

2. If the distance h between the plates is small as compared to the characteristic longitudinal and spanwise lengths of the plates, then the plates may be viewed as infinite. In this case the solution should be invariant with respect to an arbitrary shift in the x- or z-directions, which means that the velocities are independent of x and z, i.e.
$$\frac{\partial}{\partial x}(u, v, w) = 0, \quad \frac{\partial}{\partial z}(u, v, w) = 0, \tag{9.5}$$

In view of (9.5) the first and third terms in the equation (8.14d) should be disregarded, leaving

$$\frac{\partial v}{\partial y} = 0. \tag{9.6}$$

It follows that v must be a constant v_0. The boundary impermeability condition,

$$v\Big|_{y=0} = v\Big|_{y=h} = 0,$$

implies that $v_0 = 0$, and thus

$$v \equiv 0 \tag{9.7}$$

everywhere in the flow field.

Let us now consider the x-momentum equation (8.16a). Term by term inspection of this equation shows that it may be simplified significantly. In fact all the underbraced terms

$$\underbrace{\frac{\partial u}{\partial t}}_{(9.4)} + \underbrace{u\frac{\partial u}{\partial x}}_{(9.5)} + \underbrace{v\frac{\partial u}{\partial y}}_{(9.7)} + \underbrace{w\frac{\partial u}{\partial z}}_{(9.5)} = -\underbrace{\frac{1}{\rho}\frac{\partial p}{\partial x}}_{(9.2)} + \underbrace{\nu\frac{\partial^2 u}{\partial x^2}}_{(9.5)} + \nu\frac{\partial^2 u}{\partial y^2} + \underbrace{\nu\frac{\partial^2 u}{\partial z^2}}_{(9.5)}$$

vanish; the reason for this is indicated by the equation number below the corresponding term. We end up with the same equation as (9.3) as expected.

A similar inspection of the z-momentum equation (8.16c) shows that

$$\frac{\partial^2 w}{\partial y^2} = 0.$$

Obviously, the solution satisfies the boundary (no-slip) conditions,

$$w\Big|_{y=0} = w\Big|_{y=h} = 0,$$

is $w \equiv 0$ everywhere. This result together with (9.7) indicates that the flow is indeed unidirectional.

Equation (9.3) has to be solved with the boundary conditions

$$u\Big|_{y=0} = 0, \qquad u\Big|_{y=h} = U. \tag{9.8}$$

Solving (9.3) with (9.8) yields

$$u = \frac{U}{h} y. \tag{9.9}$$

Thus the fluid velocity grows linearly from zero on the lower plate to U on the upper plate, as it is shown in Figure 9.3.

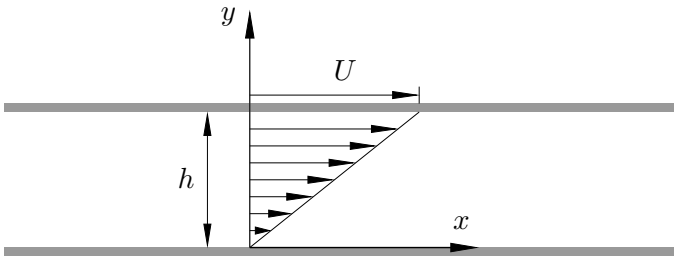

Figure 9.3: The Couette flow.

We see that in the Couette flow all the fluid particles are travelling along straight lines parallel to the x-axis with the velocity given by (9.9). For this flow, the appropriate Reynolds number is defined as

$$\mathrm{Re} = Uh/\nu.$$

This simple solution (9.9) exists for all Re, but the flow represented by it can be observed in experiments when $\mathrm{Re} < 300$. It may be noted that the shear stress at the moving plate is $p_{xy} = \frac{1}{2}\nu U/h$, and the viscous drag exerted on the plate with area S is

$$D = \frac{1}{2}\nu(U/h)S,$$

which is to be balanced by a force applied to pull the plate. By measuring this force, one can calculate the viscosity coefficient using the formula above. This forms the basis for measuring the fluid viscosity.

When Re is appreciably greater than 300, the flow assumes a complex turbulent state.

Poiseuille Flow

This is the flow through a channel between two (infinitely) large parallel plates which are *stationary* with the fluid being driven by the pressure difference, $\Delta p = p_1 - p_2$, between the two channel ends. Here p_1 and p_2 are the values of pressure in cross-sections 1 and 2, respectively; see Figure 9.4. For a practical example, one might think of a pipeline used for

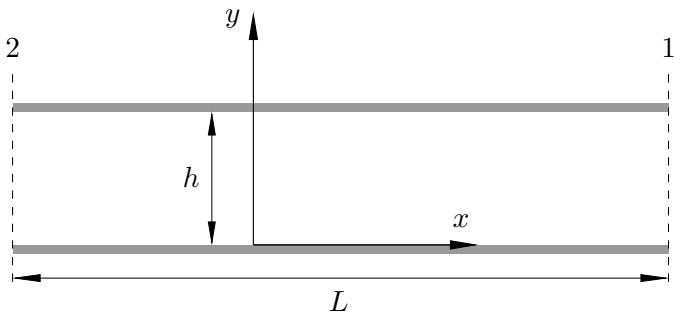

Figure 9.4: The Poiseuille flow.

transporting oil or natural gas. In order to maintain the flow through the pipeline, suitably spaced pump stations are built to create a pressure difference along the correspondent segments of the line. If we denote the length of the channel by L then an average pressure gradient along the channel may be calculated as

$$\left.\frac{dp}{dx}\right|_{\text{average}} = \frac{\Delta p}{L}. \tag{9.10}$$

Note that for the fluid to flow from left to right, Δp should be negative.

If the channel is long enough, then after initial adjustment after switching on and local adjustment near the channel intake (section 2), the longitudinal velocity profile establishes itself and for the rest of the flow would be independent of both time t and the longitudinal coordinate x, i.e.

$$\frac{\partial u}{\partial t} = 0, \quad \frac{\partial u}{\partial x} = 0, \tag{9.11}$$

Since the problem considered is invariant with respect to an arbitrary shift in spanwise direction, we can also claim that the derivative of any function with respect to z is zero,

$$\frac{\partial}{\partial z} = 0. \tag{9.12}$$

A steady unidirectional flow forms, i.e. $v = w \equiv 0$ (which can be established via the same argument in the case of the Couette flow, and so is not repeated here). With (9.11) and (9.12), equation (9.1) simplifies to

$$\frac{\partial^2 u}{\partial y^2} = \frac{1}{\mu}\frac{\partial p}{\partial x}. \tag{9.13}$$

Here $\mu = \rho\nu$ is the dynamic viscosity coefficient, and is taken to be a constant. Being steady, the pressure gradient $\partial p/\partial x$ remains constant all over the flow field, which makes formula (9.10) applicable for calculating not only an average but also the actual pressure gradient.

Integrating (9.13) with the no-slip conditions on the two plates

$$u\Big|_{y=0} = u\Big|_{y=h} = 0,$$

we find that in the flow considered the velocity profile is parabolic (see Figure 9.5),

$$u = \frac{1}{2\mu}\frac{dp}{dx}(y-h)y = -\frac{1}{2\mu}\frac{dp}{dx}\Big[(\frac{h}{2})^2 - (y-\frac{h}{2})^2\Big].$$

The maximum velocity is reached at the middle of the channel, $y = \frac{1}{2}h$, and is given by

$$u_{\max} = \frac{h^2}{8\mu}\left|\frac{dp}{dx}\right| = \frac{h^2|\Delta p|}{8\mu L}.$$

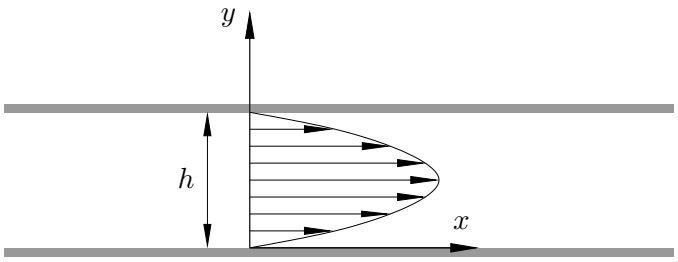

Figure 9.5: Velocity profile in the Poiseuille flow.

An appropriate Reynolds number is defined as

$$\mathrm{Re} = u_{\max}h/(2\nu).$$

The flow with the predicted parabolic profile, which is referred to as *laminar state*, exists for all Re, and indeed can be established to a good degree of accuracy when $\mathrm{Re} < 1000$. However, when Re exceeds 1000, the actually flow to be observed depends on surface roughness, unsteadiness in the pressure gradient and other perturbations which may be present in the flow environment. Unless these are kept at a very low level, the flow assumes a turbulent state.

Hagen-Poiseuille Flow

This is an axisymmetric analogue of the plane Poiseuille flow discussed in Lecture 9. An incompressible fluid flow is again driven by a pressure gradient but now through a tube of circular cross-section. This is a special case of the general unidirectional flows set up in Lecture 9. It is convenient to use the cylindrical polar coordinates in order to take advantage of the fact that the flow is symmetric with respect to the tube axis. In order to be consistent with the general description in the Cartesian coordinates (in Lecture 9), the x-axis of the cylindrical coordinate system (r, ϕ, x) (Figure 10.1) is taken to be along the centre-line of the tube (Figure 10.2). With the corresponding velocity components being

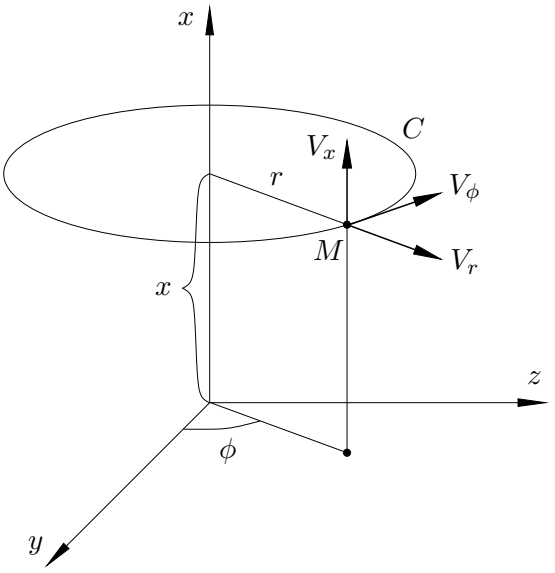

Figure 10.1: Cylindrical coordinates.

designated as shown in Figure 10.1, the Navier-Stokes equations are written as

$$\frac{\partial V_r}{\partial t}+V_r\frac{\partial V_r}{\partial r}+\frac{V_\phi}{r}\frac{\partial V_r}{\partial \phi}+V_x\frac{\partial V_r}{\partial x}-\frac{V_\phi^2}{r}=-\frac{1}{\rho}\frac{\partial p}{\partial r}+ \\ +\nu\left(\frac{\partial^2 V_r}{\partial x^2}+\frac{1}{r^2}\frac{\partial^2 V_r}{\partial \phi^2}+\frac{\partial^2 V_r}{\partial r^2}+\frac{1}{r}\frac{\partial V_r}{\partial r}-\frac{V_r}{r^2}-\frac{2}{r^2}\frac{\partial V_\phi}{\partial \phi}\right), \tag{10.1a}$$

$$\frac{\partial V_\phi}{\partial t}+V_r\frac{\partial V_\phi}{\partial r}+\frac{V_\phi}{r}\frac{\partial V_\phi}{\partial \phi}+V_x\frac{\partial V_\phi}{\partial x}+\frac{V_rV_\phi}{r}=-\frac{1}{\rho r}\frac{\partial p}{\partial \phi}+ \\ +\nu\left(\frac{\partial^2 V_\phi}{\partial x^2}+\frac{1}{r^2}\frac{\partial^2 V_\phi}{\partial \phi^2}+\frac{\partial^2 V_\phi}{\partial r^2}+\frac{1}{r}\frac{\partial V_\phi}{\partial r}-\frac{V_\phi}{r^2}+\frac{2}{r^2}\frac{\partial V_r}{\partial \phi}\right), \tag{10.1b}$$

$$\frac{\partial V_x}{\partial t}+V_r\frac{\partial V_x}{\partial r}+\frac{V_\phi}{r}\frac{\partial V_x}{\partial \phi}+V_x\frac{\partial V_x}{\partial x}=-\frac{1}{\rho}\frac{\partial p}{\partial x}+ \\ +\nu\left(\frac{\partial^2 V_x}{\partial x^2}+\frac{1}{r^2}\frac{\partial^2 V_x}{\partial \phi^2}+\frac{\partial^2 V_x}{\partial r^2}+\frac{1}{r}\frac{\partial V_x}{\partial r}\right), \tag{10.1c}$$

$$\frac{\partial V_r}{\partial r}+\frac{1}{r}\frac{\partial V_\phi}{\partial \phi}+\frac{\partial V_x}{\partial x}+\frac{V_r}{r}=0. \tag{10.1d}$$

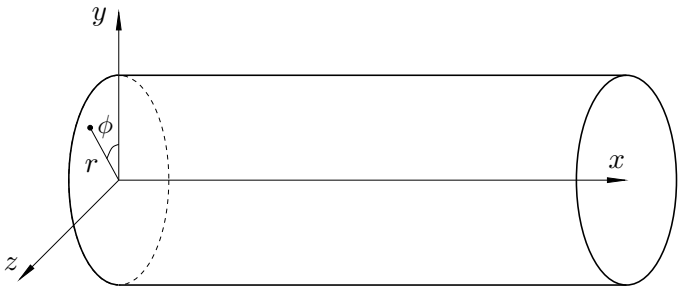

Figure 10.2: The Hagen-Poiseuille flow.

Similar to the previous examples (see Lecture 9), the tube is assumed to be long enough for the velocity field to be independent of the position along the tube, i.e.

$$\frac{\partial}{\partial x}(V_r, V_\phi, V_x)=0. \tag{10.2}$$

We can simplify the problem further by noting that the flow is axisymmetric, which implies that all the fluid dynamic functions are independent of the circumferential coordinate ϕ,

$$\frac{\partial}{\partial \phi}=0. \tag{10.3}$$

Using (10.2) and (10.3) in the continuity equation (10.1d), we find

$$\frac{\partial V_r}{\partial r}+\frac{V_r}{r}=0 \quad \text{or equivalently} \quad \frac{\partial}{\partial r}\big(rV_r\big)=0.$$

It follows that rV_r must be constant, F say. Consequently, the radial velocity component

$$V_r=\frac{F}{r}. \tag{10.4}$$

The radial velocity V_r has to be *regular* at $r = 0$, and furthermore the impermeability condition on the tube wall means that

$$V_r\Big|_{r=R} = 0, \tag{10.5}$$

where R denotes the radius of the tube. Either of the two conditions requires $F = 0$, and therefore,

$$V_r \equiv 0 \tag{10.6}$$

throughout the flow field.

Let us now turn to the circumferential momentum equation (10.1b). The flow steady and so $\partial V_\phi/\partial t = 0$. Similar to V_x, the circumferential velocity component, V_ϕ, is invariant along the tube, and both V_ϕ and the pressure, p, are independent of ϕ. Then equation (10.1b) reduces to

$$\frac{\partial^2 V_\phi}{\partial r^2} + \frac{1}{r}\frac{\partial V_\phi}{\partial r} - \frac{V_\phi}{r^2} = 0. \tag{10.7}$$

This is actually an ordinary differential equation since it involves only derivatives with respect to r. We can seek the two complementary solutions of (10.7) in the form

$$V_\phi = r^\lambda. \tag{10.8}$$

Substitution of (10.8) into (10.7) leads to the quadratic equation

$$\lambda^2 - 1 = 0,$$

which has two roots

$$\lambda_1 = 1, \qquad \lambda_2 = -1.$$

Consequently, the general solution to (10.7) is written as

$$V_\phi = G\, r + H\, \frac{1}{r}.$$

Obviously, if $H \neq 0$ the circumferential velocity V_ϕ develops a singularity at $r = 0$. This sort of behaviour could only be possible if there was a fast rotating cylinder of infinitely small radius inserted in the flow along the axis of symmetry[†]. Since our flow is free of such devices, we have to set $H = 0$.

Using further the no-slip condition on the tube wall

$$V_\phi\Big|_{r=R} = 0,$$

we find that function G is also zero, and the circumferential velocity component

$$V_\phi \equiv 0. \tag{10.9}$$

The results (10.6) and (10.9) show that the flow is indeed unidirectional, with the only non-zero velocity being in the axial direction, as was asserted earlier (at the beginning of Lecture 9) in a more general setting.

[†]When using the cylindrical coordinate system one has to keep in mind that the cylindrical coordinate system does not provide one-to-one correspondence between the position of point in space and coordinates (r, ϕ, x). Indeed, for any point situated on the axis of symmetry, the angle ϕ appears to be undetermined. This is why a singularity in the solution at $r = 0$ is to be expected.

Now it is easily found from the radial momentum equation (10.1a) that the pressure does not change with r,

$$\frac{\partial p}{\partial r} = 0.$$

Finally, an inspection of the axial momentum equation (10.1c) shows that it reduces to

$$\frac{\partial^2 V_x}{\partial r^2} + \frac{1}{r}\frac{\partial V_x}{\partial r} = \frac{1}{\mu}\frac{\partial p}{\partial x}. \tag{10.10}$$

This equation follows directly from (9.1) upon rewriting the Laplacian operator in terms of the polar coordinates via

$$y = r\cos\phi, \qquad z = r\sin\phi,$$

imposing axisymmetric and identifying u as V_x.

The flow is steady and so the pressure gradient $\partial p/\partial x$ is constant throughout the flow field, and may be calculated as

$$\frac{\partial p}{\partial x} = \frac{\Delta p}{L}.$$

Here we use the same notations as in the plane Poiseuille problem, with $\Delta p = p_2 - p_1 < 0$ being the pressure difference between the tube ends, and L the length of the tube (see Figure 9.3). Since V_x is a function of r only, we shall write equation (10.10) using ordinary derivatives, viz.

$$\frac{d^2 V_x}{dr^2} + \frac{1}{r}\frac{dV_x}{dr} = \frac{1}{\mu}\frac{\Delta p}{L}.$$

Multiplying both sides of this equation by r, we have

$$\frac{d}{dr}\left(r\frac{dV_x}{dr}\right) = \frac{1}{\mu}\frac{\Delta p}{L}\,r.$$

This equation is easily integrated to give

$$\frac{dV_x}{dr} = \frac{1}{2\mu}\frac{\Delta p}{L}\,r + \frac{C_1}{r}. \tag{10.11}$$

Integration of (10.11) results in

$$V_x = \frac{1}{4\mu}\frac{\Delta p}{L}\,r^2 + C_1 \ln r + C_2. \tag{10.12}$$

The constants of integration, C_1 and C_2, are determined by using the regularity and boundary condition. For V_x to remain finite at $r = 0$, we have to set $C_1 = 0$. The second constant, C_2, is found by using the no-slip condition,

$$V_x\Big|_{r=R} = 0.$$

We have

$$C_2 = -\frac{1}{4\mu}\frac{\Delta p}{L}\,R^2,$$

which is substituted back into (10.12) to give

$$V_x = \frac{1}{4\mu}\frac{\Delta p}{L}\big(r^2 - R^2\big) \equiv V_{\max}\big[1 - (r/R)^2\big], \tag{10.13}$$

where the maximum velocity, attained at the tube centre, is

$$V_{\max} = -\frac{1}{4\mu}\frac{R^2\Delta p}{L}.$$

With the velocity profile known, one can calculate the *volumetric flow rate*, or flux, past any cross-section of the tube as follows. If we consider an annular element of the cross-section of radius r and width dr, then the area of this element will be $2\pi r dr$, and the flux[‡]

$$dQ = V_x 2\pi r dr. \tag{10.14}$$

Substituting (10.13) into (10.14) and performing the integration, we find that the entire flux

$$Q = \frac{\pi}{2\mu}\frac{\Delta p}{L}\int_0^R (r^2 - R^2) r dr = -\frac{\pi}{8\mu}\frac{\Delta p}{L}R^4. \tag{10.15}$$

An average velocity, $\bar{V}_x$, may be defined as the ratio of the fluid flux, Q, to the cross-section area of the tube, πR^2, i.e.

$$\bar{V}_x = \frac{|\Delta p|}{8\mu L}R^2,$$

which indicates that the maximum velocity is twice the average velocity.

Using R and $V_{\max}$ as the reference length and velocity respectively, we define the Reynolds number

$$\mathrm{Re} = V_{\max} R/\nu.$$

Interestingly, formula (10.15) was deduced first by Hagen (1839) and Poiseuille (1840) not through solving the Navier-Stokes equations but based on careful experimental measurements of the flow through tubes. Their discovery was made before Reynolds number was introduced and its significance recognised. It happened that the Reynolds number was fairly low in their setup because tubes of very small radius were used since their main interest was in blood flows through vessels. Soon after their work, the mathematical solution was soon found (Stokes 1845) and the agreement with the experiments dispelled the doubt that existed at the time about the no-slip condition. Later, Reynolds (1883) in a

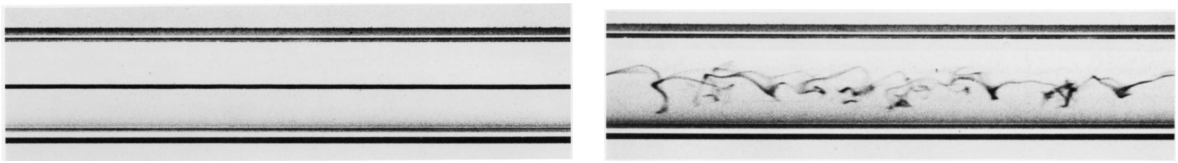

(a) Laminar flow. (b) Turbulent flow.

Figure 10.3: Laminar-turbulent transition in the Hagen-Poiseuille flow in a circular tube.

series of experiments found that the agreement appeared to hold up to $\mathrm{Re} = 13000$, and

[‡]Notice that the *mass flux* is obtained by multiplying the volumetric flux by the density ρ.

the flow remain simple laminar state ((Figure 10.3 (a)). However, the critical value was sensitive to ambient perturbations, and could be as low as just 2000. For higher Reynolds numbers, the flow becomes turbulent (Figure 10.3), and as a result the tube resistance to the flow increases significantly.

Flow	Plane Couette	Plane Poisuille	Hagen-Poisuille
Linear stability	Stable for all Re	Unstable Re $>$ 5572	Stable for all Re
Experiments	300	1000	2000
Velocity profiles			

Table 1: Instability and transition.

Remarks We have seen that the exact mathematical solutions for the three flows exist for all Reynolds numbers, yet in reality each of them is realizable and observable only up to a critical Reynolds number, beyond which the simple laminar flow is replaced by turbulent states. The latter appear random in both time and space. A time averaged velocity can be defined and measured in each case, but it turned out to be significantly different from the laminar counterpart. The change over from a laminar flow to turbulence is referred to as *laminar-turbulent transition*. It is generally attributed to instability of the laminar flow. *Linear stability theory* may serve as a first step towards explaining transition. For the plane Poiseuille flow, a critical Reynolds number of 5572 was predicted, which is much higher than the typical value at which the flow become turbulent in experiments. Even more astonishingly, the Couette flow and Hagen-Poiseuille flow both appear to be stable with respect to small perturbations at *all Reynolds numbers*. Instability and transition problems involve interesting physics and mathematics, and on the other hand are important for many technologies. My course in the Spring Term, "Hydrodynamic Stability Theory", is devoted to that subject.

The Flow Between Two Coaxial Cylinders

Let us consider two coaxial cylinders of radii R_1 and R_2 rotating with angular velocities Ω_1 and Ω_2, respectively; see Figure 10.4. The space between the cylinders is filled with a fluid, whose fluid density is ρ and viscosity coefficient μ, both assumed to be constant. The resulting flow in the gap is known as ***Taylor-Couette flow***, which can be reviewed as the axisymmetric counterpart of the plane Couette flow considered in Lecture 9. Our task is to determine the velocity and pressure distributions between the cylinders.

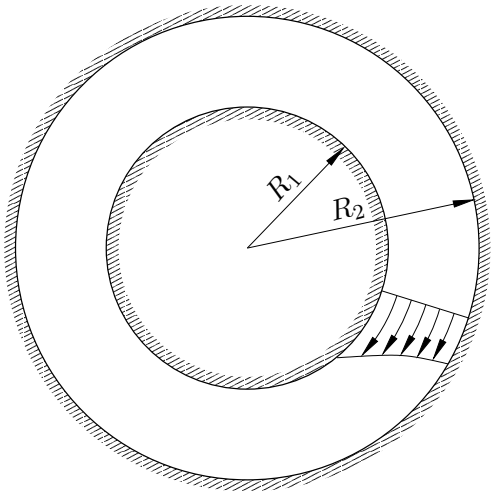

Figure 10.4: The flow between two coaxial cylinders.

It is convenient to use cylindrical coordinates (Figure 10.1) with the x-axis directed along the common axis of the cylinders. The Navier-Stokes equations written in these coordinates are given by equations (10.1). These allow for the following simplifications. Firstly, the flow considered is invariant along the x-axis, which means that the derivatives of all the fluid dynamic functions with respect to z are zeros, and also the axial velocity is zero,

$$\frac{\partial}{\partial x} = 0, \qquad V_x = 0. \tag{10.16}$$

The flow is therefor two-dimensional, taking place in the cross section. Secondly, the flow is axisymmetric so that none of the functions depend on the circumferential angle ϕ, i.e.

$$\frac{\partial}{\partial \phi} = 0. \tag{10.17}$$

In view of (10.16) and (10.17), the continuity equation (10.1d) reduces to

$$\frac{\partial V_r}{\partial r} + \frac{V_r}{r} = 0,$$

with the general solution given by (10.4),

$$V_r = \frac{F}{r}.$$

The impermeability condition on the cylinders, $V_r\Big|_{r=R_1} = V_r\Big|_{r=R_2} = 0$, is imposed on the radial velocity. It is satisfied by setting $F = 0$. We can conclude that

$$V_r \equiv 0. \tag{10.18}$$

The only non-zero velocity component is V_ϕ.

With (10.16), (10.17) and (10.18) circumferential and radial momentum equations, (10.1b) and (10.1a), reduce to

$$\frac{\partial^2 V_\phi}{\partial r^2} + \frac{1}{r}\frac{\partial V_\phi}{\partial r} - \frac{V_\phi}{r^2} = 0, \tag{10.19a}$$

$$\frac{1}{\rho}\frac{\partial p}{\partial r} = \frac{V_\phi^2}{r}. \tag{10.19b}$$

Equation (10.19b) is solved first. It is same as equation (10.7), which has been shown to have two complementary solutions, r and $1/r$. Therefore, the general solution of equation (10.19b) is written as

$$V_\phi = C_1 r + \frac{C_2}{r}. \tag{10.20}$$

In the present flow, regularity condition is irrelevant since $r = 0$ is outside of the flow domain. The constants C_1 and C_2 are determined by using the no-slip conditions on the two cylinders,

$$V_\phi\Big|_{r=R_1} = \Omega_1 R_1, \qquad V_\phi\Big|_{r=R_2} = \Omega_2 R_2. \tag{10.21}$$

Substituting (10.20) into (10.21) and solving the resulting equations for C_1 and C_2, we have

$$C_1 = \frac{\Omega_1 R_1^2 - \Omega_2 R_2^2}{R_1^2 - R_2^2}, \qquad C_2 = R_1^2 R_2^2 \frac{\Omega_1 - \Omega_2}{R_2^2 - R_1^2}. \tag{10.22}$$

This completes the solution for the azimuthal velocity, V_ϕ.

The pressure distribution between the cylinders can be determined by substituting (10.20) into the radial momentum equation (10.19a), which gives

$$\frac{dp}{dr} = \rho C_1^2 r + \frac{2\rho C_1 C_2}{r} + \frac{\rho C_2^2}{r^3}. \tag{10.23}$$

Integration of (10.23) yields

$$p = p_0 + \tfrac{1}{2}\rho C_1^2 r^2 + 2\rho C_1 C_2 \ln r - \frac{\rho C_2^2}{2r^2},$$

where the constant of integration, p_0, remains arbitrary. Notice that in the case of incompressible flows the Navier-Stokes equations (8.14) only involve the pressure gradient, not the pressure itself. Therefore, if a solution to these equations is found, they will still be satisfied with a constant "background" pressure, p_0, added to the pressure field.

The mathematical solution representing an axially uniform flow exists for all rotation speeds and the radii. The flow is controlled by the *Taylor number*,

$$T = \frac{\Omega_1^2 R_1 (R_2 - R_1)^3}{\nu^2},$$

and the ratios of radii and the rotation speeds, R_2/R_1 and Ω_2/Ω_1. However, this simple flow can be observed only when the Taylor number is below a critical value (for fixed values of the ratios). Above the critical value, the flow develops axially periodic but

stationary and axisymmetric structures, referred to as *Taylor vortices*. As the Taylor number is increased further, the so-called *wavy Taylor vortices* appear; these vortices vary in the azimuthal direction as well as in time, and in fact propagate around the cylinder. This change of the state is shown in Figure 10.5 for the case where the outer cylinder is stationary $\Omega_2 = 0$.

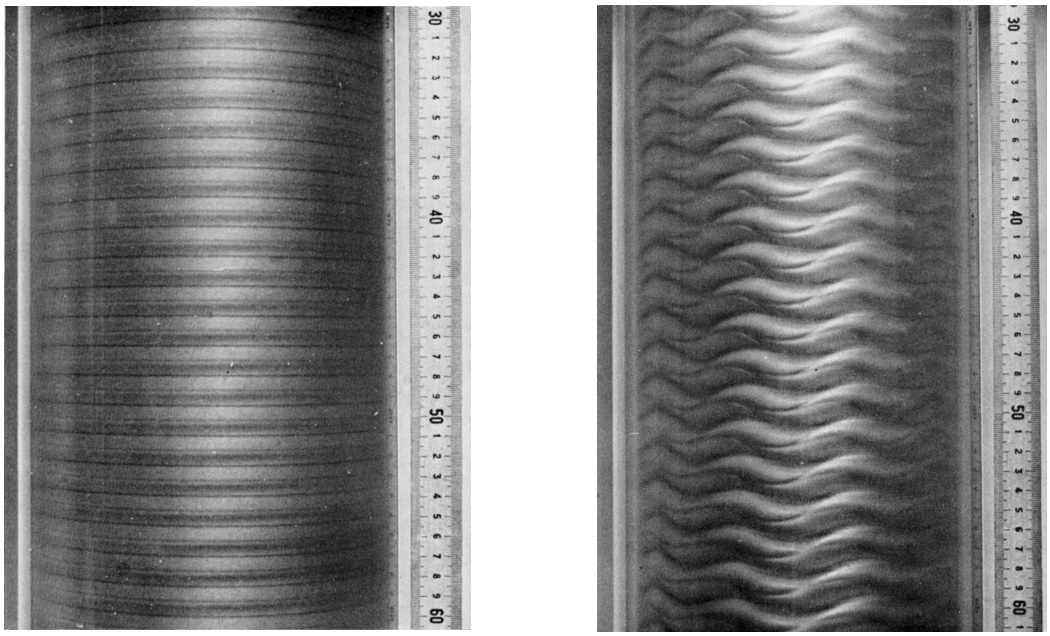

(a) Taylor vortices.

(b) Wavy Taylor vortices.

Figure 10.5: Taylor vortices and wavy Taylor vortices visualised by Burkhalter & Koschmieder (1974).

Impulsively Started Flat Plate

The configuration of this flow consists of an incompressible viscous fluid occupying a semi-infinite region above a flat surface, which is assumed to be infinitely large flat plate. Initially both the fluid and the plate were kept at rest. Then at time $t = 0$ the plate is suddenly brought into motion parallel itself with velocity U which remains constant for all $t > 0$.

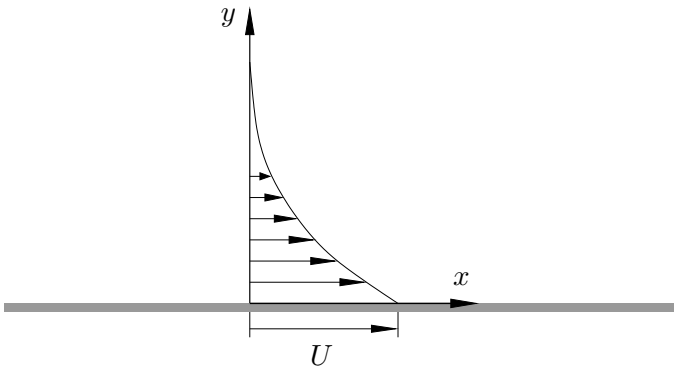

Figure 11.1: The flow above impulsively started flat plate.

Through the action of the viscous force the fluid close to the plate and then further in the field will be brought in motion, and the resulting flow is referred to as ***Rayleigh layer*** in the literature. We now describe how the flow develops. Cartesian coordinate system (x, y, z) is used with x measured along the plate in the direction of its motion, and y perpendicular to the plate surface (see Figure 11.1). The governing Navier-Stokes equations (8.14) simplify considerably.

Since the flow is invariant with respect to an arbitrary shift in the x- and z-directions, and so the derivatives of all the fluid dynamic functions with respect to x and z are zeros, i.e.

$$\frac{\partial}{\partial x} = \frac{\partial}{\partial z} = 0. \tag{11.1}$$

This reduces the continuity equation (8.16d) to

$$\frac{\partial v}{\partial y} = 0,$$

Integration of which with the impermeability condition at the plate surface, $v\Big|_{y=0} = 0$, leads to a conclusion that

$$v \equiv 0 \tag{11.2}$$

everywhere in the flow field and at any instant. The resulting flow is an *unsteady* unidirectional, and so equation (9.1) applies but noting that $\frac{\partial}{\partial z} = 0$ and no external pressure is present it simplifies to

$$\frac{\partial u}{\partial t} = \nu \frac{\partial^2 u}{\partial y^2} \tag{11.3}$$

which can also be deduced for this problem from the x-momentum equation (8.14a).

The partial differential equation (11.3) is parabolic as it has a second order derivative with respect to y and only first order derivative with respect to t. It is analogous to the standard one-dimensional parabolic equation describing heat conduction along a rod say.

In order to solve the equation (11.3), it is necessary to specify a set of *initial condition* and *boundary conditions* that are pertinent to the problem under consideration and also is compatible with the (parabolic) nature of the partial differential equation.

The initial condition is specified by noting that for all $t \leq 0$ the fluid remained at rest, we can write

$$u = 0 \quad \text{at} \quad t = 0, \;\; y \in (0, \infty). \tag{11.4}$$

Being second-order with respect to y, equation (11.3) requires two boundary conditions. The first one is the no-slip condition of the plate surface,

$$u = U \quad \text{at} \quad y = 0, \;\; t > 0. \tag{11.5}$$

The second boundary condition should be imposed at large values of y, where the fluid is expected to remain motionless for all finite values of t, that is

$$u = 0 \quad \text{at} \quad y = \infty, \;\; t > 0. \tag{11.6}$$

Now our task will be to find the solution to the problem (11.3)–(11.6). We start by noting that the flow has no characteristic length or time scale. This is an important feature with which the solution may be expected to have a *self-similar* form. This means that the solution $u(t, y)$, i.e. the distribution of the velocity u in the direction perpendicular to the plate, would look the same all the time after a suitable 'stretching' or rescaling of the coordinate y and if necessary of u itself as well. In other words, the distributions of the velocity u at different instants $t > 0$ are related to each other by means of suitable "zooming". This streching/rescaling, or 'zooming', of y and u must necessarily be time dependent, since it makes the original time-dependent flow to look the same for all time t. Mathematically, we may express this idea as

$$u(t, y)/q(t) = F\big(y/\ell(t)\big),$$

where $\ell(t)$ and $q(t)$ represent the stretching of y and rescaling of u respectively, $y/\ell(t)$ is the stretched variable and the function $F(\cdot)$ characterizes the invariant shape in terms of the stretched variable.

Suitable 'stretching' (or 'zooming') must be able to reduce the partial differential equation to an ordinary differential equation. Therefore the identification of the stretched variable, which is referred to as similarity variable, is a crucial step. We will demonstrate two ideas or procedures to find the similarity variable, in course of which the form of the self-similarity solution is also deduced. It should be pointed out that the both ideas are fairly general.

The first idea is based on the so-called ***dimensional analysis***. Since there is no natural length, the only way to non-dimensionalise y is to 'construct' a length-like quantity using the time variable t and the relevant parameter in the problem, which is the kinematic viscosity ν (while U is irrelevant since the problem is linear). The construction is aided by considering the dimensions of ν and t:

$$[\,\nu\,] = \mathrm{m}^2/\mathrm{s}, \quad [\,t\,] = \mathrm{s},$$

where the square bracket means taking the dimension. By inspection, the combination $(\nu t)^{1/2}$ has a dimension of length,

$$[(\nu t)^{1/2}] = \mathrm{m},$$

and it defines a 'length scale' that is time-dependent. We now use it to define a 'stretched' (similarity) variable

$$\eta = y/(\nu t)^{1/2}.$$

In terms of η and t, the solution can be written as

$$u(t, y) = q(t) f(\eta), \tag{11.7}$$

where $q(t)$ stands for possible rescaling of u that may be required, and is to be determined. For this purpose, we note that the boundary condition $u = U$ at $y = 0$ implies that

$$q(t) f(0) = U$$

for all $t > 0$. Hence we take $q(t) = U$, which is also expected by consideration of the dimension. In conclusion, the self-similar solution takes the form

$$u(t, y) = U f(\eta) \quad \text{with} \quad \eta = y/(\nu t)^{1/2}; \tag{11.8}$$

here η is the *similarity variable*.

The second idea is based on ***rescaling invariance***, i.e. the requirement that strechning/rescaling, or 'zooming', of y and u must render the original time-dependent problem the same for all time t. Mathematically, this 'stretching' or 'zooming' may be represented by affine transformations.

For the present problem, we seek the affine transformation in the form

$$u = A\bar{u}, \qquad t = B\bar{t}, \qquad y = C\bar{y}, \tag{11.9}$$

where A, B and C represent the stretching/rescaling mentioned. Strictly speaking they are functions of t, but for the purpose of identifying the forms of the similarity variable and solution, it suffices to treat them at this stage as if they were constants. Substitution of (11.9) into the equation (11.3) yields

$$\frac{1}{B}\frac{\partial \bar{u}}{\partial \bar{t}} = \frac{\nu}{C^2}\frac{\partial^2 \bar{u}}{\partial \bar{y}^2},$$

while the initial and boundary conditions (11.4)–(11.6) turn into

$$\bar{u} = 0 \quad \text{at} \quad \bar{t} = 0;$$

$$A\bar{u} = U \quad \text{at} \quad \bar{y} = 0, \qquad \bar{u} = 0 \quad \text{at} \quad \bar{y} = \infty.$$

If we choose

$$A = U, \qquad B\nu = C^2, \tag{11.10}$$

then the transformed problem will, at any instant, be identical to the *same canonical problem*. Let the solution to the transformed problem, which is free of any parameter, be denoted as

$$\bar{u} = F(\bar{t}, \bar{y}). \tag{11.11}$$

Returning in (11.11) to the original independent variables (11.9), we have

$$\bar{u} = F\Big(\frac{t}{B}, \frac{y}{C}\Big) = F\Big(\frac{\nu t}{C^2}, \frac{y}{C}\Big) \tag{11.12}$$

where use has been made of (11.10) in the last step.

The 'parameter' C in (11.12) may assume an arbitrary value, and yet it has been introduced artificially; the solution does not really depend on it. Furthermore, an appropriate choice of C (rescaling) should should also render $\bar{u}$, the solution to the canonical problem, independent of t (and any other parameter). Both can be fufilled by taking $C = \sqrt{\nu t}$, which leads to

$$\bar{u} = F\Big(1, \frac{y}{\sqrt{\nu t}}\Big).$$

This shows that the solution of the problem (11.3)–(11.6) has the self-similar form as given by (11.8).

The two ideas appear to be rather different as the second did not resort to dimension consideration at all, while the latter is essential to the first idea. The two ideas lead to the same conclusion, but the first is somewhat simpler.

In order to deduce a differential equation for function $f(\eta)$, we need to substitute (11.8) into the governing equation (11.3). It is easily seen that

$$\frac{\partial \eta}{\partial t} = -\frac{1}{2t}\frac{y}{(\nu t)^{1/2}} = -\frac{1}{2}\frac{\eta}{t}, \qquad \frac{\partial \eta}{\partial y} = \frac{1}{\sqrt{\nu t}}.$$

Therefore,

$$\frac{\partial u}{\partial t} = U f'(\eta)\frac{\partial \eta}{\partial t} = -\frac{U}{2}\frac{\eta}{t}f'(\eta), \qquad \frac{\partial u}{\partial y} = U f'(\eta)\frac{\partial \eta}{\partial y} = \frac{U}{\sqrt{\nu t}}f'(\eta), \qquad \frac{\partial^2 u}{\partial y^2} = \frac{U}{\nu t}f''(\eta),$$

which reduces (11.3) to

$$f'' + \frac{1}{2}\eta f' = 0. \tag{11.13}$$

The boundary conditions for this equation follows from substituting (11.8) into (11.4)–(11.6). Noting that $\eta \to \infty$ at $t \to 0^+$, we find from the initial condition (11.4) that

$$f(\infty) = 0. \tag{11.14}$$

The no-slip condition (11.5) is imposed at $y = 0$, where $\eta = 0$. We have

$$f(0) = 1. \tag{11.15}$$

We also need to use boundary condition (11.6), but it is easily seen to lead also to (11.14).

Our remaining task is to solve equation (11.13) subject to the boundary conditions (11.14) and (11.15). Equation (11.13) may be integrated first time by making use of the separation of variables,

$$\frac{f''}{f'} = -\frac{\eta}{2}.$$

We find that

$$f' = C_1 e^{-\eta^2/4}.$$

Second integration yields

$$f(\eta) = C_1 \int_0^\eta e^{-s^2/4} ds + C_2.$$

The integration constants, C_1 and C_2, may be found from the boundary conditions (11.14), (11.15) to be[†]

$$C_1 = -\frac{1}{\sqrt{\pi}}, \qquad C_2 = 1.$$

Consequently,

$$f(\eta) = 1 - \frac{1}{\sqrt{\pi}} \int_0^\eta e^{-s^2/4} ds. \tag{11.16}$$

Returning back to (11.8), we finally have the solution in the form

$$u(t, y) = U \operatorname{erfc}\Big(\frac{y}{2\sqrt{\nu t}}\Big),$$

where

$$\operatorname{erfc} x = 1 - \frac{2}{\sqrt{\pi}} \int_0^x e^{-\zeta^2} d\zeta$$

is referred to as the *complementary error function.*

We see that the thickness of the layer of the fluid involved in motion by the viscous forces may be estimated as

$$y \sim \sqrt{\nu t}; \tag{11.17}$$

within time t, the action of the moving plate spreads to a layer with thickness $\sqrt{\nu t}$.

[†]When applying condition (11.15) the following formula is used,

$$\int_0^\infty e^{-\alpha s^2} ds = \frac{1}{2}\sqrt{\frac{\pi}{\alpha}}.$$

Diffusion of A Potential Vortex

The flow to be considered is the rotational motion of a viscous fluid with the motion being initiated by the velocity represented by the so-called *potential vortex*, also referred to as a *line vortex*. The solution for its velocity is written in the cylindrical coordinates (see Figure 10.2) as

$$V_r = 0, \qquad V_\phi = \frac{\Gamma}{2\pi r}, \qquad V_x = 0, \tag{11.18}$$

which is a simple inviscid solution, i.e. solution to the Euler equations. Physically this vortex motion may be produced with a help of a circular cylinder of a small radius placed inside the fluid and brought in rotation around its axis with a large angular velocity (see Problem 3 in Exercises 3).

Suppose that having created the vortex at time $t = 0$, the cylinder suddenly "vanishes", and the fluid particles on the opposite sides of its surface come in contact with each other, generating extremely large shear stresses at the centre of rotation. This will make the singularity (the initial velocity (11.18) has at $r = 0$) to disappear immediately. We then expect the action of the viscous forces to cause a gradual deceleration of the fluid rotation, and our task to describe this process.

We start, as usual, with the continuity equation (10.1d). Since the flow is axisymmetric and invariant along the axial direction, we can disregard the derivatives with respect to ϕ and x, which yields

$$\frac{\partial V_r}{\partial r} + \frac{V_r}{r} = 0.$$

The solution of this equation is written as

$$V_r = \frac{F(t)}{r}.$$

Function $F(t)$ is related to the volumetric fluid flux through a circle centred at the axis of rotation,

$$Q = 2\pi r V_r = 2\pi F(t).$$

Therefore, assuming that there are no sources or sinks situated at the $r = 0$, we have to set $F(t) = 0$, thereby arriving at a conclusion that

$$V_r = 0 \quad \text{for all} \quad t > 0.$$

We then see that the circumferential momentum equation (10.1b) takes the from

$$\frac{\partial V_\phi}{\partial t} = \nu\left(\frac{\partial^2 V_\phi}{\partial r^2} + \frac{1}{r}\frac{\partial V_\phi}{\partial r} - \frac{V_\phi}{r^2}\right) \tag{11.19}$$

Again, the choice of the boundary conditions for equation (11.19) depends on its type. The latter is determined by the higher order derivatives. Equation (11.19) involves a first-order derivative with respect to time, which is $\partial V_\phi/\partial t$, and the second-order derivative with respect to r is $\partial^2 V_\phi/\partial r^2$. Hence, the equation is parabolic, and requires an initial and two boundary conditions.

The initial condition follows directly from (11.18), and is written as

$$V_\phi = \frac{\Gamma}{2\pi r} \quad \text{at} \quad t = 0, \;\; r > 0. \tag{11.20}$$

The far field is expected to remain undisturbed as long as time t is finite, which gives the first boundary condition,

$$V_\phi = \frac{\Gamma}{2\pi r} \quad \text{as} \quad r \to \infty, \;\; t > 0. \tag{11.21}$$

In order to formulate the second boundary condition we shall assume that, due to the action of viscous forces, the singularity at the centre of rotation will vanish momentarily, that is, there exists a positive constant M such that

$$|V_\phi| < M \quad \text{at} \quad r = 0, \;\; t > 0. \tag{11.22}$$

Similar to the Rayleigh layer considered earlier, the present problem (11.19)–(11.22) does not involve characteristic length or time scales. This feature implies that the solution may have a self-similar form.

The idea of *dimension analysis* is applicable. Specifically, with precisely the same argument as that for the Rayleigh layer, the similarity variable should be

$$\eta = r/\sqrt{\nu t}.$$

The self-similar solution is written as

$$V_\phi(t, r) = q(r) f(\eta),$$

where $q(r)$ as a function r is to be determined by using the far-field boundary condition,

$$qf(\infty) = \frac{\Gamma}{2\pi r}.$$

We anticipate $F(\infty)$ to be a constant and so take

$$q = \frac{\Gamma}{2\pi r},$$

with which $f \to 1$ as $\eta \to \infty$. The sought self-similar solution is of the form

$$V_\phi = \frac{\Gamma}{2\pi r} f(\eta) \quad \text{with} \quad \eta = r/\sqrt{\nu t}. \tag{11.23}$$

Alternatively, we may use the idea of rescaling invariance, and perform the affine transformations,

$$V_\phi = A\bar{V}_\phi, \qquad t = B\bar{t}, \qquad r = C\bar{r}. \tag{11.24}$$

Substituting (11.24) into (11.19), we find

$$\frac{A}{B}\frac{\partial \bar{V}_\phi}{\partial \bar{t}} = \frac{A}{C^2}\nu\left(\frac{\partial^2 \bar{V}_\phi}{\partial \bar{r}^2} + \frac{1}{\bar{r}}\frac{\partial \bar{V}_\phi}{\partial \bar{r}} - \frac{\bar{V}_\phi}{\bar{r}^2}\right).$$

The initial and boundary conditions (11.20)–(11.22), written in terms of the new variables, take the form

$$A\bar{V}_\phi = \frac{1}{C}\frac{\Gamma}{2\pi\bar{r}} \quad \text{at} \quad \bar{t} = 0;$$

$$A\bar{V}_\phi = \frac{1}{C}\frac{\Gamma}{2\pi\bar{r}} \quad \text{at} \quad \bar{r} \to \infty, \quad |\bar{V}_\phi| < \bar{M} \quad \text{at} \quad \bar{r} = 0.$$

In order for the transformed problem to appear the same for any time t, we set

$$B\nu = C^2, \qquad A = \frac{\Gamma}{2\pi C},$$

where C remains arbitrary.

Let the solution of the transformed problem, which is parameter free, be written as

$$\bar{V}_\phi = F(\bar{t}, \bar{r}). \tag{11.25}$$

Rewriting (11.25) in terms of the original independent variables (11.24), we have

$$\bar{V}_\phi = F\Big(\frac{t}{B}, \frac{r}{C}\Big) = F\Big(\frac{\nu t}{C^2}, \frac{r}{C}\Big). \tag{11.26}$$

Here C is arbitrary. For the solution to appear independent of time and C, we can choose $C = \sqrt{\nu t}$, which leads to

$$\bar{V}_\phi = F\Big(1, \frac{r}{\sqrt{\nu t}}\Big).$$

This suggests that the sought solution may be written in the form

$$V_\phi = \frac{\Gamma}{2\pi\sqrt{\nu t}}F(1,\eta) = \frac{\Gamma}{2\pi r}\eta F(1,\eta).$$

This form is actually the same as (11.23) upon taking $\eta F(1,\eta)$ as $f(\eta)$.

The above choice of $C = \sqrt{\nu t}$ is not unique. We may as well take $C = r$ in (11.26) so that $\bar{V}_\phi = F(1/\eta^2, 1)$, which is a function of a single variable and appears 'time-independent'. The corresponding solution for V_ϕ is again the same as (11.23) since $F(1/\eta^2, 1)$ can be identified as $f(\eta)$.

The remaining task is to derive the equation for f, which simply involves straightforward calculus. The algebra can be simplified by writing (11.19) to the form

$$\frac{\partial}{\partial t}(rV_\phi) = \nu\Big[\frac{\partial^2}{\partial r^2}(rV_\phi) - \frac{1}{r}\frac{\partial}{\partial r}(rV_\phi),\Big]$$

with rV_ϕ as the independent variable. Substituting (11.23) into the above equation gives

$$-\frac{\eta}{2}f' = \Big[f'' - \frac{1}{\eta}f'\Big],$$

which is rearranged into

$$f'' + (\frac{\eta}{2} - \frac{1}{\eta})f' = 0.$$

This is a first-order linear equation for f', and can be solved (using integration factor method or variable separation) to give

$$f' = C_1 e^{\int^\eta (\frac{1}{\eta} - \eta/2) d\eta} = C_1 e^{\ln \eta - \eta^2/4} = C_1 \eta e^{-\eta^2/4}.$$

Integrating once more, we have

$$f = C_2 - 2C_1 e^{-\eta^2/4}. \tag{11.27}$$

The constants of integration, C_1 and C_2, are determined by using the initial and boundary conditions. Substitution of (11.23)) into (11.20), (11.21) and (11.22) shows that

$$f(0) = 0, \qquad f(\infty) = 1, \tag{11.28}$$

where the first is required in order for V_ϕ to be regular. It follows from (11.28) that

$$C_2 = 1, \qquad C_1 = 1/2. \tag{11.29}$$

After substituting (11.29) back into (11.27) and then into (11.23), the circumferential velocity is given by

$$V_\phi = \frac{\Gamma}{2\pi r}\left[1 - \exp\Big(-\frac{r^2}{4\nu t}\Big)\right]. \tag{11.30}$$

It follows that the vortex has a viscous core of radius $r \sim \sqrt{\nu t}$. If $r \gg \sqrt{\nu t}$, then the velocity field is represented by the potential vortex solution

$$V_\phi = \frac{\Gamma}{2\pi r} \quad \text{for} \quad \frac{r^2}{\nu t} \gg 1.$$

If, on the other hand, $r \ll \sqrt{\nu t}$, then using the Taylor expansion for the exponential function[‡], we can find

$$V_\phi = \frac{\Gamma r}{8\pi \nu t} \quad \text{for} \quad \frac{r^2}{\nu t} \ll 1,$$

which shows that near the centre of the vortex core the circumferential velocity grows linearly with the radius r.

[‡]Recall that

$$e^x = 1 + x + \cdots \quad \text{as} \quad x \to 0.$$

Chapter 2: Inviscid Incompressible Flows

Lecture 12

In many applications, the characteristic Reynolds numbers of the flows are high, and so the flow may be treated as being inviscid. Inviscid flows exhibit some important properties, and on the other hand under certain conditions relevant solutions may be found by using special mathematical techniques.

We shall now turn to inviscid flows, which are governed by the Euler equations. It should be made clear at the outset that any inviscid flow should be viewed as an *approximation* of a real viscous flow at high-Reynolds-number limit, rather than an exact entity in itself. There are at least three reasons for this caution. Firstly, even when the majority of a flow is essentially of inviscid nature, there usually exist certain small portions of the flow field, where viscosity plays a leading-order role. The flow in those small regions may control quantities of aerodynamic significance (e.g. friction drag), and may influence the inviscid part. Secondly, the inviscid solutions may not be unique, and the conditions required to fix the solution have to be provided by considering viscous effects. Thirdly, not all inviscid solutions are physically acceptable; only those which can be approached by the viscous flow in the high-Reynolds-number limit can be considered acceptable (non-spurious).

Integrals of Motion

The motion of inviscid incompressible fluid flows is governed by the *Euler Equations*

$$\frac{\partial \mathbf{V}}{\partial t} + \big(\mathbf{V}\cdot\nabla\big)\mathbf{V} = \mathbf{f} - \frac{1}{\rho}\nabla p \quad \text{– momentum equation,} \tag{12.1a}$$

$$\text{div}\mathbf{V} = 0 \qquad \text{– continuity equation,} \tag{12.1b}$$

which are obtained from the Navier-Stokes equations (8.13a), (8.13b) by setting the viscous diffusion terms to zero. This is done on the basis of large Reynolds number even though setting the viscosity coefficient ν to zero leads to the same result.[†]

An alternative form of writing the momentum equation arises from using the well known differential identity (see Problem 1 in Exercises 2)

$$\big(\mathbf{V}\cdot\nabla\big)\mathbf{V} = \big[\boldsymbol{\omega}\times\mathbf{V}\big] + \nabla\left(\frac{V^2}{2}\right), \tag{12.2}$$

where $\boldsymbol{\omega} = \text{curl}\mathbf{V}$ and V is the modulus of the velocity vector $\mathbf{V}$. Substitution of (12.2) into (12.1) leads to the so called *Gromeko-Lamb* form of the momentum equation

$$\frac{\partial \mathbf{V}}{\partial t} + \big[\boldsymbol{\omega}\times\mathbf{V}\big] + \nabla\left(\frac{V^2}{2}\right) = \mathbf{f} - \frac{1}{\rho}\nabla p. \tag{12.3}$$

In further analysis, we will often use simplifications arising from the assumption that the body force $\mathbf{f}$ is potential.

[†]Of course, the Euler equations were deduced significantly earlier than the Navier-Stokes equations, by Euler as early as in 1755 with the assumption of $\nu = 0$.

Definition 12.1:. *A body force field* $\mathbf{f}$ *is termed* ***potential*** *(or* ***conservative****), if there exists a scalar function* U *such that*

$$\mathbf{f} = -\nabla U. \tag{12.4}$$

The gravity force is, obviously, of this kind. If we introduce Cartesian coordinate system with x and y lying in the horizontal plane and z directed vertically upwards, then the gravity force $\mathbf{f} = (0, 0, -g)$ and so equation (12.4) may be written in the coordinate decomposition form as

$$0 = -\frac{\partial U}{\partial x}, \quad 0 = -\frac{\partial U}{\partial y}, \quad -g = -\frac{\partial U}{\partial z},$$

leading to

$$U = gz + C, \tag{12.5}$$

where C is an arbitrary constant.

For a general potential (conservative) body force and a fluid with constant density, we may absorb the body force to the pressure refined as $p+\rho U$. If no interface is present, then such as a body force does not affect the velocity field, and does not have to be considered. This is the reason why mathematical solutions without considering the gravity force may be compared with experimental data acquired in laboratory. Of course, when a flow involves interface or the density varies, such as water waves, the gravity force is essential.

We shall start our discussion of inviscid incompressible fluid motion by introducing a number of important integrals of the momentum equation. The first of these is the ***Bernoulli integral***, which allows us to find the pressure distribution over a flow field once the velocity distribution is known.

Bernoulli's Integral

Theorem 1. *Let the fluid flow be steady and the body force potential. Then along any streamline the* ***Bernoulli integral***

$$\frac{V^2}{2} + \frac{p}{\rho} + U = H, \tag{12.6}$$

holds, where H *remains constant along each streamline but might be different for different streamlines.*

Proof. Since the flow is steady ($\partial \mathbf{V}/\partial t = 0$) and the body force is potential ($\mathbf{f} = -\nabla U$), we can write the momentum equation (12.3) as

$$\big[\boldsymbol{\omega} \times \mathbf{V}\big] + \nabla\big(\frac{V^2}{2} + \frac{p}{\rho} + U\big) = 0. \tag{12.7}$$

Let line $\mathcal{L}$ be a streamline. The unit vector $\boldsymbol{\tau}$ tangent to $\mathcal{L}$ is parallel to the velocity vector $\mathbf{V}$, and therefore, is perpendicular to $\big[\boldsymbol{\omega}\times\mathbf{V}\big]$, which ensures that the scalar product of $\boldsymbol{\tau}$ and $\big[\boldsymbol{\omega} \times \mathbf{V}\big]$ is nought. Hence, multiplying equation (12.7) by $\boldsymbol{\tau}$, we have

$$\boldsymbol{\tau} \cdot \nabla\big(\frac{V^2}{2} + \frac{p}{\rho} + U\big) = 0.$$

Note that $\boldsymbol{\tau} = (dx, dy, dz)/ds$, use of which allows the above to be written in the form of *directional directive* as

$$\nabla H \cdot \boldsymbol{\tau} = \frac{d}{ds} H = \frac{d}{ds}\big(\frac{V^2}{2} + \frac{p}{\rho} + U\big) = 0.$$

This proves that H really remains constant along $\mathcal{L}$. □

Kelvin's Circulation Theorem

Kelvin's circulation theorem concerns the circulation of the velocity vector along a ***fluid contour*** or ***material loop***, which fluid contour is a closed loop composed of fluid particles, and moves with the fluid particles. To understand the notion of fluid contour, we may imagine that at time $t = t_0$, we take a closed loop C_0 and mark all particles on it. Each particle $\mathbf{r}_0$ on it will move to a new position $\mathbf{r}(t, \mathbf{r}_0)$ at time $t > t_0$, in the course of which the loop C_0 moves and evolves to a new loop C, as shown in Figure 12.1. Importantly, for each $\mathbf{r}$ on C,

$$\frac{\partial \mathbf{r}}{\partial t} = \mathbf{V}. \tag{12.8}$$

The circulation along this contour is, according to its definition, given by integral (4.4),

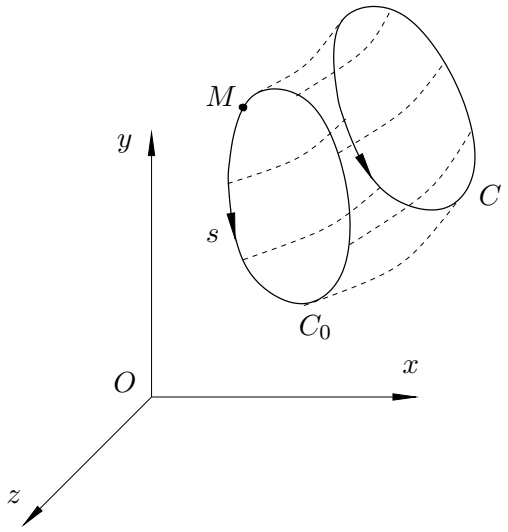

Figure 12.1: Evolution of a fluid contour.

$$\Gamma(t) = \oint_C \big(\mathbf{V} \cdot d\mathbf{r}\big). \tag{12.9}$$

The evaluation of a contour integration requires 'parameterising' the contour. We parameterise contour C_0 by s, which can be taken to be the arc length of the contour measured from a reference point. Each value of s corresponds to a point $\mathbf{r}_0$ on C_0, i.e.

$$\mathbf{r}_0 = \mathbf{r}_0(s), \tag{12.10}$$

and since C_0 is closed, $s = 0$ and $S = L$ (with L being the total arc length of C_0) represent the same point, $\mathbf{r}_0(0) = \mathbf{r}_0(L)$.

In view of (12.10), each point $\mathbf{r}(t, \mathbf{r}_0)$ on C is a function of s, and we may write $\mathbf{r}(t, \mathbf{r}_0)$ as

$$\mathbf{r} = \mathbf{r}\big(t, \mathbf{r}_0(s)\big) = \mathbf{r}(t; s),$$

which indicates that s $(0 \le s \le L)$ parameterises C as well, and

$$\mathbf{r}(t; 0) = \mathbf{r}(t; L).$$

At each instant t, the variation of the position vector along C is given by

$$d\mathbf{r} = \frac{\partial \mathbf{r}}{\partial s}\, ds. \tag{12.11}$$

Using (12.11) in (12.9), yields

$$\Gamma(t) = \int_0^L \left(\mathbf{V} \cdot \frac{\partial \mathbf{r}}{\partial s}\right) ds, \tag{12.12}$$

where $\mathbf{V} = \mathbf{V}\big[t, \mathbf{r}(t, s)\big]$. Differentiation of (12.12) with respect to t gives

$$\frac{d\Gamma}{dt} = \int_0^L \left(\frac{D\mathbf{V}}{Dt} \cdot \frac{\partial \mathbf{r}}{\partial s}\right) ds + \int_0^L \left(\mathbf{V} \cdot \frac{\partial^2 \mathbf{r}}{\partial s \partial t}\right) ds. \tag{12.13}$$

Using (12.8) (i.e. $\frac{\partial \mathbf{r}}{\partial t} = \mathbf{V}$) we can calculate the second integral in (12.13) as

$$\int_0^L \left(\mathbf{V} \cdot \frac{\partial^2 \mathbf{r}}{\partial s \partial t}\right) ds = \int_0^L \left(\mathbf{V} \cdot \frac{\partial \mathbf{V}}{\partial s}\right) ds = \int_0^L \frac{d}{ds}\left(\frac{V^2}{2}\right) ds = \frac{V^2}{2}\bigg|_{s=L} - \frac{V^2}{2}\bigg|_{s=0}; \tag{12.14}$$

this integral is zero since since $s = L$ and $s = 0$ represent the same point on contour C.

Turning to the first integral in (12.13), we shall assume the body force $\mathbf{f}$ is potential. In this case, using (12.4) in (12.1a), yields

$$\frac{D\mathbf{V}}{Dt} = -\nabla\left(U + \frac{p}{\rho}\right),$$

and we have

$$\int_0^L \left(\frac{D\mathbf{V}}{Dt} \cdot \frac{\partial \mathbf{r}}{\partial s}\right) ds = -\oint_C \nabla\left(U + \frac{p}{\rho}\right) \cdot d\mathbf{r} = -\oint_C d\left(U + \frac{p}{\rho}\right). \tag{12.15}$$

Observing that the point of integration, after making a full circle along C, returns to its original position, we can conclude that integral (12.15) is also zero.

This proves the following statement, known as the ***Kelvin's Circulation theorem***.

Theorem 2. *In an inviscid incompressible fluid flow, the circulation along any closed* ***fluid contour*** *does not change with time, i.e.*

$$\frac{d\Gamma}{dt} = 0$$

provided that the body force is potential or absent.

This theorem plays an important role in fluid dynamics; it lays a foundation for the potential flow theory. As we shall see, many inviscid flows may be treated as potential, in which case the Euler equations (12.1) reduce to a simple Laplace equation. Specifically, flows of interest may be represented by a suitable collection of concentrated vortices, each being characterised by a circulation, which remains constant due to the Kelvin's circulation theorem. In fact, it is primarily due to such simplifications that significant progress in the inviscid flow theory has been achieved.

Before turning our attention to the potential flow theory, we shall give here two examples that demonstrate how the Kelvin theorem may be used. The first one concerns fluid flows which start from the rest. If at an initial instant t_0 the flow velocity $\mathbf{V} = 0$, then the circulation along any closed contour C_0 is zero. According to the Kelvin's theorem it will remain zero after the fluid is put into motion, and at any time $t > t_0$,

$$\oint_C \big(\mathbf{V} \cdot d\mathbf{r}\big) = 0, \tag{12.16}$$

where C is the fluid contour originating from C_0.

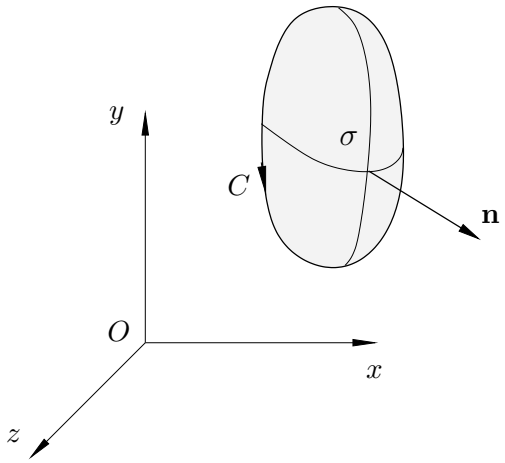

Figure 12.2: Surface σ to which the Stokes theorem is applied.

Let σ denote any surface spanned by C as is shown in Figure 12.2. We denote the unit vector normal to σ by $\mathbf{n}$ and the area of a small element of σ by ds. Then using the Stokes theorem, we have

$$\oint_C \big(\mathbf{V} \cdot d\mathbf{r}\big) = \iint_\sigma \big(\mathrm{curl}\,\mathbf{V} \cdot \mathbf{n}\big) ds = \iint_\sigma \big(\boldsymbol{\omega} \cdot \mathbf{n}\big) ds,$$

and it follows that

$$\iint_\sigma \big(\boldsymbol{\omega} \cdot \mathbf{n}\big) ds = 0.$$

Taking into account arbitrariness of C, we can conclude that any flow of this kind is *irrotational*, i.e. free of the vorticity,

$$\boldsymbol{\omega} = \mathrm{curl}\mathbf{V} = 0. \tag{12.17}$$

The argument above shows that an initially irrotational flow remains irrotational in subsequent times.

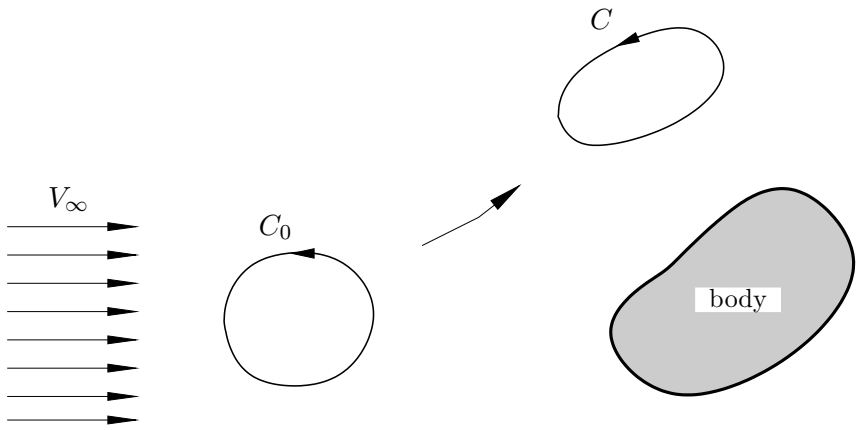

Figure 12.3: Fluid contour motion in a flow past a rigid body.

In the second example, we consider a rigid body placed into a uniform stream with the free-stream velocity V_∞, as is sketched in Figure 12.3. Assuming that there are no recirculating regions (those may form if the flow separates from the body surface), one can claim that any closed contour C in the flow field "originates" from the corresponding contour C_0 in the oncoming flow. Since on C_0 the fluid velocity is constant, $\mathbf{V} = \mathbf{V}_\infty$, the circulation along C_0 is zero. According to the Kelvin theorem, it will remain zero as C_0 deforms into C. Hence, equation (12.16) holds again, and using the Stokes theorem we can prove that the flow is irrotational.

Cauchy-Lagrange Integral

It will be shown in Lecture 13 that for any *irrotational* flow satisfying equation (12.17) there exists a scalar function $\varphi(t, \mathbf{r})$, called the *velocity potential*, such that

$$\mathbf{V} = \nabla\varphi. \tag{12.18}$$

Hence, irrotational flows are also termed ***potential flows***. Use of (12.18) in the definition of the vorticity shows that $\boldsymbol{\omega} = \mathrm{curl}\mathbf{V} = \mathrm{curl}(\nabla\varphi) = 0$, which is simply a vector identity. It follows that any potential flow is irrotational, i.e. $\boldsymbol{\omega} = 0$.

For a potential flow, steady or unsteady, we can prove the following result, which is referred to as *Cauchy-Lagrange theorem*.

Theorem 3. *Suppose that the flow of inviscid incompressible fluid is potential,* $\mathbf{V} = \nabla\varphi$. *Suppose further that the body force has potential* U, *such that* $\mathbf{f} = -\nabla U$. *Then the* ***Cauchy-Lagrange integral***

$$\frac{\partial\varphi}{\partial t} + \frac{V^2}{2} + \frac{p}{\rho} + U = \mathcal{F}(t) \tag{12.19}$$

holds with function $\mathcal{F}(t)$ *being independent on a position in the flow field.*

Proof. Under the conditions of the theorem we can write the momentum equation (12.3) as

$$\nabla\left(\frac{\partial\varphi}{\partial t}\right) + \left[\boldsymbol{\omega} \times \mathbf{V}\right] + \nabla\left(\frac{V^2}{2}\right) = -\nabla U - \nabla\left(\frac{p}{\rho}\right). \tag{12.20}$$

Noting that $\boldsymbol{\omega} = 0$, we may rewwrite (12.20) as

$$\nabla\left(\frac{\partial\varphi}{\partial t} + \frac{V^2}{2} + U + \frac{p}{\rho}\right) = 0,$$

which immediately proves that (12.19) is valid. □

If the conditions of both Theorem 1 and Theorem 3 hold simultaneously, namely,

- the flow considered is steady,
- the body force is potential,
- and the flow is irrotational,

then function H in (12.6) becomes independent of a streamline considered and function $\mathcal{F}(t)$ appears to be independent of time. Hence, we can write

$$\frac{V^2}{2} + \frac{p}{\rho} + U = C, \tag{12.21}$$

where C is a true constant.

The results (12.19) and (12.21) are often referred to as ***Bernoulli equations***. They are extremely important for steady and unsteady potential flows respectively, because they relate the pressure p to the velocity $V = |\mathbf{V}|$ and its potential φ, and so the pressure can immediately be calculated once the velocity and φ are obtained by solving the Laplace equation.

Potential Flows

We shall now prove that for any irrotational flow, i.e. a flow satisfying the equation

$$\boldsymbol{\omega} = \text{curl}\mathbf{V} = 0, \tag{13.1}$$

there exists a scalar function $\varphi(t, \mathbf{r})$, called the ***velocity potential***, such that

$$\mathbf{V} = \nabla\varphi.$$

This is actually an elementary result in vector calculus, valid for any vector $\mathbf{V}$ satisfying $\text{curl}\mathbf{V} = 0$, but it is stated here in the context of irrotational flows.

The proof is accomplished by constructing $\varphi(t, \mathbf{r})$. We start by choosing a reference point M_0, the position of which is denoted by vector $\mathbf{r}_0$; see Figure 13.1. For any other point M, we define function $\varphi(t, \mathbf{r})$ as

$$\varphi(t, \mathbf{r}) = \int_C \big(\mathbf{V} \cdot d\mathbf{r}\big), \tag{13.2}$$

where C is a contour connecting points M_0 and M.

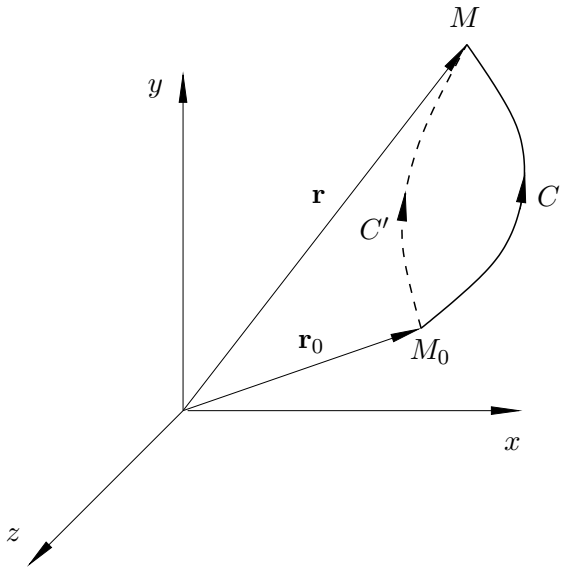

Figure 13.1: Calculation of the velocity potential.

As it stands, φ depends on the contour C and also $\mathbf{r}$ is restricted to points on C. It is necessary to show that $\varphi(t, \mathbf{r})$ is a *scalar function* and *field quatity*, i.e. it depends on the position vector $\mathbf{r}$ of point M but not on a choice of contour C, and consequently φ can be defined for any point $\mathbf{r}$. For this purpose, we choose another contour C' and write

$$\varphi'(t, \mathbf{r}) = \int_{C'} \big(\mathbf{V} \cdot d\mathbf{r}\big),$$

then the difference between $\varphi(t,\mathbf{r})$ and $\varphi'(t,\mathbf{r})$ may be expressed as

$$\varphi(t,\mathbf{r})-\varphi'(t,\mathbf{r})=\int\limits_{C}\big(\mathbf{V}\cdot d\mathbf{r}\big)-\int\limits_{C'}\big(\mathbf{V}\cdot d\mathbf{r}\big)=\oint\limits_{\widetilde{C}}\big(\mathbf{V}\cdot d\mathbf{r}\big),$$

where $\widetilde{C}$ is a closed contour composed of C and $(-C')$; the latter is C' but with the direction in the negative direction, i.e. from M to M_0.

For any open surface σ lying entirely in the flow field may be spanned by contour $\widetilde{C}$ (as in Figure 12.2) then using the Stokes theorem we can write

$$\oint\limits_{\widetilde{C}}\big(\mathbf{V}\cdot d\mathbf{r}\big)=\iint\limits_{\sigma}\big(\mathrm{curl}\mathbf{V}\cdot\mathbf{n}\big)ds, \tag{13.3}$$

and it follows from (13.1) that $\varphi(t,\mathbf{r})=\varphi'(t,\mathbf{r})$.

As the result of integration in (13.2) does not depend on a choice of contour C, it is more appropriate to write

$$\varphi(t,\mathbf{r})=\int\limits_{\mathbf{r}_0}^{\mathbf{r}}\big(\mathbf{V}\cdot d\mathbf{r}\big). \tag{13.4}$$

A small variation $\delta\mathbf{r}$ of the position vector $\mathbf{r}$ leads to

$$\varphi(t,\mathbf{r}+\delta\mathbf{r})=\int\limits_{\mathbf{r}_0}^{\mathbf{r}+\delta\mathbf{r}}\big(\mathbf{V}\cdot d\mathbf{r}\big),$$

whence

$$\varphi(t,\mathbf{r}+\delta\mathbf{r})-\varphi(t,\mathbf{r})=\int\limits_{\mathbf{r}}^{\mathbf{r}+\delta\mathbf{r}}\big(\mathbf{V}\cdot d\mathbf{r}\big). \tag{13.5}$$

By Taylor expansion, the left-hand side may be expressed

$$\frac{\partial\varphi}{\partial x}\delta x+\frac{\partial\varphi}{\partial y}\delta y+\frac{\partial\varphi}{\partial z}\delta z=\nabla\varphi\cdot\delta\mathbf{r}.$$

If $\mathbf{V}$ is a continuous function of $\mathbf{r}$, then, due to smallness of $\delta\mathbf{r}$, the integral on the right hand side of (13.5) may be approximated by $\big(\mathbf{V}(t,\mathbf{r})\cdot\delta\mathbf{r}\big)$. Thus we have

$$\nabla\varphi\cdot\delta\mathbf{r}=\big(\mathbf{V}(t,\mathbf{r})\cdot\delta\mathbf{r}\big).$$

Since $\delta\mathbf{r}$ is arbitrary, we conclude that

$$\mathbf{V}=\nabla\varphi, \tag{13.6}$$

that is, the scalar function φ that we have constructed indeed serves as a potential for $\mathbf{V}$. It should be noted that equation (13.2) defines the velocity potential φ to within an arbitrary function of time t, which depends on a choice of the reference point $\mathbf{r}_0$. However, the difference between the values of $\varphi(t,\mathbf{r})$ corresponding to two different choices of $\mathbf{r}_0$ is independent of $\mathbf{r}$, and therefore, has no effect on the velocity field using (13.6).

For potential flows, the Euler equations, which are highly nonlinear, are simplified dramatically. As is evident from the proof of Theorem 3 of Lecture 12, equation (13.6) reduces the momentum equation (12.1a) to the Cauchy-Lagrange integral (12.18), which relates the pressure to velocity field, and thus allows the former to be calculated once the latter is known. In order to determine the velocity field, one has to use the continuity equation (12.1b). Substitution of (13.6) into the continuity equation (12.1b) leads to the ***Laplace equation***

$$\nabla^2 \varphi = 0, \tag{13.7}$$

which is linear and well studied in classical mathematical physics as a standard elliptic equation.

In order to solve (13.7), it is necessary to specify appropriate *boundary conditions*, which depend on a particular problem considered. An important application of the potential flow theory is to flows past rigid bodies, for which the so called *impermeability condition* must be imposed on the body surface. This condition implies that a rigid body surface is impenetrable*, which means that the fluid particles that come in contact with the body surface will remain on this surface for some time moving along it downstream. Let the body surface be represented by the equation

$$\Phi(t, \mathbf{r}) = const,$$

and consider a particle that is at $\mathbf{r}_0$ on the surface at time t_0. Its Lagrangian position is given by $\mathbf{r} = \mathbf{r}(t, \mathbf{r}_0)$, and for the fluid particle to remain on this surface it is required that

$$\Phi\big[t, \mathbf{r}(t, \mathbf{r}_0)\big] = const. \tag{13.8}$$

Differentiation of (13.8) with respect to t for a fixed $\mathbf{r}_0$ using the chain rule yields

$$\frac{\partial \Phi}{\partial t} + \left(\nabla \Phi \cdot \frac{\partial \mathbf{r}}{\partial t} \right) = 0,$$

and since the derivative of the position vector $\partial \mathbf{r}/\partial t$ give the fluid velocity $\mathbf{V}$, we can write

$$\left(\frac{1}{|\nabla \Phi|} \frac{\partial \Phi}{\partial t} + \big(\mathbf{V} \cdot \mathbf{n} \big) \right) \Big|_S = 0. \tag{13.9}$$

Here suffix S is used to indicate that this equation holds on the body surface, $\mathbf{n}$ denotes the unit vector normal to this surface,

$$\mathbf{n} = \frac{1}{|\nabla \Phi|} \nabla \Phi.$$

*This, of course, is not true if, say, a flow over a porous (perforated) wall is studied.

If the body remains stationary in the coordinate frame used, then the impermeability condition (13.9) reduces to

$$\big(\mathbf{V}\cdot\mathbf{n}\big)\Big|_S = 0, \tag{13.10}$$

which means that the velocity vector should be tangent to the body surface[†]. Condition (13.10) may be rewritten for the velocity potential φ as follows

$$\big(\nabla\varphi\cdot\mathbf{n}\big)\Big|_S = \frac{\partial\varphi}{\partial n}\Big|_S = 0.$$

One can intuitively expect that the flow past a rigid body depends on the body shape as well as on characteristics of the oncoming flow. The information about the body shape is given by the impermeability condition. A second boundary condition, termed the *free-stream condition*, is needed to specify the oncoming flow. If far from the body the flow is uniform with the velocity being $\mathbf{V}_\infty$, then we can write

$$\mathbf{V}\to\mathbf{V}_\infty \quad \text{as} \quad |\mathbf{r}|\to\infty. \tag{13.11}$$

This may be reformulated for the potential function φ as

$$\varphi = \big(\mathbf{V}_\infty\cdot\mathbf{r}\big) + \cdots \quad \text{as} \quad |\mathbf{r}|\to\infty.$$

In summary, to describe the potential flow past a stationary rigid body one needs to solve the following *boundary-value problem*:

Problem 13.1. *Find the velocity potential φ that satisfies the Laplace equation*

$$\nabla^2\varphi = 0 \tag{13.12a}$$

almost everywhere inside the flow field. It should satisfy the impermeability condition

$$\frac{\partial\varphi}{\partial n}\Big|_S = 0, \tag{13.12b}$$

on the body surface, and the free-stream condition

$$\varphi = \big(\mathbf{V}_\infty\cdot\mathbf{r}\big) + \cdots \quad \textit{as} \quad |\mathbf{r}|\to\infty. \tag{13.12c}$$

in the far field.

Next, we shall discuss various techniques by which the Laplace equation (13.12a) can be solved. Let us start with the *principle of superposition*, which is applicable to any linear equation. It is easily seen that if functions φ_1 and φ_2 satisfy the Laplace equation, then their linear combination $\varphi = c_1\varphi_1 + c_2\varphi_2$, with arbitrary coefficients c_1 and c_2, is also a solution of the Laplace equation. Keeping this in mind, we shall introduce some simple examples of potential flows, which correspond to fundamental solutions of the Laplace equation, and may be used as building blocks to construct solutions for more complicated flows that may be of interest in reality.

[†]Of course, when the body surface is perforated to allow for suction or blowing, boundary conditions (13.9), (13.10) should be appropriately modified.

The Flow from a Source or Sink

Let us start with the flow from a ***point source***(or sink) in an otherwise stagnant fluid. For simplicity, we will place the source at the coordinate origin. The intensity of the source q is defined as a quantity which, being multiplied by the fluid density ρ, gives the mass of fluid produced by the source per unit time. Taking into account spherical symmetry of the flow, we expect that at any point with position vector $\mathbf{r}$, the velocity is directed from the source, i.e. along $\mathbf{r}$.

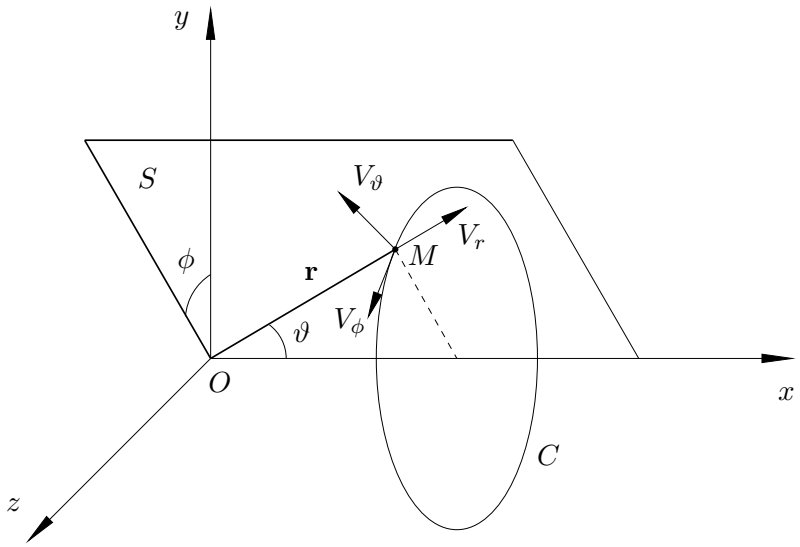

Figure 13.2: Spherical polar coordinates.

For this type of configuration, it is natural to use *spherical polar coordinates*; see Figure 13.2. In spherical coordinates the position of arbitrary point M is given by three numbers, (r, ϑ, ϕ). The first is the distance, $r = |\mathbf{r}|$, from point M to the coordinate origin O; the second is the angle, ϑ, made by the position vector $\mathbf{r}$ with the x-axis, and the third is the angle, ϕ, between xy-plane and plane S drawn through the point of interest, M, and the x-axis. Correspondingly, the velocity vector $\mathbf{V}$ is represented by three components, V_r, V_ϕ and V_ϑ. The radial component, V_r, is parallel to the radius $\mathbf{r}$. The azimuthal component, V_ϕ, is tangent to circle C which lies in the plane drawn through point M perpendicular to the x-axis and has its centre on the x-axis. Finally, the meridional velocity component, V_ϑ, lies in plane S and is perpendicular to the radius $\mathbf{r}$.

In the flow from a source only, the radial velocity V_r is non-zero, and it does not depend on angles ϕ and ϑ. Therefore, if we consider a sphere of radius r whose centre coincides with the source then, using the mass conservation law, we can write

$$V_r \cdot 4\pi r^2 = q, \tag{13.13}$$

where $4\pi r^2$ stands for the area of the sphere surface. Solving (13.13) for V_r we have

$$V_r = \frac{q}{4\pi r^2}. \tag{13.14}$$

To find the velocity potential φ for this flow, we have to use equation (13.6). In the spherical polar coordinates coordinates it is written as

$$V_r = \frac{\partial \varphi}{\partial r}, \qquad V_\vartheta = \frac{1}{r}\frac{\partial \varphi}{\partial \vartheta}, \qquad V_\phi = \frac{1}{r\sin\vartheta}\frac{\partial \varphi}{\partial \phi}. \tag{13.15}$$

Combining the first of equations (13.15) with (13.14) yields

$$\frac{\partial \varphi}{\partial r} = \frac{q}{4\pi r^2}, \tag{13.16}$$

while from the second and third equations in (13.15) show that φ is independent of ϑ and ϕ.

Integration of (13.16) results in[‡]

$$\varphi = -\frac{q}{4\pi r}, \tag{13.17}$$

which is the sought potential of a source (sink for $q < 0$) situated at the origin. If a source is placed at point $\mathbf{r}_0$ then (13.17) should be rewritten as

$$\varphi = -\frac{q}{4\pi|\mathbf{r} - \mathbf{r}_0|}. \tag{13.18}$$

It is easy to check that (13.17) and (13.18) satisfy the Laplace equation, and they are referred to ***source*** if $q > 0$ and ***sink*** if $q < 0$.

[‡]An arbitrary constant may be always added to (13.17) since the velocity potential is defined to within an arbitrary choice of the reference position vector $\mathbf{r}_0$.

Dipole.

Let us now consider a source and a sink of the same intensity placed close to one another. We shall assume that the source is situated at the coordinate origin, and the sink at the point with the position vector $\delta\mathbf{r}_0$. Then, using the *principle of superposition*, we have

$$\varphi = \underbrace{-\frac{q}{4\pi|\mathbf{r}|}}_{\text{source}} + \underbrace{\frac{q}{4\pi|\mathbf{r}-\delta\mathbf{r}_0|}}_{\text{sink}}. \tag{14.1}$$

If $|\delta\mathbf{r}_0|$ is small, then neglecting squares of small quantities we can write

$$\begin{aligned}|\mathbf{r}-\delta\mathbf{r}_0| &= \sqrt{(x-\delta x_0)^2+(y-\delta y_0)^2+(z-\delta z_0)^2} = \\ &= \sqrt{x^2+y^2+z^2-2x\delta x_0-2y\delta y_0-2z\delta z_0+\cdots},\end{aligned}$$

or, equivalently,

$$|\mathbf{r}-\delta\mathbf{r}_0| = \sqrt{r^2-2\big(\mathbf{r}\cdot\delta\mathbf{r}_0\big)+\cdots} = r\left[1-2\frac{\big(\mathbf{r}\cdot\delta\mathbf{r}_0\big)}{r^2}+\cdots\right]^{1/2}. \tag{14.2}$$

Formula (14.2) may be simplified further using the Taylor expansion

$$(1+\varepsilon)^\alpha = 1+\alpha\varepsilon+O(\varepsilon^2) \tag{14.3}$$

with $\alpha=\frac{1}{2}$. We have

$$|\mathbf{r}-\delta\mathbf{r}_0| = r\left[1-\frac{\big(\mathbf{r}\cdot\delta\mathbf{r}_0\big)}{r^2}\right]+O\big(|\delta\mathbf{r}_0|^2\big). \tag{14.4}$$

Substitution of (14.4) into (14.1) gives

$$\varphi = -\frac{q}{4\pi r}+\frac{q}{4\pi r}\frac{1}{\left[1-\frac{(\mathbf{r}\cdot\delta\mathbf{r}_0)}{r^2}\right]},$$

and using (14.3) again, now with $\alpha=-1$, we find

$$\begin{aligned}\varphi &= -\frac{q}{4\pi r}+\frac{q}{4\pi r}\left[1+\frac{\big(\mathbf{r}\cdot\delta\mathbf{r}_0\big)}{r^2}\right]+O\big(|\delta\mathbf{r}_0|^2\big) \\ &= \frac{q}{4\pi}\frac{\big(\mathbf{r}\cdot\delta\mathbf{r}_0\big)}{r^3}+O\big(|\delta\mathbf{r}_0|^2\big).\end{aligned} \tag{14.5}$$

Finally, we assume that $|\delta\mathbf{r}_0|$ tends to zero and q tends to infinity such that their product remains finite. The source-sink pair satisfying this condition is referred to as ***dipole***. This leads to the following expression for the dipole potential

$$\varphi = \frac{\big(\mathbf{m}\cdot\mathbf{r}\big)}{4\pi r^3}. \tag{14.6}$$

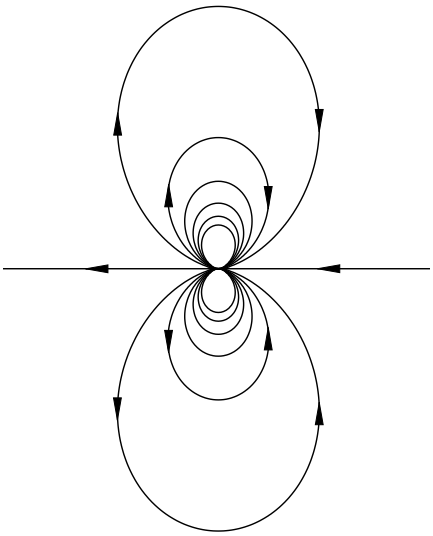

Figure 14.1: Dipole streamline pattern.

Here vector $\mathbf{m} = q\,\delta\mathbf{r}_0$ is referred to as the ***dipole moment***. Once again, it may be verified that (14.6) satisfied the Laplace equation in three dimensions; this is left as an exercise.

The dipole flow (14.6) is symmetric with respect to the axis drawn along vector $\mathbf{m}$. In particular, if $\mathbf{m} = (m, 0, 0)$, then the axis of symmetry coincides with the x-axis, and the streamline pattern in the S-plane of Figure (13.2) appears to be independent of the azimuthal angle ϕ. It is shown in Figure 14.1.

If a dipole is centred at $\mathbf{r}_0$, then the corresponding velocity potential is given by

$$\varphi = \frac{\big(\mathbf{m} \cdot (\mathbf{r} - \mathbf{r}_0)\big)}{4\pi(r - r_0)^3}.$$

The Flow past a Sphere

We shall now show that a superposition of the uniform flow and suitable dipole gives a solution of problem (13.12) which describes the flow past a rigid sphere. For any direction of the oncoming flow, one can always rotate the coordinate system to make the x-axis aligned with the free-stream velocity (see Figure 14.2). Then the potential of the uniform flow (13.12c) becomes

$$\varphi = V_\infty x. \tag{14.7}$$

Let us place the dipole into the sphere centre and assume that it is also aligned with the x-axis, i.e. its moment $\mathbf{m} = (m, 0, 0)$. In this case (14.6) reduces to

$$\varphi = \frac{mx}{4\pi r^3}. \tag{14.8}$$

Superposing (14.7) with (14.8) we have

$$\varphi = V_\infty x + \frac{mx}{4\pi r^3}. \tag{14.9}$$

The value of m is to be determined.

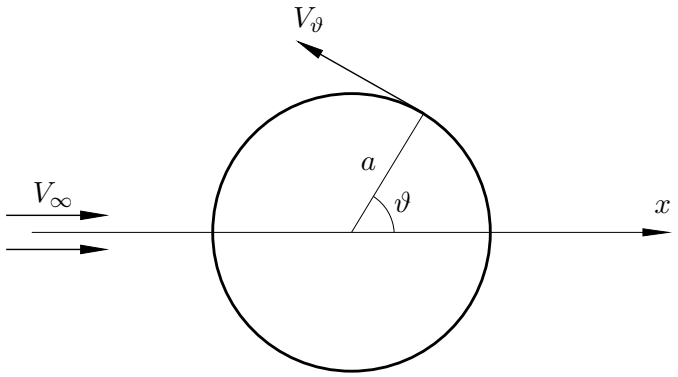

Figure 14.2: The flow view in the plane S of Figure 13.2.

Let us now examine the boundary conditions (13.12b) and (13.12c). As $r \to \infty$ the second term in (14.9) tends to zero, reducing (14.9) to (14.7), which proves that the free-stream boundary condition is satisfied.

Turning to the impermeability condition (13.12b), we note that at any point situated outside the sphere, $x = r\cos\vartheta$, and equation (14.9) may be written as

$$\varphi = V_\infty r\cos\vartheta + \frac{m\cos\vartheta}{4\pi r^2}. \tag{14.10}$$

With a being the radius of the sphere, we have

$$\left.\frac{\partial\varphi}{\partial n}\right|_S = \left.\frac{\partial\varphi}{\partial r}\right|_{r=a} = \left(V_\infty - \frac{m}{2\pi a^3}\right)\cos\vartheta.$$

Therefore, by choosing

$$m = 2\pi a^3 V_\infty, \tag{14.11}$$

we can satisfy the impermeability condition (13.12b) for all values of ϑ, i.e. on the entire surface of the sphere. This proves that formula (14.10) really represents the solution for the flow past the sphere. Substituting (14.11) back into (14.10) results in

$$\varphi = V_\infty\left(r + \frac{a^3}{2r^2}\right)\cos\vartheta. \tag{14.12}$$

In this flow the azimuthal velocity V_ϕ is obviously zero. The radial and meridional velocities may be calculated using formulae (13.15):

$$V_r = \frac{\partial\varphi}{\partial r} = V_\infty\left(1 - \frac{a^3}{r^3}\right)\cos\vartheta, \qquad V_\vartheta = \frac{1}{r}\frac{\partial\varphi}{\partial\vartheta} = -V_\infty\left(1 + \frac{a^3}{2r^3}\right)\sin\vartheta.$$

On the sphere surface ($r = a$) the radial velocity component vanishes, as it should in view of the impermeability condition. Hence, the velocity vector is tangent to the sphere surface and given by

$$\left.V_\vartheta\right|_{r=a} = -\frac{3}{2}V_\infty\sin\vartheta. \tag{14.13}$$

The minus sign in this formula implies that the velocity is directed against increasing ϑ; see Figure 14.2. It turns zero at the front ($\vartheta = \pi$) and rear ($\vartheta = 0$) *stagnation points*, and reaches maximum at the equator ($\vartheta = \pi/2$), where $|V_\vartheta| = \frac{3}{2}V_\infty$.

It is interesting to notice that the velocity (14.13) appears to be symmetric with respect to the equator ($\vartheta = \frac{1}{2}\pi$), exhibit *front-rear symmetry*. Let us now find the pressure distribution. Since the flow considered is steady and potential, one can use the Bernoulli equation in the form given by (12.20). Disregarding the body force and using the free-stream conditions to calculate constant C on the right hand side of (12.20), we have

$$\frac{V^2}{2} + \frac{p}{\rho} = \frac{V_\infty^2}{2} + \frac{p_\infty}{\rho}. \tag{14.14}$$

Substituting (14.13) into (14.14), wee find that on the surface of the sphere the pressure is given by

$$p = p_\infty + \frac{1}{2}\rho V_\infty^2 \left(1 - \frac{9}{4}\sin^2\vartheta\right).$$

Since the pressure is symmetric with respect to the equator, the integral pressure force acting upon the front hemisphere is entirely balanced by the pressure force acting upon the rear hemisphere, which suggests that the sphere should experience no resistance when moving through a fluid with constant velocity. This result is an example of the ***d'Alembert paradox***. As unrealistic as it appears to be, zero drag prediction is not a unique property of the sphere flow, but rather a common feature of inviscid flow theory. It highlights a fundamental weakness of this theory. Historically, the efforts to resolve this paradox drove further developments of theoretical fluid dynamics.

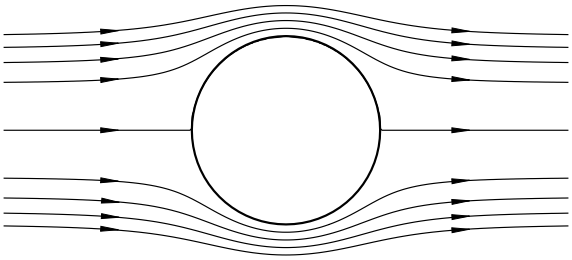

(a) Theoretical streamline pattern.

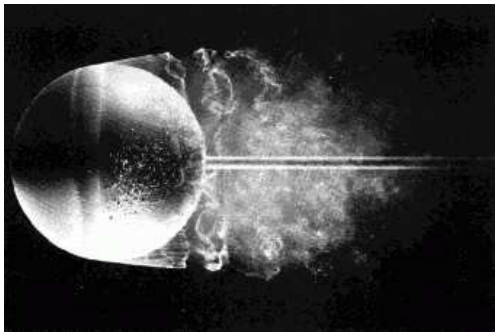

(b) Visualization by Werlé (1980).

Figure 14.3: Comparison of the prediction by the potential flow theory with experimental observations.

In Figure 14.3 the streamline pattern, drawn using solution (14.12), is compared with an experimental visualization of the flow. As can be seen, in reality the flow does not remain attached to the sphere surface. Instead near the equator streamlines on and close the surface deviate significantly from the surface, leading to a distortion in the flow field. The flow looses its front-rear symmetry, and consequently a non-zero drag is produced. This rather drastic change is known as ***flow separation***.

Experimental observations also show that once separated, the flow normally develops unsteadiness, which causes an additional drag. At the same time an unsteady flow might remain attached for a period of time. For example, suppose that the sphere is initially kept at rest and is surrounded by a fluid which is also at rest. Then the sphere is brought into motion causing the fluid around it to move. Numerous experiments show that the resulting fluid flow remains fully attached for a certain of time. However, separation eventually occurs.

Two-Dimensional Flows

We now focus on incompressible inviscid flows that are two-dimensional. A typical example is that of an incompressible fluid past a rigid body of cylindrical shape whose cross-section is shown in Figure 15.1; the generatrix of the body surface is a straight line perpendicular to the sketch plane, and the cylinder is assumed to be infinite in its axial direction[†]. Let us further assume that the velocity vector of the oncoming flow is perpendicular to the body generatrix. In this case, none of the fluid dynamic functions is expected to vary in the direction of the generatrix, which is taken to aligned with the z-axis, that is,

$$\frac{\partial}{\partial z} = 0, \tag{15.1}$$

and the velocity component in this direction, w, is expected to be zero so that

$$\mathbf{V} = (u, v, 0). \tag{15.2}$$

Fluid flows satisfying conditions (15.1) and (15.2) are termed *two-dimensional*.

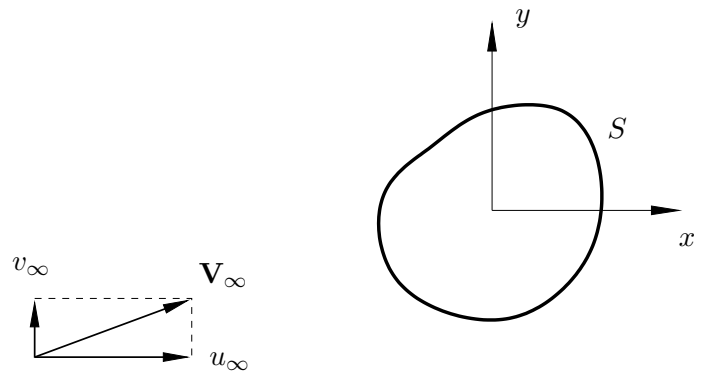

Figure 15.1: A two-dimensional flow.

In a two-dimensional flow, the vorticity vector $\boldsymbol{\omega}$ has just one component ω_z perpendicular to the plane of fluid motion. Indeed, using (15.1) and (15.2) in (4.1), we have

$$\boldsymbol{\omega} = \mathbf{k}\left(\frac{\partial v}{\partial x} - \frac{\partial u}{\partial y}\right) = \omega_z \mathbf{k}.$$

If the flow considered is irrotational, i.e.

$$\omega_z = \frac{\partial v}{\partial x} - \frac{\partial u}{\partial y} = 0 \tag{15.3}$$

almost everywhere. Then there exists a velocity potential, φ. It is related to the velocity field through the integral (13.2) as in the case of three-dimensional flows. For a two-dimensional flow, this integral assumes a simpler form

$$\varphi(t, \mathbf{r}) = \int_{\mathbf{r}_0}^{\mathbf{r}} \big(\mathbf{V} \cdot d\mathbf{r}\big) = \int_{\mathbf{r}_0}^{\mathbf{r}} (u\, dx + v\, dy). \tag{15.4}$$

[†]In practice, it is sufficient for the length of a cylinder to be much larger than the characteristic dimension of its cross-section.

In Lecture 13, it was demonstrated that the integral for $\varphi(t, \mathbf{r})$ does not depend on a choice of contour C connecting points $\mathbf{r}_0$ and $\mathbf{r}$. We now exam this result more closely.

Recall that we took two contours C and C' (see Figure 13.1) connecting $\mathbf{r}_0$ and $\mathbf{r}$, and denoted the results of the integration along C and C' by $\varphi(t, \mathbf{r})$ and $\varphi'(t, \mathbf{r})$, respectively. Then the difference between $\varphi(t, \mathbf{r})$ and $\varphi'(t, \mathbf{r})$ was calculated using the Stokes theorem

$$\varphi(t, \mathbf{r}) - \varphi'(t, \mathbf{r}) = \int\limits_{C} \big(\mathbf{V} \cdot d\mathbf{r}\big) - \int\limits_{C'} \big(\mathbf{V} \cdot d\mathbf{r}\big) = \oint\limits_{\widetilde{C}} \big(\mathbf{V} \cdot d\mathbf{r}\big) = \iint\limits_{\sigma} \big(\boldsymbol{\omega} \cdot \mathbf{n}\big) ds.$$

Here $\widetilde{C}$ is a closed contour composed of C and C', and σ is an open surface spanned by $\tilde{C}$ as is shown in Figure 13.1. We see that if $\boldsymbol{\omega} = 0$ everywhere on σ, then $\varphi(t, \mathbf{r}) = \varphi'(t, \mathbf{r})$. This conclusion, however, relies on an assumption that the region occupied by the moving fluid is *singly-connected*, i.e. for any closed contour $\widetilde{C}$ there exists a surface σ, resting on $\widetilde{C}$, which lies entirely inside the flow field. Two-dimensional flows past cylindrical bodies, obviously, do not share this property; one path connecting points $\mathbf{r}_0$ and $\mathbf{r}$ might go round one side of the body and the other might go round the other side, and the integrals along these two paths as defined by (15.4) can not be proven to be the same.

Corresponding to this, we can subdivide all closed contours into two classes. In the first one are contours like C_1 in Figure 15.2 which may be reduced to a point by a continuous deformation (shrinking). When the position vector $\mathbf{r}$ in the integral (15.4) makes a circle around such a contour, the potential $\varphi(t, \mathbf{r})$ returns to it initial value. In the second category are contours like C_2. When traversing around such a contour, the potential increases by a value

$$\Delta\varphi = \oint\limits_{C_2} \big(\mathbf{V} \cdot d\mathbf{r}\big) = \Gamma, \tag{15.5}$$

which is equal to the velocity circulation in the flow past a rigid body.

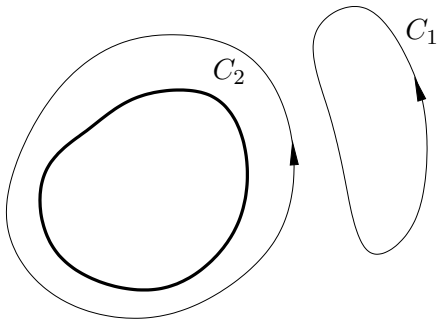

Figure 15.2: Classification of closed contours in two-dimensional flows.

It is easily shown that the circulation Γ is independent on a choice of contour embracing the body and hence an 'intrinsic' constant of a given two-dimensional flow. To show this, we take two contours C_2 and C_2', both of which go around the body as shown in Figure 15.3,

and write

$$\Gamma = \oint\limits_{C_2} \big(\mathbf{V}\cdot d\mathbf{r}\big), \qquad \Gamma' = \oint\limits_{C_2'} \big(\mathbf{V}\cdot d\mathbf{r}\big).$$

Then using the Stokes theorem (which actually degenerates to Green's theorem), we will have

$$\oint\limits_{C_2} \big(\mathbf{V}\cdot d\mathbf{r}\big) - \oint\limits_{C_2'} \big(\mathbf{V}\cdot d\mathbf{r}\big) = \iint\limits_{\sigma} \omega_z ds, \tag{15.6}$$

with σ now denoting the region between C_2 and C_2'. Since in this region equation (15.3) holds, we can conclude that the two integrals on the left hand side of (15.6) coincide to one another.

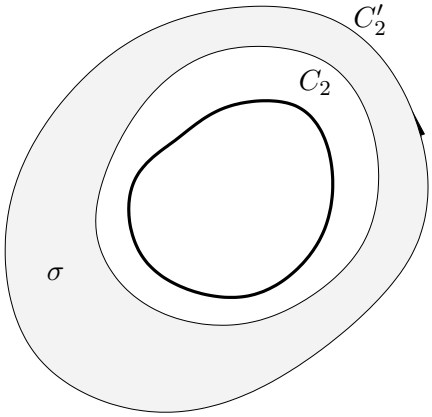

Figure 15.3: Two closed contours, C_2 and C_2', and surface σ exploited in equation (15.6).

Thus, when studying two-dimensional irrotational flows past solid bodies, one can still introduce a velocity potential φ with the help of the integral (15.4). However, in general case, φ will not be a single-valued function, although the non-uniqueness in φ is rather simple. When the contour makes each loop around the body, the value of φ at a given point, $\mathbf{r}$, increases by the circulation, Γ. In what follows, the integral in (15.5) is calculated in the counter-clockwise direction.

Of course, each single-valued branch of the velocity potential, φ, still satisfies the Laplace equation (13.7), which is written in two dimensions as

$$\frac{\partial^2\varphi}{\partial x^2} + \frac{\partial^2\varphi}{\partial y^2} = 0.$$

Stream Function

For two-dimensional flows, the continuity equation (12.1b) reduces to

$$\frac{\partial u}{\partial x} + \frac{\partial v}{\partial y} = 0. \tag{15.7}$$

An important consequence of two-dimensionality is that there exists a scalar function $\psi(t,\mathbf{r})$, termed the ***stream function*** such that

$$u = \frac{\partial\psi}{\partial y}, \qquad v = -\frac{\partial\psi}{\partial x}. \tag{15.8}$$

Despite that ψ is a special property of two-dimensionality, the *proof of its existence* is similar to that for the existence of the velocity potential $\varphi(t, \mathbf{r})$, which has been introduced for a general three-dimensional flow based on the zero-vorticity equation (15.3). To prove, we define an auxiliary vector field

$$\mathbf{A} = (A_x, A_y, A_z) = (-v, u, 0), \tag{15.9}$$

which would play the role of $\mathbf{V}$ in the proof. Now calculate the curl of A,

$$\text{curl}\mathbf{A} = \begin{vmatrix} \mathbf{i} & \mathbf{j} & \mathbf{k} \\ \frac{\partial}{\partial x} & \frac{\partial}{\partial y} & \frac{\partial}{\partial z} \\ -v & u & 0 \end{vmatrix} = \mathbf{k}\left(\frac{\partial u}{\partial x} + \frac{\partial v}{\partial y}\right) = 0,$$

where use has been made of the fact that neither u nor v is dependent on z. Hence, the vector field $\mathbf{A}$ is irrotational. Analogous to (15.4), there exists a scalar function $\psi(t, \mathbf{r})$, such that $\mathbf{A} = \nabla\psi$, and furthermore $\psi(t, \mathbf{r})$ may be constructed as the integral

$$\psi(t, \mathbf{r}) = \int_{\mathbf{r}_0}^{\mathbf{r}} \big(\mathbf{A} \cdot d\mathbf{r}\big) = \int_{\mathbf{r}_0}^{\mathbf{r}} (-v\, dx + u\, dy). \tag{15.10}$$

Writing the relation

$$\nabla\psi = \mathbf{A} = (-v, u, 0). \tag{15.11}$$

into the coordinate decomposition form

$$\frac{\partial\psi}{\partial x} = A_x = -v, \qquad \frac{\partial\psi}{\partial y} = A_y = u,$$

proves the validity of equations (15.8).

The existence of the stream function ψ relies solely on the continuity equation or, more precisely, on the form (15.7) that it assumes in two-dimensional incompressible flows. It does not matter if the flow is steady or unsteady, inviscid or viscous, irrotational or with non-zero vorticity, one can still introduce the stream function. In the case of irrotational flow, the stream function ψ satisfies the Laplace equation

$$\nabla^2\psi = \frac{\partial^2\psi}{\partial x^2} + \frac{\partial^2\psi}{\partial y^2} = 0,$$

as can be shown by substituting (15.8) into equation (15.3).

The stream function is more than a mathematical concept. It has interesting physical meanings. In order to demonstrate them, we consider two points M and M' in the xy-plane (see Figure 15.4) and calculate the fluid volume flux across a curve $\mathcal{L}$ joining M and M' or, more precisely, the flux across an open surface swept out by translating curve $\mathcal{L}$ through a unit distance in the z-direction. Taking the flux to be positive when it is in the direction shown by the arrow in Figure 15.4, we write

$$Q = -\int_{\mathcal{L}} \big(\mathbf{V} \cdot \mathbf{n}\big) dl = -\int_{\mathcal{L}} (un_x + vn_y)\, dl, \tag{15.12}$$

where $\mathbf{n} = (n_x, n_y)$ is a unit vector normal to $\mathcal{L}$ and dl is the length of a small element of $\mathcal{L}$. Notice that unlike for the mass flux (7.3), volume flux integral (15.12) does not involve the fluid density ρ.

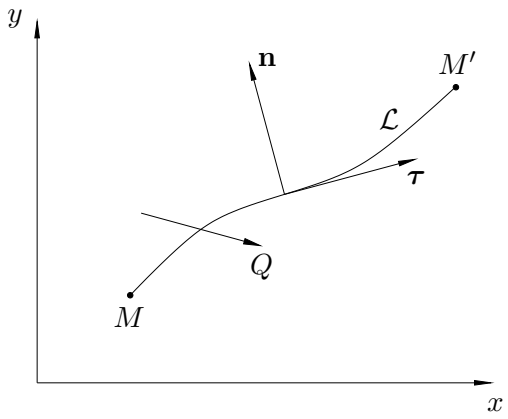

Figure 15.4: Calculation of volume flux Q through curve $\mathcal{L}$ between points M and M'.

Let us now introduce a unit vector $\boldsymbol{\tau} = (\tau_x, \tau_y) = (dx, dy)/dl$ which is *tangent* to $\mathcal{L}$, and is related to the normal vector through

$$n_x = -\tau_y, \qquad n_y = \tau_x.$$

Hence, using (15.8), we can express the integral in (15.12) as

$$Q = \int\limits_{\mathcal{L}} \left(\frac{\partial \psi}{\partial x} \tau_x + \frac{\partial \psi}{\partial y} \tau_y \right) d\, l = \int\limits_{\mathcal{L}} \big(\nabla \psi \cdot \boldsymbol{\tau} \big) d\, l = \int\limits_{\mathcal{L}} \big(\nabla \psi \cdot d\mathbf{r} \big),$$

with $d\mathbf{r}$ being an increment of the position vector $\mathbf{r}$ along $\mathcal{L}$. We see that the volume flux across any curve joining two points in the flow field equals the difference between the values of ψ at these points:

$$Q = \psi(M') - \psi(M). \tag{15.13}$$

The *stream function* that we just introduced and the *streamlines* (which was introduced in Lecture 3) are two different concepts. For two-dimensional flows, they are closely related as is stated in the following theorem, which we now prove by using the result (15.13).

Theorem 1. *The stream function is constant along any streamline, and any line defined by the equation*

$$\psi = const \tag{15.14}$$

is a streamline.

Proof. Let the line $\mathcal{L}$ in Figure 15.4 be a streamline. Then according to its definition (Definition 3.1 of Lecture 3) the velocity vector is tangent to $\mathcal{L}$, and therefore there is no fluid flux across $\mathcal{L}$ and $Q = 0$. Combining this with (15.13), we can conclude that for any two points M and M' on the streamline $\mathcal{L}$, $\psi(M') = \psi(M)$. This proves the first part of the theorem.

To prove that any line defined by equation (15.14) is a streamline, we note that for a line represented by equation (15.14), the unit normal vector $\mathbf{n}$ may be calculated as

$$\mathbf{n} = \frac{\nabla \psi}{|\nabla \psi|} = \frac{1}{|\nabla \psi|} \left(\frac{\partial \psi}{\partial x}, \frac{\partial \psi}{\partial y} \right).$$

Let us consider the scalar product of the velocity vector $\mathbf{V}$ and normal vector $\mathbf{n}$,

$$\big(\mathbf{V}\cdot\mathbf{n}\big)=\frac{1}{|\nabla\psi|}\bigg(u\frac{\partial\psi}{\partial x}+v\frac{\partial\psi}{\partial y}\bigg). \tag{15.15}$$

Using (15.8) in (15.15) we see that $\big(\mathbf{V}\cdot\mathbf{n}\big)=0$, which proves that the velocity vector $\mathbf{V}$ is perpendicular to $\mathbf{n}$, and therefore, is tangent to the line considered. □

It should be pointed out that the result (15.13) as well as the relations between the stream function and streamlines as stated in the above theorem hold for any two-dimensional flows whether inviscid or viscous, steady or unsteady and irrotational or rotational.

Complex Potential

If an incompressible flow is both *two-dimensional flow* and *irrotational*, then equations (15.3) and (15.7) hold,

$$\frac{\partial v}{\partial x} - \frac{\partial u}{\partial y} = 0, \qquad \frac{\partial u}{\partial x} + \frac{\partial v}{\partial y} = 0. \tag{16.1}$$

From the first of these it follows that there exists the velocity potential φ related to the velocity vector by means of equation (13.6) in Lecture 13. For a two-dimensional flow, it is written as

$$u = \frac{\partial \varphi}{\partial x}, \qquad v = \frac{\partial \varphi}{\partial y}. \tag{16.2}$$

The second of equations (16.1) guarantees the existence of the stream function ψ, and we can use equations (15.8),

$$u = \frac{\partial \psi}{\partial y}, \qquad v = -\frac{\partial \psi}{\partial x}. \tag{16.3}$$

Comparing (16.2) with (16.3), we see that

$$\frac{\partial \varphi}{\partial x} = \frac{\partial \psi}{\partial y}, \qquad \frac{\partial \varphi}{\partial y} = -\frac{\partial \psi}{\partial x}. \tag{16.4}$$

These are the *Cauchy-Riemann equations* representing the necessary and sufficient conditions for the function

$$w(z) = \varphi + i\psi \tag{16.5}$$

to be an *analytic function* of the complex variable $z = x + iy$. This function is called the ***complex potential***.

If $w(z)$ is known, then the velocity component u and v could be obtained by means of differentiating $w(z)$. We have

$$\frac{dw}{dz} = \frac{\partial \varphi}{\partial x} + i\frac{\partial \psi}{\partial x},$$

which, on using (16.2) and (16.3), may be written as

$$\overline{V}(z) = u - iv = \frac{dw}{dz}. \tag{16.6}$$

Function $\overline{V}(z) = u - iv$ is called the ***complex conjugate velocity***. Being the derivative of analytic function, the complex conjugate velocity, $\overline{V}(z)$, is also an analytic function. The latter is confirmed by equations (16.1), which are the Cauchy-Riemann conditions for $\overline{V}(z) = u - iv$. The pressure can be obtained from the Bernoulli equation. It follows that a complex potential $w(z)$ encapsules all the information of a two-dimensional irrotational (potential) flow.

It is worth pointing out that *any* analytic function $w(z)$ would give a velocity field and pressure that satisfy the Euler equations, and thus could represent a *possible* two-dimensional irrotational flow. However, the boundary conditions may not be readily satisfied. The simplest flow configuration is an unbounded domain, in which case the velocity is usually required to be finite. If the velocity $\overline{V}(z)$ is required to be non-singular and also bounded in the far field, then the only possibility is that $\overline{V}(z)$ is constant, corresponding

to a completely uniform flow. This follows directly from *Liouville's theorem* on analytic functions, which states "*a function that is analytic everywhere on the entire complex plane and bounded can only be a constant*". It may be inferred that any non-uniform flow that is bounded must necessarily be singularity driven in the sense that $w(z)$ must contain a singularity.

In the following, we shall consider several simple analytic functions $w(z)$, and find out the corresponding elementary two-dimensional flows. Conversely, one may consider elementary two-dimensional flows and deduce the corresponding expressions for the complex potential $w(z)$. These elementary flows and the corresponding analytic functions can be used as basic building blocks to construct solutions for flows of interest.

Uniform Flow.

We consider the complex potential in the simplest form, a linear function of z,

$$w(z) = e^{-i\alpha} V_\infty z. \tag{16.7}$$

where V_∞ and α are real constants. The complex conjugate velocity can be found as[†]

$$\overline{V}(z) = u - iv = V_\infty e^{-i\alpha} = V_\infty(\cos\alpha - i\sin\alpha). \tag{16.8}$$

Equating the real and imaginary parts, we have

$$u = V_\infty \cos\alpha, \qquad v = V_\infty \sin\alpha. \tag{16.9}$$

In the Cartesian coordinate system (x, y), the velocity components above represent a uniform flow in the direction that makes an angle α with the x-axis, and the magnitude of the velocity is V_∞ (see Figure 16.1).

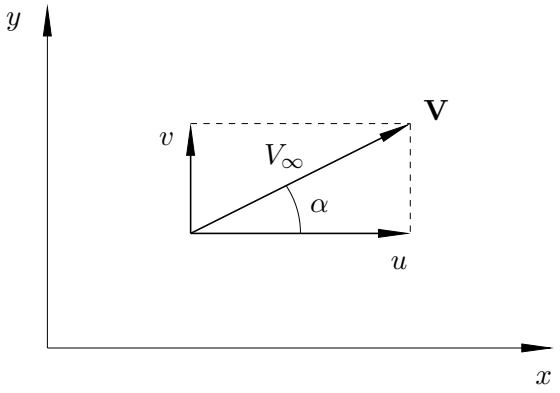

Figure 16.1: Uniform flow.

Of course if given the velocity (16.9), one could follow the steps opposite to the above to find the corresponding complex potential (16.7).

[†]Here use has been made of the well known *Euler formula*

$$e^{i\alpha} = \cos\alpha + i\sin\alpha.$$

Two-Dimensional Source.

Rather than finding the flow from a prescribed complex potential $w(z)$, we now start with a flow in physical space and try to find the corresponding $w(z)$. The flow that we consider is the two-dimensional analogue of the point source in three dimensions, which was considered in Lecture 13. It may be viewed as a superposition of three-dimensional sources continuously and *uniformly* distributed along an infinite straight line, $\mathcal{L}$, drawn perpendicular to the (x, y)-plane. Such a source is also called ***two-dimensional*** or ***line source***. The resulting flow will be a two-dimensional one in the (x, y)-plane (see Problem 1 in Exercises 5).

Let us define the strength, q, of the two-dimensional source as the volume of the fluid produced (per unit time) by a segment of the line $\mathcal{L}$ with unit length in the direction perpendicular to the (x, y)-plane. Assume that the two-dimensional source is centred at

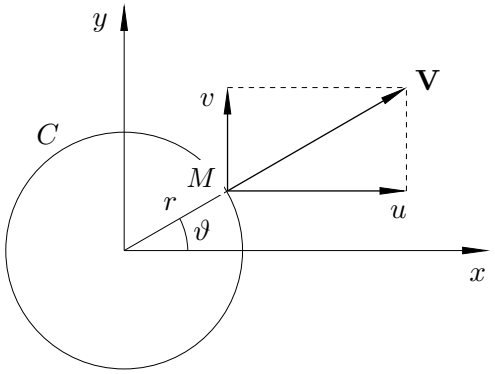

Figure 16.2: Two-dimensional source.

the coordinate origin ($x = y = 0$). Due to the symmetry of the flow, the velocity vector has only radial component, V_r, which is the same at all points on a C, a circle of radius r. The law of mass conservation implies that

$$2\pi r \cdot V_r = q,$$

from the velocity, V_r, at a point M situated at distance r from the source is found as

$$V_r = \frac{q}{2\pi r}.$$

Denoting by ϑ the angle made by the velocity vector with the x-axis, we can write

$$u = V_r \cos\vartheta = \frac{q}{2\pi}\,\frac{\cos\vartheta}{r}, \qquad v = V_r \sin\vartheta = \frac{q}{2\pi}\,\frac{\sin\vartheta}{r},$$

and therefore,

$$\overline{V}(z) = u - iv = \frac{q}{2\pi}\,\frac{\cos\vartheta - i\sin\vartheta}{r} = \frac{q}{2\pi}\,\frac{1}{r(\cos\vartheta + i\sin\vartheta)} = \frac{q}{2\pi z}. \tag{16.10}$$

Integration of (16.10) leads to

$$w(z) = \frac{q}{2\pi}\ln z, \tag{16.11}$$

which is the sought complex potential of two-dimensional point source centred at $z = 0$. If a two-dimensional source is centred at $z = z_0$, then the complex potential is

$$w(z) = \frac{q}{2\pi}\ln(z - z_0).$$

Note the flow is *bounded*, but $w(z)$ is *singular* at $z = z_0$. Obviously, the case with $q < 0$ represents the flow due to a ***sink***.

Dipole.

Similar to a three-dimensional dipole, a two-dimensional dipole is introduced as a superposition of a source and a sink. If a source is situated at $z = 0$ and the sink of equal strength at $z = \delta z_0$, then we can write

$$w(z) = \frac{q}{2\pi}\ln z - \frac{q}{2\pi}\ln(z - \delta z_0) = \\ = \frac{q}{2\pi}\ln z - \frac{q}{2\pi}\ln\left[z\left(1 - \frac{\delta z_0}{z}\right)\right] = -\frac{q}{2\pi}\ln\left(1 - \frac{\delta z_0}{z}\right). \tag{16.12}$$

We shall now suppose $|\delta z_0|$ to be small as compared to $|z|$. In this case Taylor expansion for the logarithm, $\ln(1 + \varepsilon) = \varepsilon + \cdots$, may be used. We have

$$\ln\left(1 - \frac{\delta z_0}{z}\right) = -\frac{\delta z_0}{z} + \cdots,$$

which reduces (16.12) to

$$w(z) = \frac{me^{i\alpha}}{2\pi z}. \tag{16.13}$$

Here $m = q|\delta z_0|$ is the moment of the dipole, and $\alpha = \arg\{\delta z_0\}$ defines the orientation of the dipole in the (x, y)-plane. The expression (16.13) is the complex potential for a ***two-dimensional dipole*** centred at $z = 0$. For a dipole centred at z_0, the complex potential of the flow is

$$w(z) = \frac{me^{i\alpha}}{2\pi(z - z_0)}.$$

Potential Vortex.

The complex potential of the source (16.11) is given by the logarithmic function $\ln z$ with a *real factor* $q/2\pi$. The complex potential for the flow due to a ***potential vortex*** is of $\ln z$, with the difference that the factor is *imaginary*, i.e.

$$w(z) = \frac{\kappa}{2\pi i}\ln z, \tag{16.14}$$

where κ is a real constant. A potential vortex is also referred to as ***line vortex***.

In order to determine the form of the streamlines and velocity in this flow we shall rely on Theorem 1 of Lecture 15. We first separate the real and imaginary parts in the complex potential (16.14). Expressing z in the exponential form, $z = re^{i\vartheta}$, we have

$$w(z) = \varphi + i\psi = \frac{\kappa}{2\pi i}(\ln r + i\vartheta) = \frac{\kappa}{2\pi}\vartheta - i\frac{\kappa}{2\pi}\ln r.$$

Hence, the velocity potential and stream function are given by

$$\varphi = \frac{\kappa}{2\pi}\vartheta, \qquad \psi = -\frac{\kappa}{2\pi}\ln r.$$

It is easily seen that the potential, φ, increases by the value of κ each time a point in the complex z-plane makes a full circle around the vortex centre. Therefore, according to (15.5), κ is the circulation, Γ, and we can rewrite (16.14) as

$$w(z) = \frac{\Gamma}{2\pi i} \ln z. \tag{16.15}$$

Correspondingly, the stream function takes the form

$$\psi = -\frac{\Gamma}{2\pi} \ln r.$$

Theorem 1 in Lecture 15 states that ψ remains constant along streamline, which can only happen if the radius, r, stays constant. This means that the streamlines have the form of concentric circles with the centre situated at the origin $z = 0$ (see Figure 16.3).

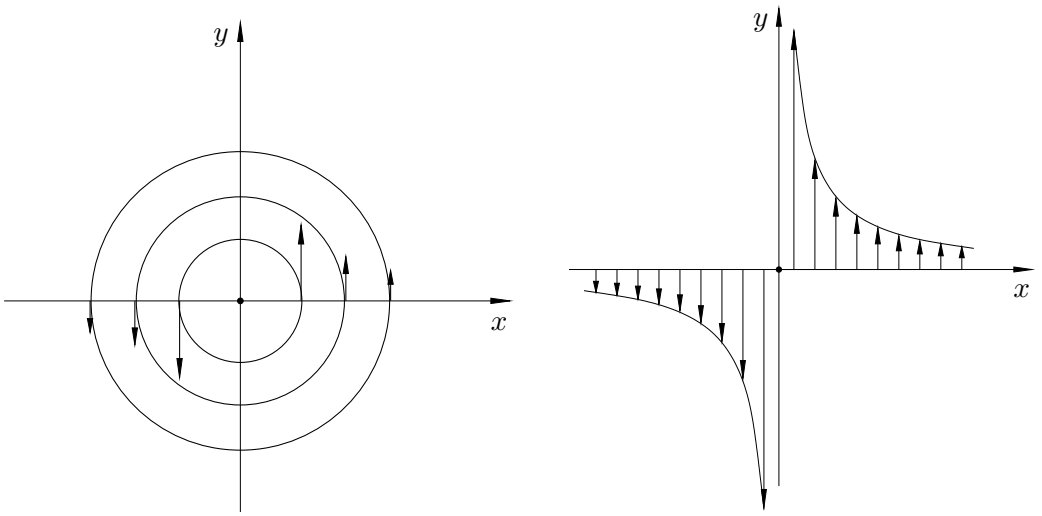

Figure 16.3: Streamline pattern (left) and velocity profile (right) for the potential vortex flow (16.14), the flow due to a line vortex.

In order to make φ and consequently $w(z)$ (or more precisely $\ln z$ in $w(z)$) single-valued, we choose the branch by restricting $-\pi \leq \vartheta < \pi$, i.e. by placing a *branch cut* along the negative real axis.

In order to find the velocity, we differentiate (16.15) with respect to z,

$$\overline{V}(z) = \frac{dw}{dz} = \frac{\Gamma}{2\pi i z}. \tag{16.16}$$

As the velocity vector is tangent to the stream lines, the shape of which is already known, we only need to find the modulus of the velocity

$$|\mathbf{V}| = |\overline{V}(z)| = \frac{\Gamma}{2\pi|z|} = \frac{\Gamma}{2\pi r}, \tag{16.17}$$

indicating that $|\mathbf{V}|$ is inversely proportional to the distance from the vortex centre; see Figure 16.3. Alternatively, from the velocity potential φ, the velocity in the polar coordinate system is found as

$$v_r = \frac{\partial \varphi}{\partial r} = 0, \quad v_\theta = \frac{1}{r}\frac{\partial \varphi}{\partial \theta} = \frac{\Gamma}{2\pi r},$$

or from the stream function ψ,

$$v_r = \frac{1}{r}\frac{\partial \psi}{\partial \theta} = 0, \quad v_\theta = -\frac{\partial \psi}{\partial r} = \frac{\Gamma}{2\pi r}.$$

Clearly, the direction of the velocity is anti-clockwise if $\Gamma > 0$ and clockwise if $\Gamma < 0$.

The complex potential (16.15) and the velocity magnitude are pertinent to a ***potential*** or ***line vortex*** centred at $z = 0$. For a vortex centred at z_0,

$$w(z) = \frac{\Gamma}{2\pi i}\ln(z - z_0), \quad |\mathbf{V}| = |\overline{V}(z)| = \frac{\Gamma}{2\pi|z - z_0|}.$$

Boundary-Value Problem for the Complex Potential

Unlike the elementary flows considered in the previous lecture, which are in an unbounded domain, flows of practical interest involve boundaries. It is important to formulate the corresponding boundary-value problem properly. Such a formulation provides a strict mathematical basis for analysis. In three dimensions, the behaviour of potential flow past a stationary body is governed by Problem 13.1 (see Lecture 13). For two-dimensional flows, it is advantageous to reformulate that problem in terms of the complex potential $w(z)$ as mathematical techniques of analytic functions could be used. In two-dimensions, Problem 13.1 is equivalent to the following one.

Problem 17.1. *Find the complex potential $w(z) = \varphi + i\psi$ such that*

1. *$w(z)$ is an analytic function of the complex variable $z = x + iy$ everywhere outside the body contour S,*

2. *it satisfies the impermeability condition on the body contour*

$$\Im\big\{w(z)\big\}\Big|_S = const, \tag{17.1}$$

3. *and the free-stream condition*

$$\frac{dw}{dz} = u_\infty - iv_\infty \quad as \quad z \to \infty, \tag{17.2}$$

where u_∞ and v_∞ are the components of the velocity vector $\mathbf{V}_\infty$ in the oncoming flow.

Condition *1* is equivalent to the requirement that the velocity potential, φ, satisfies the Laplace equation. This is automatically guaranteed by any analytic function $w(z) = \varphi(x, y) + i\psi(x, y)$ because of the Cauchy-Riemann conditions,

$$\frac{\partial\varphi}{\partial x} = \frac{\partial\psi}{\partial y}, \qquad \frac{\partial\varphi}{\partial y} = -\frac{\partial\psi}{\partial x}. \tag{17.3}$$

Cross-differentiation of (17.3) leads to the Laplace equation for φ.

Condition *2* is a reformulation of, and hence equivalent to, the impermeability condition on the surface of a stationary body as was expressed in the form of equation (13.10) or equivalently by equation (13.12b) in the formulation of Problem (13.1). The impermeability condition means that the fluid velocity must be tangent to the body surface. According to Theorem 1 of Lecture 15, the contour of $\psi =$ constant coincides with one of the streamlines. Since $\psi = \Im\big\{w(z)\big\}$, Condition *2* implies that the body surface itself is a streamline, and so the fluid velocity at the surface is tangent to the body surface.

Finally, equation (17.2) simply recasts the free-stream condition (13.12c) of Problem 13.1 in terms of the complex conjugate velocity, $\overline{V}$.

The Flow past a Circular Cylinder.

Here we shall demonstrate that the solution of Problem 17.1 for the two-dimensional flow past a circular cylinder may be constructed as a superposition of the uniform flow (16.8) and dipole (16.13). Without losing generality, we can choose the x-axis to be parallel to the oncoming flow and set $\alpha = 0$ in (16.8). We have

$$w(z) = V_\infty z. \tag{17.4}$$

We then place a dipole into the coordinate origin and assume that it is also aligned with the x-axis. We therefore choose $\alpha = 0$ in (16.13) leading to

$$w(z) = \frac{m}{2\pi z}, \tag{17.5}$$

but the dipole strength m is to be fixed in order to satisfy the boundary condition on the surface of the cylinder. Adding (17.4) and (17.5) together, we write

$$w(z) = V_\infty z + \frac{m}{2\pi z}. \tag{17.6}$$

Function (17.6) obviously satisfies condition *1* of Problem 17.1, as $w(z)$ is analytic everywhere except at point $z = 0$. We will see that this point lies inside the body contour; meanwhile analyticity of $w(z)$ should be ensured in the flow field.

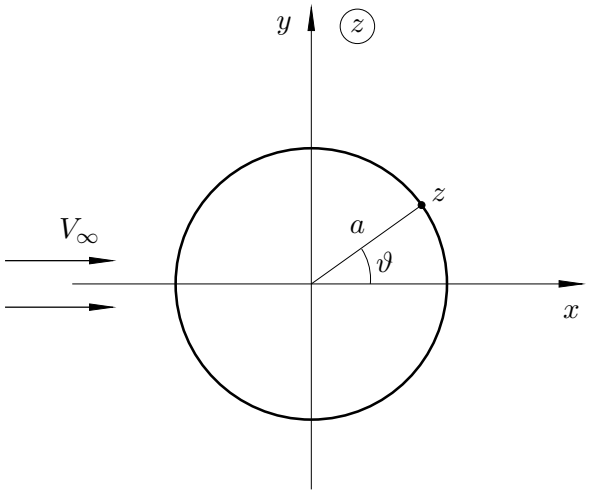

Figure 17.1: Flow past a circular cylinder.

Turning to condition *2*, we shall assume that the cylinder has its centre at $z = 0$, with the radius being a. Then for any point on the cylinder surface

$$z = ae^{i\vartheta}, \tag{17.7}$$

where ϑ is the position angle measured from the real positive semi-axis, as shown in Figure 17.1. Substitution of (17.7) into (17.6) results in

$$w(z) = V_\infty a e^{i\vartheta} + \frac{m}{2\pi a} e^{-i\vartheta}. \tag{17.8}$$

The stream function of the cylinder surface is given by the imaginary part of (17.8),

$$\psi\Big|_{r=a} = \Im\big\{w(z)\big\} = \left(V_\infty a - \frac{m}{2\pi a}\right) \sin\vartheta.$$

It may be made a constant (zero) for all values of ϑ by choosing

$$m = 2\pi V_\infty a^2. \tag{17.9}$$

Substituting (17.9) back into (17.6), we have

$$w(z) = V_\infty\left(z + \frac{a^2}{z}\right). \tag{17.10}$$

It remains to check that function (17.10) also satisfies condition *3* of Problem 17.1. Indeed, as $z \to \infty$, the second term in the parenthesis tends to zero, and (17.10) reduces to $w(z) = V_\infty z$, which represents a uniform flow parallel to the x-axis.

Differentiating (17.10) we find that at any point z in the flow field the complex conjugate velocity

$$\overline{V}(z) = \frac{dw}{dz} = V_\infty\left(1 - \frac{a^2}{z^2}\right). \tag{17.11}$$

In particular, on the cylinder surface, where z is given by (17.7),

$$\overline{V}\Big|_{r=a} = u - iv = V_\infty\big(1 - e^{-2i\vartheta}\big), \tag{17.12}$$

which can be rearranged (17.12) as

$$\overline{V}\Big|_{r=a} = V_\infty e^{-i\vartheta}\big(e^{i\vartheta} - e^{-i\vartheta}\big) = 2iV_\infty e^{-i\vartheta}\sin\vartheta.$$

The modulus of the velocity vector $\mathbf{V}$ is calculated as $|\mathbf{V}| = \sqrt{u^2 + v^2}$, and obviously coincides with the modulus of the complex conjugate velocity $\overline{V} = u - iv$. Therefore one can conclude that on the cylinder surface

$$|\mathbf{V}| = 2V_\infty \sin\vartheta. \tag{17.13}$$

We see that there are two points where $|\mathbf{V}| = 0$, the *front stagnation point* ($\vartheta = \pi$) and the *rear stagnation point* ($\vartheta = 0$). Between them the fluid velocity (17.13) appears to be symmetric with respect to the middle point ($\vartheta = \pi/2$), where it reaches its maximum,

$$|\mathbf{V}|_{\max} = 2V_\infty.$$

The pressure distribution can be found by using the Bernoulli equation (14.14),

$$\frac{V^2}{2} + \frac{p}{\rho} = \frac{V_\infty^2}{2} + \frac{p_\infty}{\rho}. \tag{17.14}$$

Substitution of (17.13) into (17.14) gives the pressure on the cylinder surface,

$$p = p_\infty + \frac{1}{2}\rho V_\infty^2\big(1 - 4\sin^2\vartheta\big).$$

Similar to the sphere flow the solution for a circular cylinder appears to be symmetric with respect to the y-axis (see Figure 17.1), which implies again a zero drag force. However, in reality the flow *separates* from the cylinder surface as the flow visualization due to Prandtl & Tietjens (1934) clearly shows; see Figure 17.2(a). The separation leads to

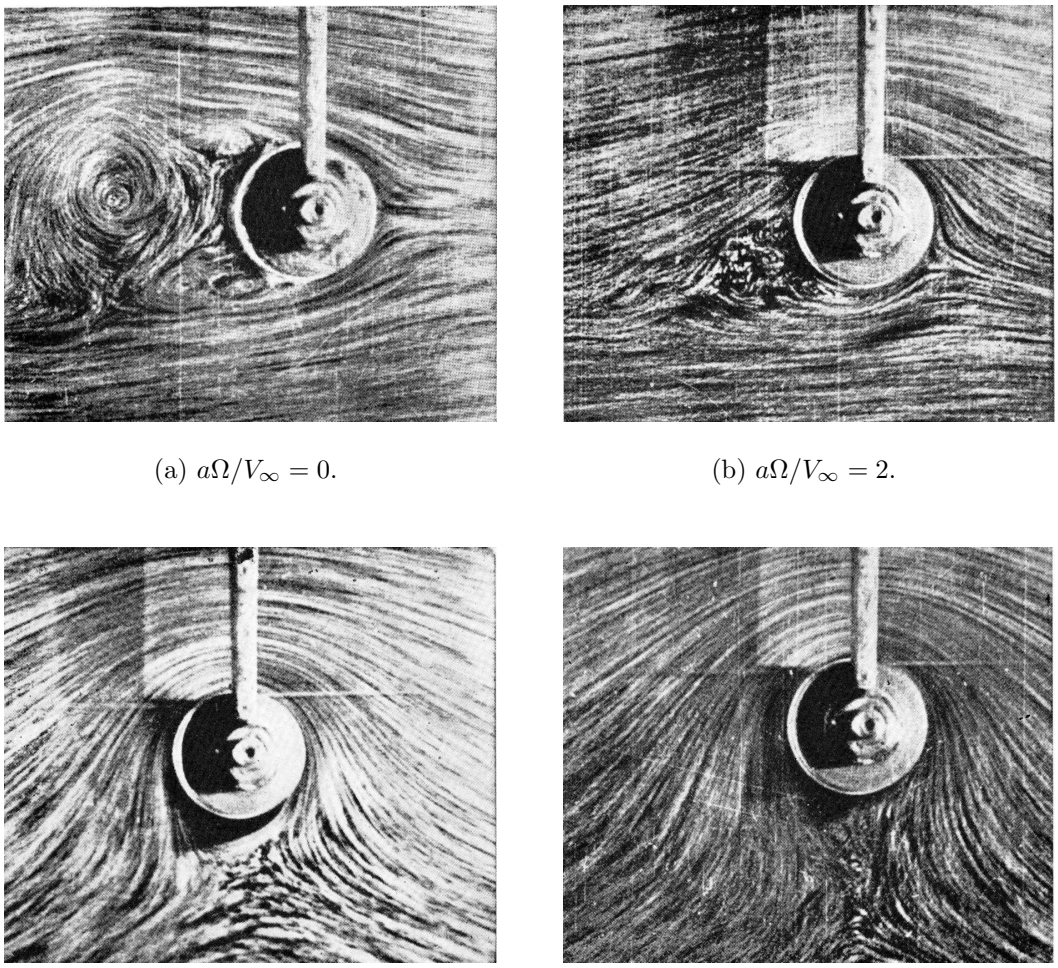

(a) $a\Omega/V_\infty = 0$.

(b) $a\Omega/V_\infty = 2$.

(c) $a\Omega/V_\infty = 4$.

(d) $a\Omega/V_\infty = 6$.

Figure 17.2: Visualization of the flow past a rotating cylinder (Prandtl & Tietjens 1934). The flow is from right to left.

a redistribution of the pressure on the cylinder surface. As a result a non-zero drag is produced.

Interestingly enough, Prandtl & Tietjens (1934) demonstrated that the separation may be suppressed by rotating the cylinder around its centre. A non-dimensional parameter that governs the flow past a rotating cylinder can be identified as

$$a\Omega/V_\infty,$$

where Ω is the angular velocity of the cylinder rotation. Figure 17.2 shows that with increasing Ω, the separation region becomes smaller, and disappears all together when $a\Omega/V_\infty$ reaches a critical value slightly above 4; see Figure 17.2(d).

In order to model theoretically the effect of the cylinder rotation on the flow, the potential vortex (16.15) is added to the solution (17.10) for the flow past the cylinder, leading to

$$w(z) = V_\infty\left(z + \frac{a^2}{z}\right) + \frac{\Gamma}{2\pi i}\ln z. \tag{17.15}$$

In order to confirm that this is a true solution to Problem 17.1, we first note that function

$w(z)$ as defined by (17.15) is analytic everywhere in the flow field ($|z| > a$). Secondly, on the cylinder surface, where $z = ae^{i\vartheta}$, we have

$$w(z) = V_\infty\big(ae^{i\vartheta} + ae^{-i\vartheta}\big) - i\frac{\Gamma}{2\pi}(\ln a + i\vartheta) = 2V_\infty a\cos\vartheta + \frac{\Gamma\vartheta}{2\pi} - i\frac{\Gamma}{2\pi}\ln a,$$

which shows that the imaginary part of $w(z)$ is, indeed, constant on the cylinder surface,

$$\Im\big\{w(z)\big\}\Big|_{|z|=a} = -\frac{\Gamma}{2\pi}\ln a.$$

Thirdly, the complex conjugate velocity is calculated as

$$\overline{V}(z) = \frac{dw}{dz} = V_\infty\left(1 - \frac{a^2}{z^2}\right) + \frac{\Gamma}{2\pi iz}, \tag{17.16}$$

and obviously satisfies the free-stream condition (17.2).

The following two comments are appropriate here. Firstly, while it is clear that the circulation, Γ, in (17.15) is somehow linked to the speed of rotation of the cylinder, its effect mimics that of the rotation, in the inviscid-flow formulation, there is neither physical nor mathematical basis on which a link can be established. The inviscid flow cannot 'sense' the rotation at all. Indeed, mathematically the impermeability condition on the cylinder surface, (17.1), remains the same whether the cylinder is stationary or rotating. Secondly, what have demonstrated is that the boundary-value problem of the two-dimensional inviscid flow theory (Problem 17.1) is not a well-posed problem in the classical sense as it does not define a unique solution. Instead it admits a family of solutions with the circulation, Γ, being a free parameter.

In order to see how changing Γ influences the flow past a circular cylinder, let us consider the velocity distribution along the cylinder surface. Substituting (17.7) into (17.16), we have

$$\overline{V}(z) = u - iv = V_\infty\big(1 - e^{-2i\vartheta}\big) - \frac{i\Gamma}{2\pi a}e^{-i\vartheta} = ie^{-i\vartheta}\left(2V_\infty\sin\vartheta - \frac{\Gamma}{2\pi a}\right). \tag{17.17}$$

It follows from (17.17) that a point on the cylinder surface whose position angle, ϑ, satisfies the equation

$$\sin\vartheta = \frac{\Gamma}{4\pi aV_\infty}, \tag{17.18}$$

is a stagnation point where both velocity components, u and v, simultaneously vanish.

In the case of zero circulation, $\Gamma = 0$, the flow is symmetric with respect to the x-axis, and the stagnation points are located at $\vartheta = 0$ and $\vartheta = \pi$. The corresponding streamline pattern is shown in Figure 17.3(a). In order to mimic the visualization results in Figure 17.2, where the stagnation points lie on the lower side of the cylinder, we have to assume that the circulation, Γ, is negative. If $-4\pi aV_\infty < \Gamma < 0$, then equation (17.18) has two solutions which represent two stagnation points situated symmetrically on the lower surface of the cylinder as shown in Figure 17.3(b). When $\Gamma = -4\pi aV_\infty$, these points come together and the streamline pattern takes the form shown in Figure 17.3(c). Finally, for $\Gamma < -4\pi aV_\infty$, no solutions of (17.18) can be found, which suggests that the stagnation point moves from the cylinder surface into the interior of the flow field; see Figure 17.3(d)[†]

[†]Finding the location of the stagnation point and thereby deciding the flow pattern shown in the figure is left as an exercise.

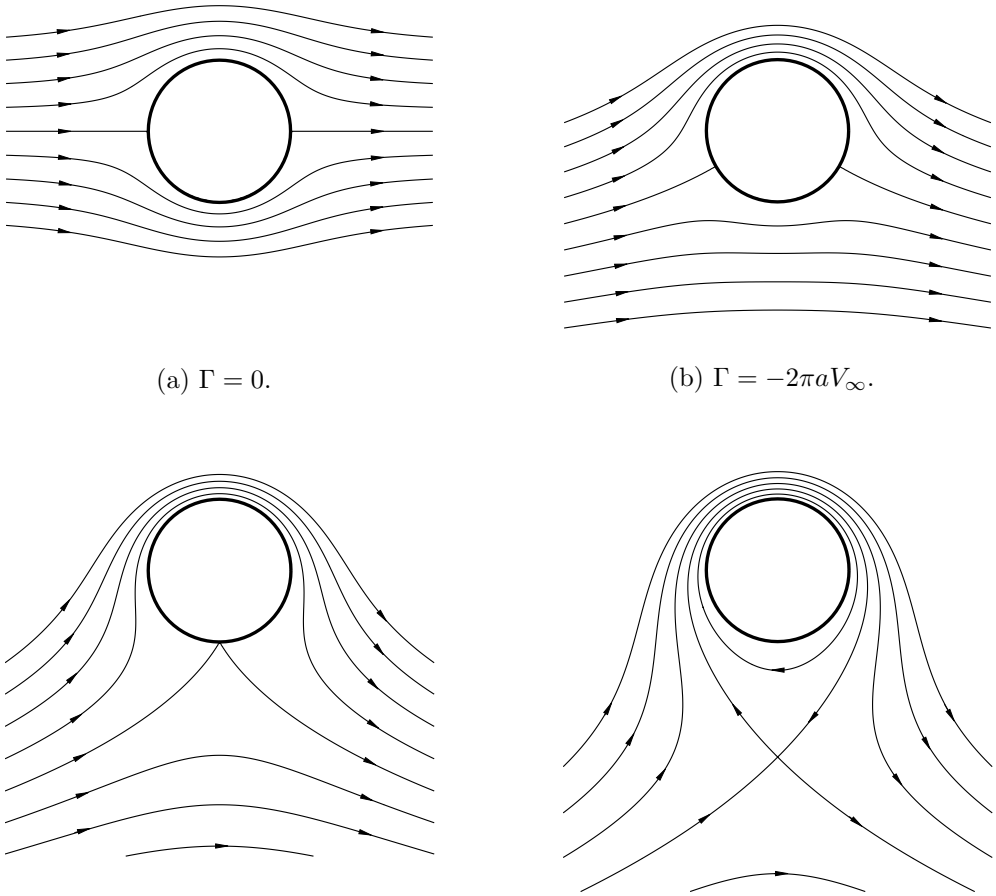

(a) $\Gamma = 0$.

(b) $\Gamma = -2\pi a V_\infty$.

(c) $\Gamma = -4\pi a V_\infty$.

(d) $\Gamma = -6\pi a V_\infty$.

Figure 17.3: The flow past a circular cylinder for different values of the circulation Γ.

. It is interesting to note that at this stage the theoretical streamline pattern starts to show a good agreement with the experimental observations (see Figure 17.2d) and so does the pressure distribution on the cylinder surface.

We have seen that with $\Gamma \neq 0$ the flow past the cylinder loses its symmetry with respect to the x-axis. As a result the pressure below the cylinder appears to be larger than the pressure above it, and a side force acting perpendicular to the direction of the oncoming flow is created. Its value is given by the *Joukovskii formula*,

$$L = -\rho V_\infty \Gamma,$$

which will be deduced in Lecture 18 (see also Problem 5 in Exercises 6).

The formation of the side force on a rotating cylinder is known as the *Magnus effect*, named after the scientist who first performed a detailed experimental study of the flow around a rotating cylinder (Magnus 1852). In everyday life, the Magnus effect may be observed in a variety of situations. In particular, it represents an integral part of various sports, ranging from football to table tennis. It would be, perhaps, too optimistic to suggest that the sportsmen understand the theory behind the phenomenon, but they certainly know how by spinning a ball they can influence its behaviour (e.g. trajectory) in the flight.

Quiz Football: Discus how you might, in a free kick facing a 'wall' of opposing players, spin the ball to get it to go around the 'wall' (and possibly score!); Or if tennis is your game, discuss how the top, under and side spinning each influences the trajectory of the ball.

References

Magnus, H. G. (1852) Über die abweichung der geschosse. *Abh. Berl. Akad* (Phys.), 1–24.

Prandtl, L. and Tietjens, O. G. 1934 Applied Hydro- and Aeromechanics. McGraws-Hill (reprinted by Dover Pulications in 1957).

The Force on a Cylindric Body

Let us consider a steady two-dimensional flow past a cylindrical body of an arbitrary cross section shown in Figure 18.1(a). If we assume that the body force $\mathbf{f}$ acting on the moving fluid is negligibly small, then the pressure at any point in the flow field may found using the Bernoulli equation (12.6),

$$\frac{p}{\rho} + \frac{V^2}{2} = H. \tag{18.1}$$

Provided that the oncoming flow is uniform, Bernoulli's function H is a constant which does not depend on a streamline considered. Indeed, using the free-stream conditions one can find that

$$H = \frac{p_\infty}{\rho} + \frac{V_\infty^2}{2}.$$

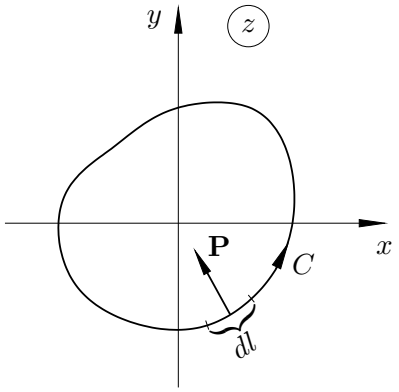

(a) Pressure force, $\mathbf{P}$, on an element dl of the body surface.

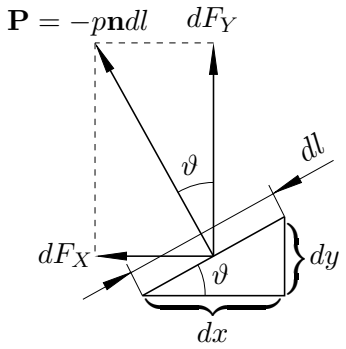

(b) Coordinate decomposition of the pressure force acting on an element dl of the body surface.

Figure 18.1: Calculation of the pressure force on the cylinder surface.

In order to calculate the resultant force acting on the cylinder, we consider a small element dl of the cylinder contour; in Figure 18.1(a) the body contour being denoted by C. The integration along this contour will be performed in the counter-clockwise direction. In the case of a inviscid flow, the stress is given by $-p\mathbf{n}$, with $\mathbf{n}$ being the outward unit normal vector of C. The pressure force acting on the contour element dl (per unit length in the spanwise direction) is

$$\mathbf{P} = -p\mathbf{n}\, dl. \tag{18.2}$$

The projections of this force to the x- and y-axes are; see Figure 18.1(b)

$$dF_X = -p\, dl \sin\vartheta, \qquad dF_Y = p\, dl \cos\vartheta, \tag{18.3}$$

where ϑ is the angle between the tangent to the body contour and the x-axis. Use of the geometric relations

$$dx = dl\cos\vartheta, \qquad dy = dl\sin\vartheta,$$

in (18.3) gives

$$dF_X = -p\,dy, \quad dF_Y = p\,dx. \tag{18.4}$$

The same expression follows alternatively from (18.2) and that the outward unit normal vector of C is

$$\mathbf{n} = (dy/dl, -dx/dl).$$

Integrating (18.4) around the cylinder surface, we have the following formulae for the components of the resultant force,

$$F_X = -\oint_C p\,dy, \qquad F_Y = \oint_C p\,dx.$$

It is convenient to combine them into the so called "*complex conjugate force*",

$$F_X - iF_Y = -\oint_C p(dy + i\,dx) = -i\oint_C p(dx - i\,dy) = -i\oint_C p\,d\bar{z}. \tag{18.5}$$

The pressure p follows from the Bernoulli equation (18.1),

$$p = \rho H - \frac{\rho}{2}V^2,$$

substitution of which into (18.5) gives[†]

$$F_X - iF_Y = i\,\frac{\rho}{2}\oint_C V^2 d\bar{z}. \tag{18.6}$$

Let dz be a small element of the integration contour C, and ϑ the angle made by dz with

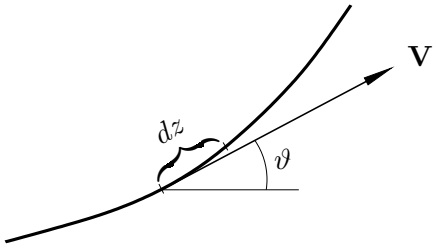

Figure 18.2: Relation between tangent direction and the velocity on the surface.

the x-axis (see Figure 18.2). Then

$$dz = |dz|e^{i\vartheta} \quad \text{and} \quad d\bar{z} = |dz|e^{-i\vartheta}. \tag{18.7}$$

Since the velocity vector is tangent to the surface, we can write $u + iv = Ve^{i\vartheta}$, and it follows that the complex conjugate velocity

$$\overline{V}(z) \equiv u - iv = Ve^{-i\vartheta},$$

and hence

$$V = \overline{V}e^{i\vartheta}. \tag{18.8}$$

[†]Here it is taken into account that the integral of a constant along a closed contour is always zero.

Substitution of (18.7) and (18.8) into (18.6) yields

$$F_X - iF_Y = i\,\frac{\rho}{2}\oint\limits_C \overline{V}^2 e^{i2\vartheta}|dz|e^{-i\vartheta} = i\,\frac{\rho}{2}\oint\limits_C \overline{V}^2|dz|e^{i\vartheta} = i\,\frac{\rho}{2}\oint\limits_C \left(\frac{dw}{dz}\right)^2 dz. \tag{18.9}$$

The above equation is known as the ***Blasius-Chaplygin formula***.

Taking the advantage of the fact that the integrand in (18.9) is an analytic function, we can, by appealing to Cauchy's theorem, deform the integration path of the body contour C, which may be rather complicated, to a suitable closed contour embracing the body. In particular, the integration may be performed along a *circle* C_R of large enough radius, and then $\overline{V}(z)$ may be represented by its far-field asymptotic expansion.

The above procedure can be carried through under the assumption that there are no discontinuities of the velocity in the flow field[‡], we can treat $\overline{V}(z)$ as a single-valued analytic function. According to the free-stream boundary condition (17.2), $\overline{V}(z)$ is finite at $z=\infty$, and therefore, the *Laurent series* for $\overline{V}(z)$ is written as

$$\overline{V}(z) = \frac{dw}{dz} = a_0 + \frac{a_1}{z} + \frac{a_2}{z^2} + \cdots \qquad \text{as} \quad z \to \infty. \tag{18.10}$$

The leading order term is easily seen to be

$$a_0 = u_\infty - iv_\infty = V_\infty e^{-i\alpha}.$$

In order to clarify the physical meaning of factor a_1 in the second term, we integrate (18.10), which gives

$$w(z) = V_\infty e^{-i\alpha} z + a_1 \ln z + O\big(1/z\big).$$

Let us assume that the point of observation z makes a full circle around the body. This results in an increment of the complex potential,

$$\Delta w = \Delta\varphi + i\Delta\psi = a_1 2\pi i. \tag{18.11}$$

According to (15.5), $\Delta\varphi$ coincides with the circulation Γ. For a body with impenetrable surface, $\Delta\psi = 0$ (see Problem 3 in Exercises 5). Consequently, it follows from (18.11) that

$$a_1 = \Gamma/(2\pi i),$$

and (18.10) may be written as

$$\frac{dw}{dz} = V_\infty e^{-i\alpha} + \frac{\Gamma}{2\pi i z} + O\left(\frac{1}{z^2}\right). \tag{18.12}$$

[‡]Flows with discontinuities do however exist, an example of which is the so-called Kirchhoff flow.

Deform the original integral contour C in (18.9) to a large circle C_R and making use of the far-field asymptote (18.12), we have

$$F_X - iF_Y = i\,\frac{\rho}{2}\oint_{C_R}\left(V_\infty^2 e^{-i2\alpha} + \frac{V_\infty e^{-i\alpha}\Gamma}{\pi i z} + \cdots\right)dz$$
$$= i\,\frac{\rho}{2}\,\frac{V_\infty e^{-i\alpha}\Gamma}{\pi i}\,2\pi i = i\rho V_\infty e^{-i\alpha}\Gamma.$$

Separation of the real and imaginary parts yields

$$F_X = \rho V_\infty \Gamma \sin\alpha, \qquad F_Y = -\rho V_\infty \Gamma \cos\alpha. \tag{18.13}$$

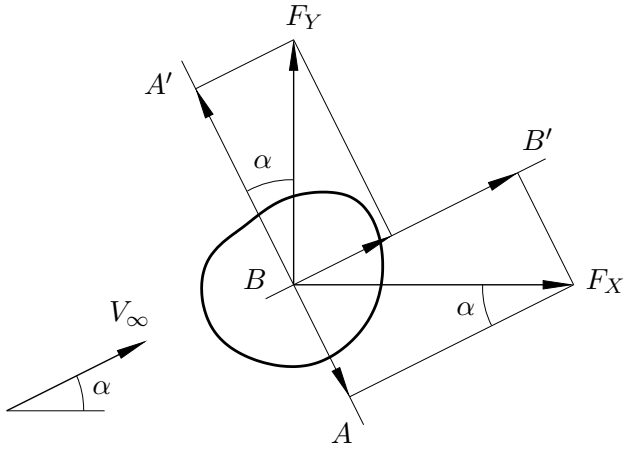

Figure 18.3: Calculation of the lift and drag forces.

The ***lift force*** L is defined as the projection of the resultant force to the direction perpendicular to the free stream. It is calculated by projecting F_X and F_Y upon line AA' in Figure 18.3,

$$L = F_Y \cos\alpha - F_X \sin\alpha. \tag{18.14}$$

Inserting (18.13) into (18.14), we find that

$$L = -\rho V_\infty \Gamma. \tag{18.15}$$

The ***drag force*** D is the projection of the resultant force to line BB' parallel to the direction of the free-stream

$$D = F_Y \sin\alpha + F_X \cos\alpha.$$

Using (18.13), we can see that $D = 0$, which indicates that d'Alembert's paradox arises for an arbitrary two-dimensional body.

Formula (18.15) gives a surprisingly simple relationship between the lift force L to the circulation Γ, and it is known as the ***Joukovskii-Kutta formula***.

Lecture 19

(The topics of Lecture 19 are primarily of review nature, and will be explained rather briefly in the in-person lecture. It would be helpful if you preview the content.)

The Method of Conformal Mapping

One of the powerful mathematical tools is the method of conformal mapping, which is based on the theory for functions of complex variables. It has many applications not least to fluid dynamics; in fact it played an important role in the development of the theory of two-dimensional inviscid flows. Before turning to fluid dynamics applications of the method, we shall discuss basic mathematical aspects of conformal mapping.

Any complex function $\zeta = f(z)$ serves the purpose of defining the value of $\zeta = \xi + i\eta$ for a given value of the argument $z = x + iy$. It therefore may be thought of as a mapping of points in the z-plane into the corresponding points in the ζ-plane. Using such mappings defined by suitable $f(z)$, we may map a complex region in the z-plane to a simpler one (e.g. a circle or a straight line) in the ζ-plane.

Mapping with Linear Function

We start by considering the mapping defined by the linear function

$$\zeta = az + b, \tag{19.1}$$

where a and b are complex numbers. If, in particular, $a = 1$, then denoting the real and imaginary parts of b by b_r and b_i repsectively, we have

$$\xi = x + b_r, \qquad \eta = y + b_i.$$

This shows that mapping with function $\zeta = z + b$ represents parallel translation of all the points in the complex plane.

Let us now consider the case when b in (19.1) is zero, and a is an arbitrary complex number different from zero and infinity. It then may be represented in the exponential form

$$a = \kappa e^{i\delta}, \tag{19.2}$$

where κ is the modulus of a, and δ its argument. With a given by (19.2) and $b = 0$ the mapping (19.1) takes the form

$$\zeta = \kappa e^{i\delta} z.$$

Since z may also be written in the exponential form (see Figure 19.1a),

$$z = re^{i\vartheta},$$

we have

$$\zeta = \kappa e^{i\delta} r e^{i\vartheta} = (\kappa r) e^{i(\delta+\vartheta)}.$$

Thus, the mapping $\zeta = az$ leads to magnification of $|z|$ by factor $\kappa = |a|$ and rotation through angle $\delta = \arg a$ (see Figure 19.1b).

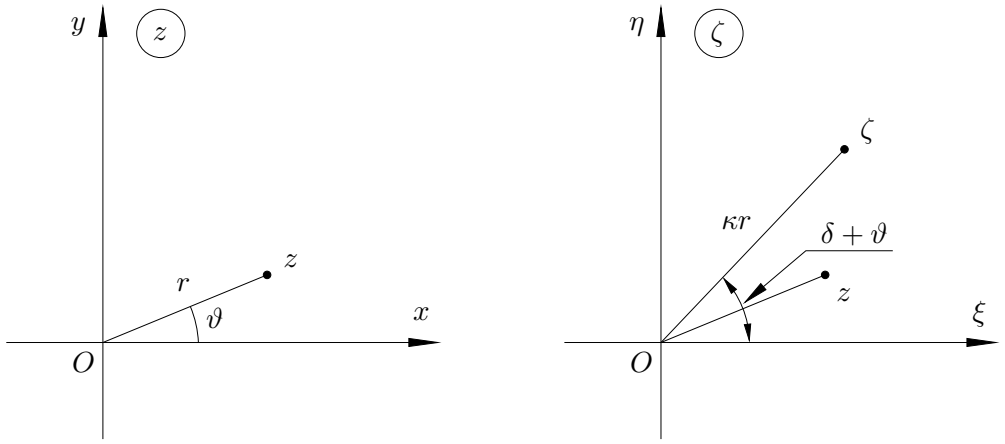

(a) z-plane. (b) ζ-plane.

Figure 19.1: Mapping with function $\zeta = az$.

Let us now return to the general linear function (19.1) and consider two points z' and z'' in the z-plane. Their images in the ζ-plane are

$$\zeta' = az' + b, \qquad \zeta'' = az'' + b,$$

and we see that

$$\zeta'' - \zeta' = a(z'' - z'). \tag{19.3}$$

If we use again the exponential form (19.2) for a and represent $z'' - z'$ as

$$z'' - z' = |z'' - z'|\, e^{i\vartheta},$$

then (19.3) turns into

$$\zeta'' - \zeta' = \kappa e^{i\delta}\, |z'' - z'| e^{i\vartheta} = \kappa |z'' - z'|\, e^{i(\delta+\vartheta)}.$$

This shows that the mapping with linear function (19.1) rotates a segment of a straight line through angle angle δ and stretches it κ times (compresses, if $\kappa < 1$).

Since the angle of the rotation does not depend on the initial orientation of the segment in z-plane nor on its length, the following two statements are valid:

(i) a straight line in the z-plane is mapped by the linear function (19.1) onto a straight line in the ζ-plane;

(ii) if two lines in the z-plane make an angle θ at the point of their intersection, then this angle is preserved in the course of the mapping with linear function; see Figure 19.2.

We can further prove the following theorem.

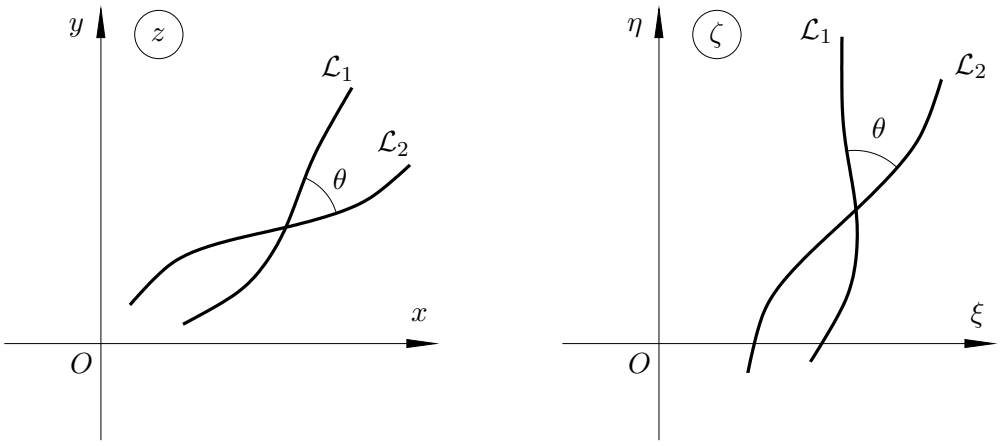

(a) z-plane. (b) ζ-plane.

Figure 19.2: Preservation of the angle θ between intersecting lines $\mathcal{L}_1$ and $\mathcal{L}_2$ when mapping with the linear function (19.1).

Theorem 1. *The linear function*

$$\zeta = az + b,$$

where $a \neq 0$, transforms any circle on the z-plane into a circle on the ζ-plane.

Proof. Let us consider circle C_z of radius r centred at point z_0 in the z-plane (see Figure 19.3). Its image in the ζ-plane we denote as C_ζ. For any point z lying on C_z the following equation is valid

$$|z - z_0| = r.$$

Using z_0 instead of z' and z instead of z'' in (19.3), we have

$$\zeta - \zeta_0 = a(z - z_0). \tag{19.4}$$

Here ζ_0 is the image of the centre z_0 and ζ lies on the image C_ζ of circle C_z.

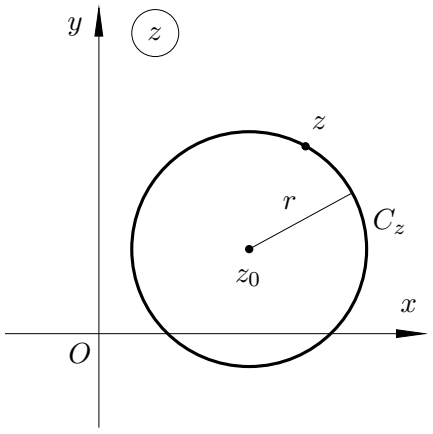

Figure 19.3: Mapping of a circle.

It follows from (19.4) that

$$|\zeta - \zeta_0| = |a|\,|z - z_0| = \kappa r,$$

which proves that C_ζ is a circle (centred at ζ_0 with a radius κr). □

Conformal Mapping

We shall use the following definition of conformal mapping.

Definition 19.1:. *The mapping $\zeta = f(z)$ is said to be conformal at point z_0 if function $f(z)$ is analytic at z_0 and $f'(z_0) \neq 0$.*

As the definition states, 'conformal' is a local feature. Remind that a function $f(z)$ is called *analytic* at point z_0 if it is differentiable at this point, i.e. there exists the limit

$$f'(z_0) = \lim_{\Delta z \to 0} \frac{f(z_0 + \Delta z) - f(z_0)}{\Delta z},$$

independent of the orientation of Δz in the complex plane. It follows that in a small vicinity of z_0,

$$f(z_0 + \Delta z) - f(z_0) = f'(z_0)\Delta z + \alpha(z_0, \Delta z)\Delta z,$$

where function $\alpha(z_0, \Delta z)$ is such that

$$\lim_{\Delta z \to 0} \alpha(z_0, \Delta z) = 0.$$

Therefore, if we restrict our attention to a small vicinity of z_0, then we can write

$$f(z_0 + \Delta z) - f(z_0) = f'(z_0)\Delta z.$$

Now denoting $z = z_0 + \Delta z$ and taking into account that $\zeta = f(z)$, we have

$$\zeta - \zeta_0 = f'(z_0)\,(z - z_0). \tag{19.5}$$

Comparing (19.5) with (19.4), we can conclude that any conformal mapping behaves *locally* as linear mapping (19.1). In particular, it maps small circles onto small circles, and preserves the angles between intersecting lines. It further follows from comparison of (19.5) with (19.4) that $|f'(z)|$ is the magnification factor κ of the mapping $\zeta = f(z)$ while the angle of rotation δ is given by

$$\delta = \arg\left(\frac{df}{dz}\right). \tag{19.6}$$

Mapping with the Power Function

The power function is given by

$$\zeta = z^\alpha, \tag{19.7}$$

with α being a real constant. If α is not an integer, function (19.7) is multi-valued. If one wants to define single-valued analytic branch of the power function, a branch cut should be made in the z-plane connecting points $z = 0$ and $z = \infty$.

The derivative of (19.7)

$$\frac{d\zeta}{dz} = \alpha z^{\alpha - 1}$$

remains finite at all finite z. As $z \to 0$ it tends to zero for all $\alpha > 1$. If, on the other hand, $\alpha < 1$, then $d\zeta/dz$ becomes infinite at $z = 0$. This suggests that the mapping performed by (19.7) preserves the angles at all finite points of the complex plane, but not at $z = 0$.

In order to see the action of the mapping defined by (19.7), let z be expressed in the exponential form

$$z = re^{i\vartheta}, \tag{19.8}$$

and substituting (19.8) into (19.7), yields

$$\zeta = r^{\alpha} e^{i\alpha\vartheta}.$$

This shows that the mapping with the power function (19.7) increases all the angles by factor α.

As an example let us consider the corner made of two rays, OA and OB, emanating from point O at angle $\pi - \theta$ to one another; see Figure 19.4(a). For our purposes it is convenient to place the coordinate origin into the point O and draw the real axis along one of the rays, say, OA.

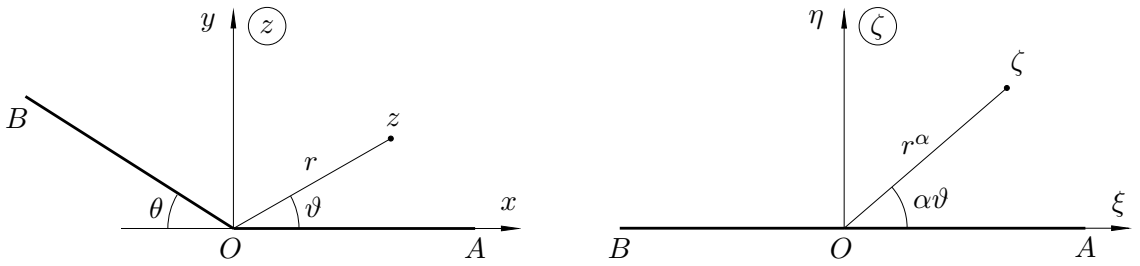

(a) z-plane. (b) ζ-plane.

Figure 19.4: Mapping with the power function (19.7).

Since any z on the first ray OA is real, $z = x$, the power function mapping (19.7) leaves OA at the original place. The second ray, OB, rotates around point O changing its angle from $\pi - \theta$ to $\alpha(\pi - \theta)$. We see that if, for example, we need to map the region above the corner (wedge) region between OA and OB in the z-plane onto the upper half of the ζ-plane, then we have to set

$$\alpha(\pi - \theta) = \pi.$$

A power function (19.7) performs the desired mapping provided that

$$\alpha = \frac{\pi}{\pi - \theta}.$$

Lecture 20

Linear Fractional Transformation

A *linear fractional transformation* is defined by the mapping

$$\zeta = \frac{az+b}{cz+d}, \tag{20.1}$$

where a, b, c and d are complex constants subject to the restriction that

$$ad - bc \neq 0.$$

If $c = 0$, then (20.1) reduces to the linear transformation (19.1), but if $c \neq 0$, then (20.1) may be written in the form

$$\zeta = \frac{a}{c} + \frac{bc-ad}{c}\frac{1}{cz+d}, \tag{20.2}$$

which shows that the condition $ad-bc \neq 0$ is necessary to ensure that the linear fractional transformation (20.1) is not a constant function mapping all the points in the z-plane into just one point in the ζ-plane.

When cleared of fractions, equation (20.1) takes the form

$$c\,\zeta z + d\zeta - az - b = 0, \tag{20.3}$$

which is linear in z and linear in ζ, or bilinear in z and ζ. Hence, another name for the linear fractional transformation (20.1) is *bilinear transformation.*

Solving equation (20.3) for z, we find the *inversion* of the mapping (20.1),

$$z = \frac{-d\zeta + b}{c\zeta - a}. \tag{20.4}$$

It follows from (20.1) and (20.4) that each point in the z-plane (except, may be, $z = -d/c$) has one and only one image-point in the ζ-plane. Conversely, each point in the ζ-plane (except, may be, $\zeta = a/c$) has one and only one image-point in the z-plane. In order to include these points into consideration we adopt the following conventions for the *complex infinity* ∞.

1. If a is a finite number, then
$$\frac{a}{\infty} = 0.$$
2. If $a \neq 0$, then
$$\frac{a}{0} = \infty.$$

With this *complex infinity* as defined above, we can introduce the notion of *extended complex plane.*

Definition 20.1:. *The complex z-plane including the complex infinite $z = \infty$ is called* extended z-plane.

This is a set of all 'finite' complex numbers plus the complex infinity $z = \infty$.

Equipped with the notions of complex infinity and extended complex, we now return to the mapping (20.1) and its inversion (20.4), which may be written as

$$\zeta = \frac{az+b}{cz+d} = \frac{a+b/z}{c+d/z}, \qquad z = \frac{-d\zeta+b}{c\zeta-a} = \frac{-d+b/\zeta}{c-a/\zeta},$$

where in the second step of each equation, we take z and ζ to be large but finite, respectively. If z approaches $-d/c$,, then we have formally,

$$\zeta = \frac{b-ad/c}{0},$$

and with the aid of the property 2 of the infinite we will say that

$$\zeta = \infty \quad \text{at} \quad z = -\frac{d}{c}. \tag{20.5}$$

On the other hand, the inversion indicates that

$$z = -\frac{d}{c} \quad \text{at} \quad \zeta = \infty,$$

with the first property of the infinite. Thus $z = -d/c$ is mapped to $\zeta = \infty$, and vice visa.

Likewise, as ζ approaches a/c, the inverse mapping formally becomes

$$z = \frac{b-ad/c}{0},$$

and we will say that

$$z = \infty \quad \text{at} \quad \zeta = \frac{a}{c},$$

while the mapping itself indicates

$$\zeta = \frac{a}{c} \quad \text{at} \quad z = \infty. \tag{20.6}$$

It follows that $z = \infty$ is mapped to $\zeta = a/c$, and vice visa.

With extensions (20.6) and (20.5), the linear fractional function (20.1) performs one-to-one mapping of *extended* z-plane onto *extended* ζ-plane.

Let us now return to formula (20.2). It shows that the linear fractional mapping (20.1) can be obtained by the *composition* of the sequence of three more elementary mappings:

$$z_1 = cz + d, \tag{20.7a}$$

$$\zeta_1 = \frac{1}{z_1}, \tag{20.7b}$$

$$\zeta = \frac{a}{c} + \frac{bc-ad}{c}\zeta_1. \tag{20.7c}$$

The first and third are linear mappings, the properties of which have already been discussed. Hence, we only need to examine the properties of the second mapping (20.7b). Changing the notations, we write

$$\zeta = \frac{1}{z}. \tag{20.8}$$

If we use the exponential form for z, i.e. $z = |z|e^{i\vartheta}$, then (20.8) gives

$$\zeta = \frac{1}{|z|}e^{-i\vartheta}.$$

We see that the transformation (20.8) consists of (i) reflection of point z in the circle of unit radius (in this reflection the image of z stays on the same radius but its modulus changes to $1/|z|$), and (ii) reflection in the real axis (see Figure 20.1).

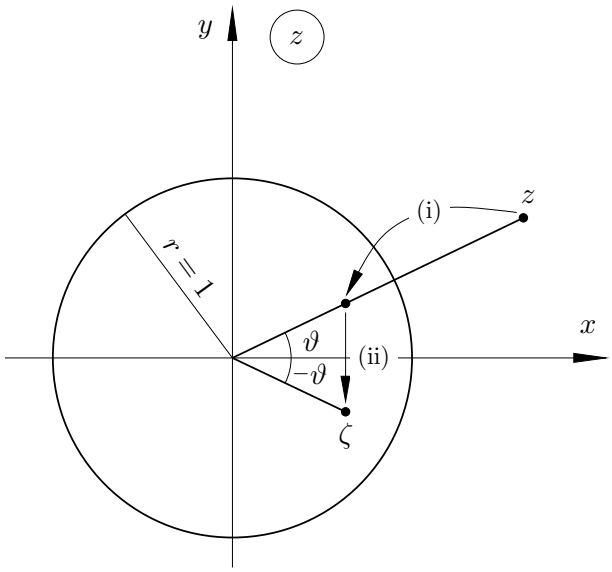

Figure 20.1: Two steps of the transformation (20.1).

The main property of the linear fractional transformation is the *circle property* which is expressed by the following theorem.

Theorem 1. *The linear fractional transformation*

$$\zeta = \frac{az + b}{cz + d}$$

maps any circle on the extended z-plane into a circle on the extended ζ-plane.

Proof. Consider, first, the mapping with the function (20.8). The inverse to (20.8) is written as

$$z = \frac{1}{\zeta}.$$

Expressing z and ζ via their real and imaginary parts

$$z = x + iy, \qquad \zeta = \xi + i\eta,$$

we have

$$x + iy = \frac{1}{\xi + i\eta} = \frac{\xi - i\eta}{\xi^2 + \eta^2}.$$

Hence,

$$x = \frac{\xi}{\xi^2 + \eta^2}, \qquad y = -\frac{\eta}{\xi^2 + \eta^2}. \tag{20.9}$$

Any circle in the z-plane may be written as

$$A(x^2 + y^2) + Bx + Cy + D = 0, \tag{20.10}$$

where A, B, C and D are real numbers. Substitution of (20.9) into (20.10) leads to

$$D(\xi^2 + \eta^2) + B\xi - C\eta + A = 0, \tag{20.11}$$

which represents a circle in the ζ-plane.

Note two 'extreme cases'. The first is with $D = 0$, for which the circle (20.10) in the z-plane passes through the origin ($x = y = 0$). Its image (20.11) in the ζ-plane appears to be a straight line. The second is for $A = 0$, with which the circle (20.11) in the ζ-plane passes through the origin ($\xi = \eta = 0$), while the circle (20.10) in the z-plane degenerates into a straight line. In order to include these 'extreme cases', we will view straight lines on the extended complex plane as circles of infinite radius.

This completes the proof of the circle property for the transformation (20.8). It remains to recall that the linear fractional transformation (20.1) may be performed in three steps (20.7), linear mapping (20.7a), mapping with function (20.7b) and then linear mapping (20.7c). All of these transformations possess the *circle property*, and therefore, so does their composition, the linear fractional transformation (20.1). □

Application to Fluid Dynamics

We now discuss how the method of conformal mapping can be applied to study two-dimensional incompressible inviscid flows that can be treated as being irrotational. In this case, the flow analysis may be conducted in the complex plane z, where the body contour is denoted by S_z; see Figure 20.2(a). In what follows we shall refer to this plane as the physical plane.

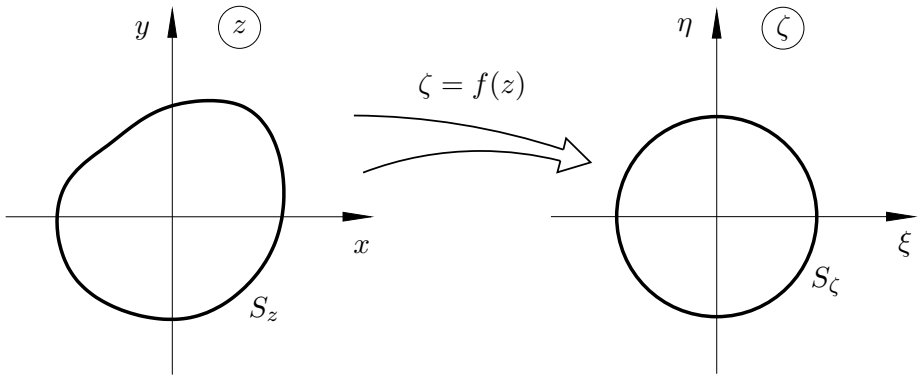

(a) Physical plane. (b) Auxiliary plane.

Figure 20.2: Conformal mapping.

Let us further suppose that corresponding to this flow we can introduce an auxiliary complex plane ζ with the body contour S_ζ simple enough, a circle say, such that the

complex potential $W(\zeta)$ for this flow is known; see Figure 20.2(b). Suppose that we also know the conformal mapping

$$\zeta = f(z),$$

which maps the exterior of the body contour S_z in the z-plane onto the exterior of the body contour S_ζ in the auxiliary plane ζ, then the composite function

$$w(z) = W\big[f(z)\big] \tag{20.12}$$

represents the sought complex potential of the flow in the physical z-plane.

Indeed, since function $W(\zeta)$ represents the complex potential of a fluid flow, it should be an analytic function as condition *1* of Problem (17.1) requires. Function $f(z)$ performing the conformal mapping of the $z-$plane onto $\zeta-$plane is also an analytic function. Therefore we can claim that function $w(z)$, being a superposition of $W(\zeta)$ and $f(z)$, is an analytic function everywhere outside S_z.

Turning to condition *2* of Problem (17.1), we note that since $W(\zeta)$ represents a fluid flow, the imaginary part of $W(\zeta)$ should be constant along the body contour S_ζ in the ζ-plane, i.e.

$$\Im\big\{W(\zeta)\big\}\Big|_{S_\zeta} = const. \tag{20.13}$$

The principle of the correspondence of boundaries in a conformal mapping states that any two points ζ_1 and ζ_2 that lie on the boundary S_ζ in the ζ-plane are images of points z_1 and z_2 which lie on the boundary S_z in the $z-$plane (see Figure 20.3), i.e.

$$\zeta_1 = f(z_1), \qquad \zeta_2 = f(z_2). \tag{20.14}$$

It follows from (20.13) that

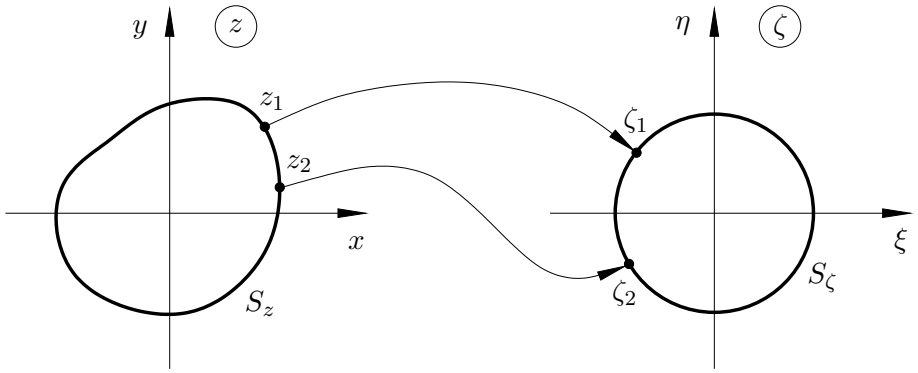

Figure 20.3: Correspondence of the boundary points.

$$\Im\big\{W(\zeta_1)\big\} = \Im\big\{W(\zeta_2)\big\}.$$

Therefore, combining (20.14) and (20.12), we see that

$$\Im\big\{w(z_1)\big\} = \Im\big\{w(z_2)\big\},$$

which, due to the arbitrariness of z_1 and z_2 on S_z, proves that

$$\Im\{w(z)\}\Big|_{S_z} = const,$$

indicating that the boundary condition on the surface in the physical plane is satisfied if its counterpart in the auxiliary ζ-place is.

Unfortunately, conformal mapping does not preserve the far-field condition *3* of Problem 17.1 to be satisfied automatically. For this reason, the flow behaviour in the free-stream should be verified each time when the method of conformal mapping is employed.

Circular Cylinder with an Angle of Attack

We now demonstrates how the method of conformal mapping may be used to generalize the solution for the flow past a circular cylinder (17.15) to include an angle of attack. Suppose that in the physical z-plane we have a circular cylinder of radius a centred at the coordinate origin $z = 0$. The oncoming flow is such that the free-stream velocity vector has modulus V_∞ and makes an angle α with the x-axis (see Figure 20.4).

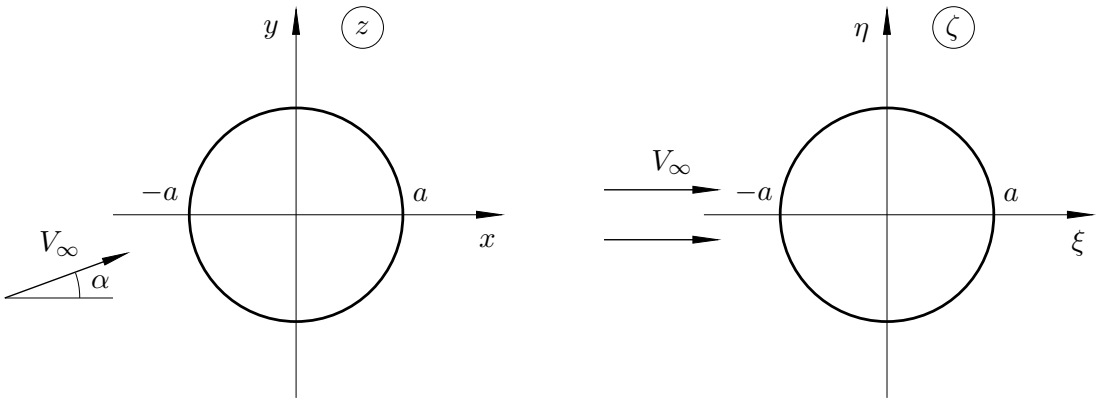

Figure 20.4: Rotation of the cylinder through angle α.

To reduce this problem to the one considered before, we introduce an auxiliary plane ζ, which is "obtained" by rotating the $z-$plane through an angle α in the clockwise direction. This can be realised via a simple linear mapping,

$$\zeta = e^{-i\alpha} z. \tag{20.15}$$

This rotation annuls the angle of attack, and therfore using (17.15), we can write the complex potential in the auxiliary plane as

$$W(\zeta) = V_\infty \left(\zeta + \frac{a^2}{\zeta}\right) + \frac{\Gamma}{2\pi i} \ln \zeta. \tag{20.16}$$

Substituting (20.15) into (20.16) we find that in the $z-$plane

$$w(z) = V_\infty \left(z e^{-i\alpha} + \frac{a^2}{z\, e^{-i\alpha}}\right) + \frac{\Gamma}{2\pi i} \ln z. \tag{20.17}$$

Additive constant $-\alpha\Gamma/2\pi$ has been disregarded.

Joukovskii Transformation

A conformal mapping that is a particularly useful for studying fluid flows is the Joukovskii transformation. Although its final form looks rather complicated and nonintuitive, the transformation can be constructed as a composition of a sequence of elementary mappings, including the linear fractional and power functions.

In order to introduce this transformation, let us try to find the conformal mapping of a circular arc onto a full circle. More precisely, we shall consider a region that consists of the entire $z-$plane with the exception of a 'slit', a branch cut along a circular arc. The circular arc is of course part of a circle, and it is taken to have a depth h with the interval $[-a, a]$ of the real axis serving as the arc chord; see Figure 21.1(a). This region is to be

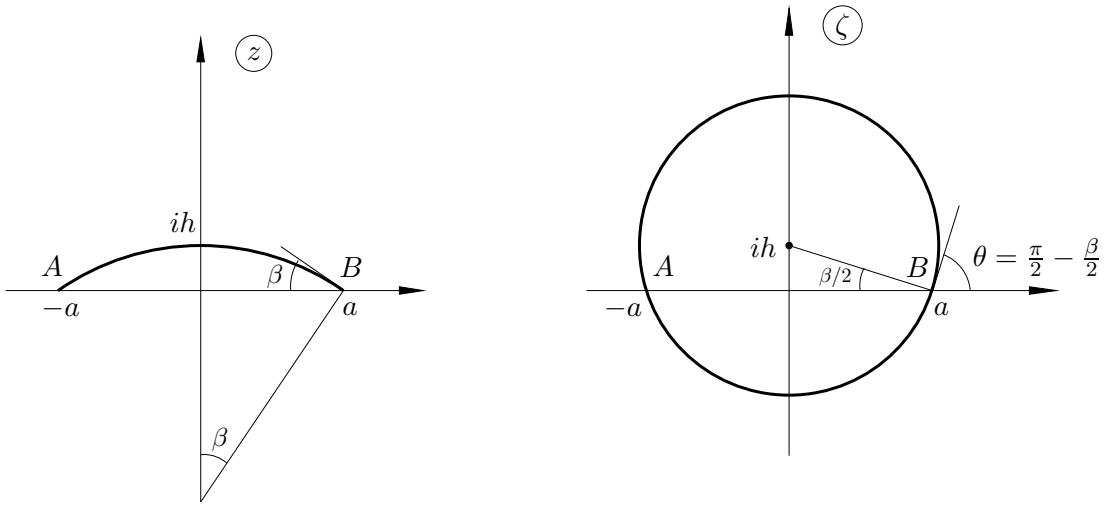

(a) z-plane. (b) ζ-plane.

Figure 21.1: Joukovskii transformation.

mapped onto the exterior of a circle which is centered at $\zeta = ih$ and intersects the real axis at points $-a$ and a as shown in Figure 21.1(b). We shall denote the angle between the tangent to the arc at point B and the real axis in the z-plane as β. It can be shown that the line connecting the centre of the circle and point B in the ζ-plane, makes an angle $\frac{1}{2}\beta$ with the real axis.

In order to achieve the desired mapping, we will transform the circular arc 'slit' in the z-plane and the full circle in the ζ-plane to simple 'images', respectively, and then map the 'images' from one to another via another mapping.

We start with the $z-$plane to which the following transformation linear fractional transformation will be first applied

$$z_1 = \frac{z-a}{z+a} \equiv f_1(z). \tag{21.1}$$

The transformation (21.1) assumes the circle property, i.e. it maps a circle (or circular arc) in the $z-$plane onto a circle (or a straight line) in the z_1-plane.

It is easily seen that function (21.1) maps point B, situated at the right hand side end of the arc in the z-plane into the origin $z_1 = 0$ in the z_1-plane. The image of the left hand side end A of the arc where $z = -a$ is easily seen to be $z_1 = \infty$. Thus the arc is transformed into a ray emerging from the origin and extending to infinity.

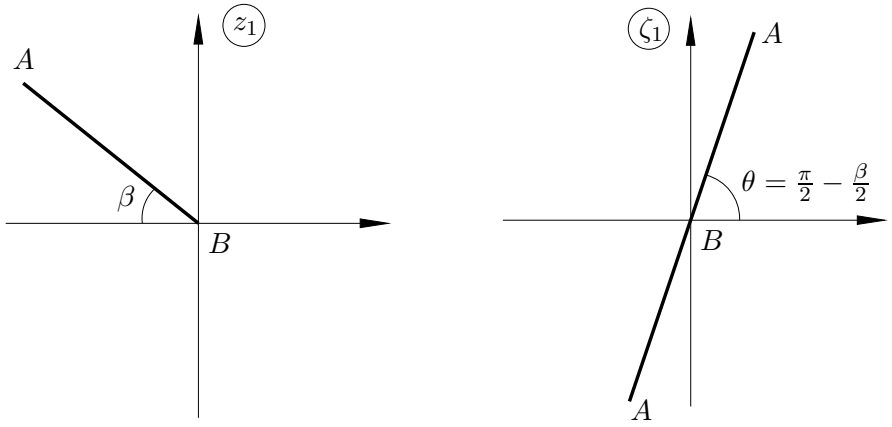

(a) z_1-plane. (b) ζ_1-plane.

Figure 21.2: Auxiliary planes z_1 and ζ_1.

The orientation of the ray may be found using formula (19.6) which gives the angle δ of rotation of any line (more precisely, a small segment of a line) in the z-plane when it is mapped onto the z_1-plane. Differentiating (21.1), we have

$$\frac{dz_1}{dz} = f_1'(z) = \frac{2a}{(z+a)^2}\,.$$

At point B, $z = a$ and the derivative appears to be *real* and *positive*

$$\left.\frac{dz_1}{dz}\right|_{z=a} = f_1'(a) = \frac{1}{2a},$$

and hence $\delta \equiv \arg\big(f_1'(a)\big) = 0$, which means that a small segment of the arc in Figure 21.1(a) near point B does not experience any rotation. Hence, the angle made by the ray with the negative real semi-axis in the z_1-plane equals β. The image of the circular arc is shown in Figure 21.2(a).

We now apply the same transformation to the circle in the ζ-plane, see Figure 21.1(b),

$$\zeta_1 = \frac{\zeta - a}{\zeta + a}. \tag{21.2}$$

As a result point B is mapped into $\zeta_1 = 0$ and point A into an infinite point $\zeta_1 = \infty$. The derivative of function (21.1) at $\zeta = a$ is] *real* and *positive*, which means again that a

small segment of the circle in Figure 21.1(b) near $\zeta = a$ does not experience any rotation. Its image in the ζ_1-plane is a straight line that makes an angle $\theta = \frac{\pi}{2} - \frac{\beta}{2}$ with the real positive axis; see Figure 21.2(b). The image is the whole line AA with the part of the circle in the upper/lower half of the ζ-plane being mapped to the upper/lower half of the ζ_1-plane, and the exterior of the circle is mapped onto the half-plane to the right of this line.

Noting that the orientation angle of the ray in the z_1-plane is twice the orientation angle of the line BA in the upper half of the ζ_1-plane, the mapping between the z_1- and ζ_1-planes is performed by the function

$$z_1 = \zeta_1^2. \tag{21.3}$$

Note that the ray BA in the lower half of the ζ_1 has the phase angle $\pi/2 - \beta/2 + \pi$, and becomes, after the mapping (21.3), $\pi - \beta + 2\pi$, and thus overlaps with BA in the z_1-plane, that is, a 'folding' has taken place.

Substitution of (21.1) and (21.2) into (21.3) gives

$$\frac{z-a}{z+a} = \left(\frac{\zeta - a}{\zeta + a}\right)^2. \tag{21.4}$$

The following simple manipulations

$$\frac{z+a-2a}{z+a} = \left(\frac{\zeta + a - 2a}{\zeta + a}\right)^2,$$
$$1 - \frac{2a}{z+a} = \left(1 - \frac{2a}{\zeta + a}\right)^2 = 1 - \frac{4a}{\zeta + a} + \frac{4a^2}{(\zeta + a)^2},$$
$$\frac{1}{z+a} = \frac{2}{\zeta + a} - \frac{2a}{(\zeta + a)^2} = \frac{2\zeta}{(\zeta + a)^2},$$
$$z + a = \frac{(\zeta + a)^2}{2\zeta} = a + \frac{\zeta^2 + a^2}{2\zeta}$$

show that

$$z = \frac{1}{2}\left(\zeta + \frac{a^2}{\zeta}\right), \tag{21.5}$$

which is the sought function performing the conformal mapping of the exterior of the circle in the ζ-plane (see Figure 21.1) onto the exterior of the arc in the z-plane.

Multiplying both sided of (21.5) by 2ζ

$$\zeta^2 - 2z\,\zeta + a^2 = 0, \tag{21.6}$$

and solving quadratic (21.6) for ζ we find that ζ in terms of z is given by

$$\zeta = z \pm \sqrt{z^2 - a^2},$$

Notice that this is double-valued, while (21.5) is a single-valued function. For each point in the z-plane it produces two points in the ζ-plane. One of them is situated outside the circle (see Figure 21.1), while the other finds itself inside the circle. If we take, for instance, $z = 2a$, then

$$\zeta_{1,2} = (2 \pm \sqrt{3})\, a.$$

We see that in order to deal with the exterior of the circle in the auxiliary plane ζ, we have to write transformation from z to ζ as

$$\zeta = z + \sqrt{z^2 - a^2}. \tag{21.7}$$

The transformation (21.7) and its inversion (21.5) are referred to as ***Joukovskii transformation***.

Flat Plate at an Incidence.

We now apply the Joukovskii transformation to describe the flow past a flat plate that has a finite length but is infinitely thin. Returning to Figure 21.1, we note that the camber of the circular arc in the physical plane z depends on parameter h. If h is chosen zero, then the arc turns into a segment of a straight line connecting points A and B; their coordinates $z = -a$ and $z = a$ remain the same for all values of h. With $h = 0$, the centre of the circle in the auxiliary ζ-plane moves into the coordinate origin. The radius of the circle becomes a, since it still has to be drawn through points A and B. We see that the Joukovskii transformation (21.7) performs conformal mapping of the entire z-plane except a branch cut along a segment $[-a, a]$ of the real axis, onto the exterior of the circle that has radius a and is centred at the origin $\zeta = 0$ in the auxiliary plane ζ; see Figure 21.3.

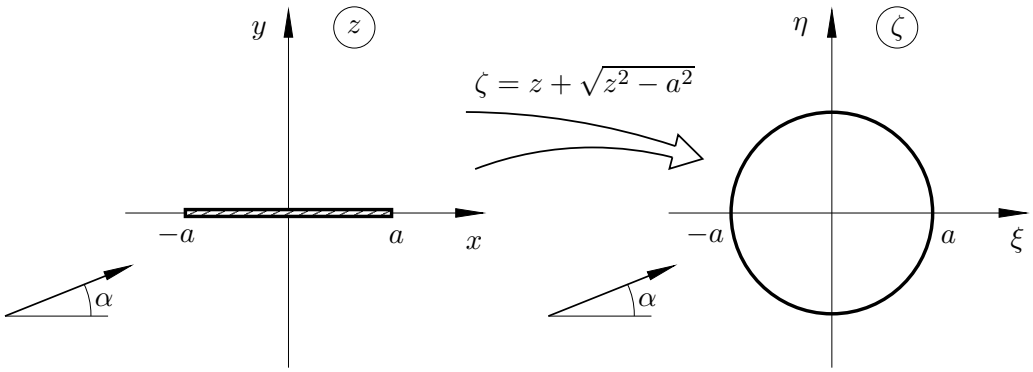

(a) Physical plane. (b) Auxiliary plane.

Figure 21.3: Transformation of a flat plate onto a circle.

According to (20.17), the complex potential in the auxiliary plane is written as

$$W(\zeta) = \tilde{V}_\infty \left(\zeta e^{-i\alpha} + \frac{a^2}{\zeta e^{-i\alpha}} \right) + \frac{\Gamma}{2\pi i} \ln \zeta. \tag{21.8}$$

Here $\tilde{V}_\infty$ denotes the free-stream velocity in the auxiliary plane which does not necessarily coincide with the free-stream velocity in the physical z-plane. In order to obtain the complex potential $w(z)$ in the physical plane, we have to combine (21.8) with Joukovskii transformation (21.7), viz. $w(z) = W\big[\zeta(z)\big]$.

The complex conjugate velocity in the z-plane may be calculated as

$$\overline{V}(z) = \frac{dw}{dz} = \frac{dW}{d\zeta}\frac{d\zeta}{dz} = \frac{dW}{d\zeta}\frac{1}{dz/d\zeta}. \tag{21.9}$$

From (21.8) it follows that

$$\frac{dW}{d\zeta} = \tilde{V}_\infty \left(e^{-i\alpha} - \frac{a^2}{\zeta^2 e^{-i\alpha}} \right) + \frac{\Gamma}{2\pi i \zeta}. \tag{21.10}$$

Differentiating (21.5), we find

$$\frac{dz}{d\zeta} = \frac{1}{2}\left(1 - \frac{a^2}{\zeta^2} \right). \tag{21.11}$$

In the far field ($z \to \infty$, $\zeta \to \infty$), formulae (21.10) and (21.11) reduce to

$$\frac{dW}{d\zeta} = \tilde{V}_\infty e^{-i\alpha}, \qquad \frac{dz}{d\zeta} = \frac{1}{2}.$$

Therefore

$$\overline{V}(z) \to 2\tilde{V}_\infty e^{-i\alpha} \quad \text{as} \quad z \to \infty,$$

and if the modulus of the velocity in the oncoming flow in the physical plane is V_∞, then in the auxiliary plane we have to take

$$\tilde{V}_\infty = \frac{1}{2} V_\infty. \tag{21.12}$$

The solution is non-unique; it involves one unknown parameter, the circulation Γ, and our next task is to study its influence on the flow behaviour and then determine the correct value of Γ such that the solution is physically acceptable. Note immediately that according to (21.11) the derivative $dz/d\zeta$ has singularities at $\zeta = -a$ and $\zeta = a$, which are translated respectively into the so-called ***leading-edge*** and ***trailing-edge singularities*** in the velocities (21.9) at $z = -a$ and $z = a$, unless $dW/d\zeta = 0$ at these points. The latter would require a particular value of Γ and is not satisfied in general. For example, if we set $\Gamma = 0$, then

$$\frac{dW}{d\zeta}\Big|_{\zeta = \pm a} = \frac{1}{2} V_\infty \left[e^{-i\alpha} - \frac{a^2}{a^2 e^{-i\alpha}} \right] = -iV_\infty \sin\alpha \neq 0$$

for $\alpha \neq 0$. Instead, $dW/d\zeta$ would vanish elsewhere other than at $\zeta = \pm a$. Their positions is found by setting $dW/d\zeta$ as given by (21.10) to zero,

$$\frac{dW}{d\zeta} = \frac{1}{2} V_\infty \left[e^{-i\alpha} - \frac{a^2}{\zeta^2 e^{-i\alpha}} \right] = 0 \quad \Longrightarrow \quad \zeta = \pm a e^{i\alpha}.$$

These are the two *stagnation points* on S'. Their locations in the z-plane may be found using (21.5):

$$z = \pm \frac{1}{2}\left(a e^{i\alpha} + \frac{a^2}{a e^{i\alpha}} \right) = \pm a \cos\alpha.$$

These are the two *stagnation points* on the plate surface S. In the case of $\Gamma = 0$, the streamline pattern will have the form shown in Figure 21.4. We see that the flow goes round the leading and trailing edges of the plate, where the velocity should becomes infinite[†]. Experimental observations show that the flow normally leaves the trailing edge in a smooth fashion. On the other hand, it is known that near the trailing edge the boundary layer (the notion of the viscous boundary layer will be discussed in Fluid Dynamics II in the next term) is well developed, and this local flow is incapable of sustaining the violent

[†]See Problem 3 in Exercises 7.

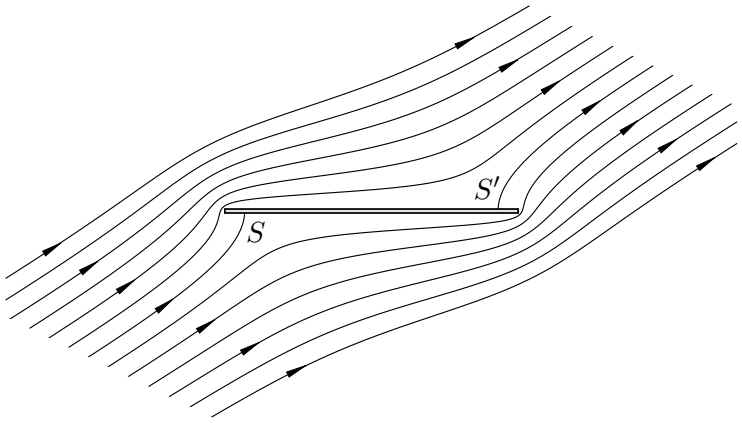

Figure 21.4: The streamline pattern for the flow past a flat plate with $\Gamma = 0$ and incidence $\alpha = 30°$. This figure was drawn by introducing a uniform mesh in the z-plane and calculating ζ for each node point z using (21.7). Then ζ was used in formula (21.11) to calculate the complex potential. Its imaginary part gives the stream function at the node points. As soon as the distribution of the stream function over the mesh is calculated, the contour plot may drawn using a standard plotting package.

variations of the pressure that would happen if the flow was really going round the trailing edge as shown in the Figure 21.4. The considerations above led to the proposition that *the velocity at the trailing edge should be finite*, and this is referred to as the ***Joukovskii-Kutta hypothesis***. The analysis performed later in the limit of high Reynolds number ($V_\infty a/\nu \gg 1$) for the viscous flow in a small region near the trailing edge provided the mathematical justification for requirement of the regularity of the velocity at the trailing edge, which is now also referred to as ***Joukovskii-Kutta condition***. This is an example showing the importance of treating an inviscid flow as a limiting case of the viscous flow at high Reynolds numbers.

The Joukovskii-Kutta condition allows the circulation Γ to be determined. It may be easily seen that the flow may be made smooth near the trailing edge by a proper choice of the circulation Γ. In the present case, the singularity in (21.9), i.e.

$$\overline{V}(z) = \frac{dw}{dz} = \frac{dW}{d\zeta}\frac{d\zeta}{dz} = \frac{dW}{d\zeta}\frac{1}{dz/d\zeta},$$

may be avoided if we set $dW/d\zeta$ as given by (21.10) to zero at point $\zeta = a$, which represents the trailing edge of the plate in the auxiliary ζ-plane. Substituting (21.12) into (21.10) gives

$$\frac{dW}{d\zeta} = \frac{1}{2}V_\infty\left(e^{-i\alpha} - \frac{a^2}{\zeta^2 e^{-i\alpha}}\right) + \frac{\Gamma}{2\pi i\zeta},$$

and on setting $\zeta = a$ and equating $dW/d\zeta$ to zero, we have

$$\frac{V_\infty}{2}\left(e^{-i\alpha} - e^{i\alpha}\right) + \frac{\Gamma}{2\pi i a} = 0,$$

from which, we will find the circulation

$$\Gamma = -2\pi a V_\infty \sin\alpha. \tag{21.13}$$

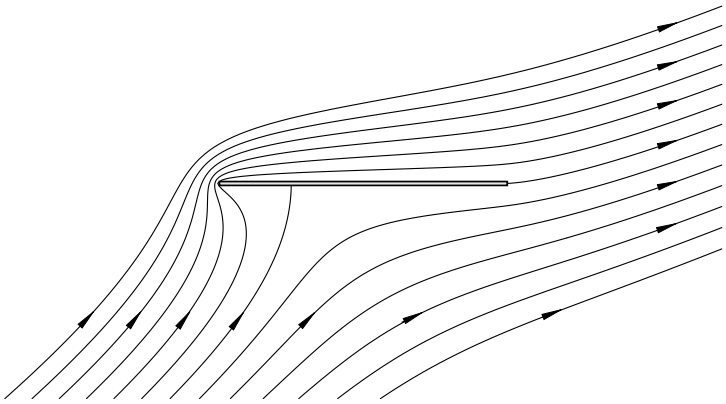

Figure 21.5: Incidence $\alpha = 30°$.

The streamline pattern for the flow field with the circulation given by (21.13) is shown in Figure 21.5.

Let us now calculate the velocity field for this flow. Substitution of (21.12) and (21.13) into (21.10) yields

$$\begin{aligned}\frac{dW}{d\zeta} &= \frac{V_\infty}{2}\left(e^{-i\alpha} - \frac{a^2}{\zeta^2 e^{-i\alpha}}\right) - V_\infty \frac{a\sin\alpha}{i\zeta} \\ &= \frac{V_\infty}{2}\cos\alpha - i\frac{V_\infty}{2}\sin\alpha - \frac{V_\infty}{2}\frac{a^2}{\zeta^2}\cos\alpha - i\frac{V_\infty}{2}\frac{a^2}{\zeta^2}\sin\alpha + iV_\infty\frac{a}{\zeta}\sin\alpha \\ &= \frac{V_\infty}{2}\left(1 - \frac{a^2}{\zeta^2}\right)\cos\alpha - i\frac{V_\infty}{2}\left(1 - \frac{a}{\zeta}\right)^2\sin\alpha. \end{aligned} \tag{21.14}$$

Substitution of (21.14) and (21.11) into (21.9) yields

$$\overline{V} = \frac{dW}{d\zeta}\frac{1}{dz/d\zeta} = V_\infty\cos\alpha - iV_\infty\sin\alpha\frac{\zeta - a}{\zeta + a}.$$

Finally, in order to express the velocity field in terms of z, we use (21.7) and note that

$$\frac{\zeta - a}{\zeta + a} = \frac{z - a + \sqrt{z^2 - a^2}}{z + a + \sqrt{z^2 - a^2}} = \frac{\sqrt{z-a}(\sqrt{z-a} + \sqrt{z+a})}{\sqrt{z+a}(\sqrt{z+a} + \sqrt{z-a})} = \sqrt{\frac{z-a}{z+a}},$$

and therefore,

$$\overline{V}(z) = V_\infty\cos\alpha - iV_\infty\sin\alpha\sqrt{\frac{z-a}{z+a}}.$$

Notice that at the trailing edge ($z = a$) the velocity is directed parallel to the plate surface and has a finite modulus $|\overline{V}| = V_\infty\cos\alpha$.

Joukovskii Aerofoils

In Lecture 21, we have demonstrated that the Joukovskii transformation

$$\zeta = z + \sqrt{z^2 - a^2} \tag{22.1}$$

maps the circular arc slit in the z-plane onto the circle in the ζ-plane (see Figure 22.1). The arc connects points $-a$ and a on the real axis in the z-plane and crosses the imaginary axis at point $z = ih$. Its image in the ζ-plane is a circle which has its centre at $\zeta = ih$ and intersects the real axis at points $-a$ and a.

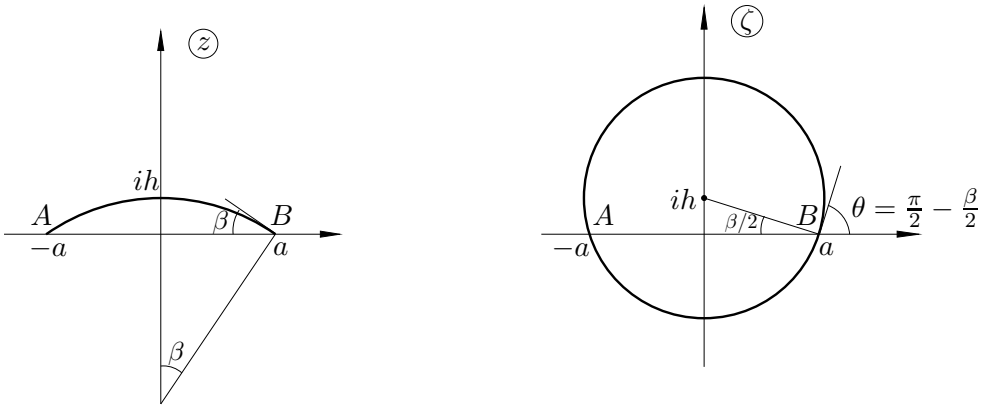

(a) z-plane. (b) ζ-plane.

Figure 22.1: Joukovskii transformation.

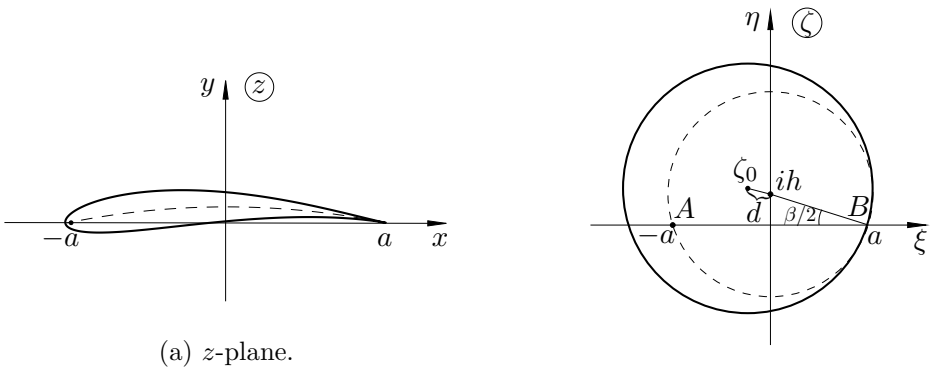

(a) z-plane.

(b) ζ-plane.

Figure 22.2: Mapping of a circle in the auxiliary plane onto Joukovskii aerofoil in the physical plane. The particular shape of the aerofoil shown in the z-plane has been calculated for $h/a = 0.1$ and $d/a = 0.1$.

We shall now use this mapping to introduce a family of aerofoil shapes known as ***Joukovskii aerofoils***. These are generated in the following way. We extend the segment

of a straight line connecting points $\zeta = ih$ and $\zeta = a$ in the ζ-plane beyond point $\zeta = ih$ as shown in Figure 22.2(b), and place point ζ_0 on the extension a distance d from the point ih. We then use ζ_0 as the centre of a new circle, and choose its radius to be

$$R = d + \sqrt{a^2 + h^2},$$

which ensures that the circle passes through point B, where $\zeta = a$. In Figure 22.2(b) this new circle is drawn with the solid line; we also reproduce here the "old circle" of Figure 22.1(b) with the dashed line. In what follows we shall refer to these as "large" and "small" circles, respectively.

The inverse Joukovskii transformation

$$z = \frac{1}{2}\left(\zeta + \frac{a^2}{\zeta}\right) \tag{22.2}$$

maps the small circle onto the circular arc in the z-plane, shown in Figure 22.2(a) with the dashed line. The image of the large circle represents a *Joukovskii aerofoil*. Since at point B in the ζ-plane the two circles are tangent to one another, their images in the z-plane should also be tangent. This means that at the trailing edge both the upper and lower surfaces of the aerofoil (see Figure 22.2a) are tangent to the arc, and therefore the aerofoil contour forms a *cusp* at the trailing edge. Moving away from point B in the auxiliary ζ-plane results in wider separation of the two circles. Correspondingly in the z-plane the distance between the arc and the upper and lower surfaces of the aerofoil contour grows larger. Since

$$\frac{dz}{d\zeta} = \frac{1}{2}\left(1 - \frac{a^2}{\zeta^2}\right)$$

is the finite at any point other than $\zeta = \pm a$, but the point A (where $\zeta = -a$) in the ζ-plane is situated inside the large circle, the leading edge of the aerofoil must be rounded.

Apart from parameter a, which may be used to change the aerofoil cord, there are two more parameters controlling the aerofoil shape, the camber parameter, h, and thickness parameter, d. The particular shape shown in Figure 22.2 was drawn for $h/a = 0.1$ and $d/a = 0.1$. This was done numerically by placing sufficiently large number of points distributed uniformly round the circle in the ζ-plane and using Joukovskii transformation (22.2) to calculate their coordinates in the z-plane.

Now we need to adjust the complex potential (17.15) that describes the flow past a circular cylinder in Figure 17.1 to the flow past the "large circle" in the auxiliary ζ-plane (Figure 22.2b). Taking into account that the radius of the circle now equals R and its centre is shifted to point ζ_0, we write

$$W(\zeta) = \tilde{V}_\infty\left[(\zeta - \zeta_0)e^{-i\alpha} + \frac{R^2}{(\zeta - \zeta_0)e^{-i\alpha}}\right] + \frac{\Gamma}{2\pi i}\ln(\zeta - \zeta_0). \tag{22.3}$$

Recall that with the method of conformal mapping conditions *1* and *2* in the formulation of Problem 17.1 are satisfied automatically, but the free-stream condition *3* requires special attention.

The complex conjugate velocity in the physical plane (Figure 22.2a) is calculated as

$$\overline{V}(z) = \frac{dW}{d\zeta}\frac{d\zeta}{dz}, \tag{22.4}$$

where

$$\frac{dW}{d\zeta} = \tilde{V}_\infty \left[e^{-i\alpha} - \frac{R^2}{(\zeta - \zeta_0)^2 e^{-i\alpha}} \right] + \frac{\Gamma}{2\pi i} \frac{1}{\zeta - \zeta_0}, \tag{22.5}$$

and

$$\frac{d\zeta}{dz} = 1 + \frac{z}{\sqrt{z^2 - a^2}}. \tag{22.6}$$

At large values of z and ζ,

$$\frac{dW}{d\zeta} = \tilde{V}_\infty e^{-i\alpha}, \qquad \frac{d\zeta}{dz} = 2,$$

which being substituted into (22.4) yield

$$\overline{V}(z) = 2\tilde{V}_\infty e^{-i\alpha} + \cdots \quad \text{as} \quad z \to \infty.$$

We see that the free-stream condition is satisfied with

$$\tilde{V}_\infty = \tfrac{1}{2} V_\infty. \tag{22.7}$$

Let us now return to finite values of z. It follows from (22.6) that there are two singular points $z = -a$ and $z = a$. However, now the first of these, $z = -a$, is situated inside the aerofoil, and we only need to consider the point $z = a$, which lies at the trailing edge of the aerofoil. Its image in the auxiliary plane is the point B, where $\zeta = a$; see Figure 22.2. According to the Joukovskii-Kutta condition, the complex conjugate velocity, $\overline{V}(z)$, has to be finite at the trailing edge, which is only possible if

$$\left. \frac{dW}{d\zeta} \right|_B = 0. \tag{22.8}$$

It may be easily seen from Figure 22.2(b) that at point B

$$\zeta - \zeta_0 = a - \zeta_0 = Re^{-i\beta/2}. \tag{22.9}$$

Using (22.8) and (22.7) in (22.5) allows to express equation (22.8) in the form

$$\frac{V_\infty}{2} \left(e^{-i\alpha} - \frac{1}{e^{-i(\alpha+\beta)}} \right) - i \frac{\Gamma}{2\pi} \frac{1}{Re^{-i\beta/2}} = 0,$$

which, being solved for Γ, yields

$$\Gamma = -2\pi R V_\infty \frac{e^{i(\alpha+\beta/2)} - e^{-i(\alpha+\beta/2)}}{2i} = -2\pi R V_\infty \sin\big(\alpha + \beta/2\big). \tag{22.10}$$

This completes the task of finding the complex potential of the flow past Joukovskii aerofoil. Now any fluid dynamic function may be easily determined. In particular, in Figure 22.3 we show the streamline pattern for Joukovskii aerofoil with $h/a = 0.1$ and $d/a = 0.1$ at incidence $\alpha = 20°$. It was obtained numerically by distributing the mesh points on a set of concentric circles surrounding the large circle in Figure 22.2(b). For each such point the location of its image in the physical z-plane is calculated using Joukovskii transformation (22.2). The value of the complex potential at this point is found using equation (22.3) with (22.7) and (22.10). Separating the imaginary part of W yields the stream function, ψ. The contours of constant ψ produce the streamline pattern.

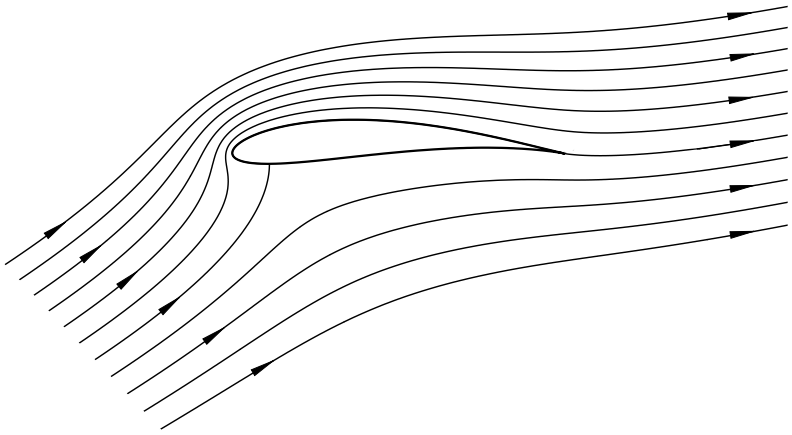

Figure 22.3: Streamline pattern for the aerofoil in Figure 22.2(a); incidence $\alpha = 20°$.

If one wants to find the velocity field, then equation (22.4) should be used. Once the velocity is known, the pressure at any point in the flow field and on the aerofoil surface can be found using the Bernoulli equation

$$\frac{V^2}{2} + \frac{p}{\rho} = \frac{V_\infty^2}{2} + \frac{p_\infty}{\rho}.$$

Of course, one does not need to integrate the pressure to determine the lift force since the latter can be calculated using the Joukovskii-Kutta formula,

$$L = -\rho V_\infty \Gamma = \rho V_\infty^2 2\pi R \sin\big(\alpha + \beta/2\big). \tag{22.11}$$

The theoretical predictions for the lift force prove to be in a good agreement with the experimental data but only for angles of attack below some critical value which depends on the aerofoil shape. The reason is that the Joukovskii-Kutta condition presumes that the flow remains attached to the aerofoil surface. While aerofoils are especially designed to maintain attached form of the flow, in reality the separation can be avoided only within a narrow range of angles of attack. As an example, in Figure 22.4 the flow past NACA 4412 aerofoil is shown. We see that at angle of attack $\alpha = 5°$ the flow is attached to the aerofoil surface, but at $\alpha = 10°$ the separation occurs near the trailing edge. It leads to a reduction of the circulation, Γ, produced by an aerofoil, and hence, to a loss in the lift force.

Despite it failed completely to predict the drag force, the inviscid flow theory has been used extensively is aerofoil design. The analysis of Joukovskii aerofoils presented above takes advantage of the fact that the function performing the conformal mapping of the aerofoil on a circle in the auxiliary plane can be expressed in the explicit analytical form (22.1). This is however not possible in general case, where the mapping function could be found numerically. As this task is quite complicated, the flow field past an aerofoil is normally predicted through direct numerical solution of the boundary-value Problem 13.1 (see Lecture 13).

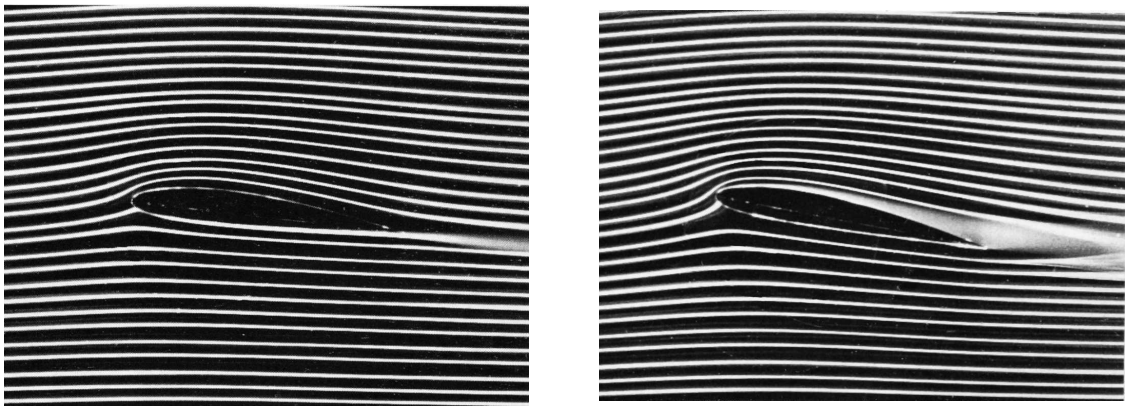

(a) Incidence $\alpha = 5°$.

(b) Incidence $\alpha = 10°$.

Figure 22.4: Visualization of the flow past NACA 4412 aerofoil.